NOTICE

The quality of this microform is heavily dependent upon the quality of the original thesis submitted for microfilming. Every effort has been made to ensure the highest quality of reproduction possible.

If pages are missing, contact the university which granted the degree.

Some pages may have indistinct print especially if the original pages were typed with a poor typewriter ribbon or if the university sent us an inferior photocopy.

Reproduction in full or in part of this microform is governed by the Canadian Copyright Act, R.S.C. 1970, c. C-30, and subsequent amendments.

AVIS

La qualité de cette microforme dépend grandement de la qualité de la thèse soumise au microfilmage. Nous avons tout fait pour assurer une qualité supérieure de reproduction.

S'il manque des pages, veuillez communiquer avec l'université qui a conféré le grade.

La qualité d'impression de certaines pages peut laisser à désirer, surtout si les pages originales ont été dactylographiées à l'aide d'un ruban usé ou si l'université nous a fait parvenir une photocopie de qualité inférieure.

La reproduction, même partielle, de cette microforme est soumise à la Loi canadienne sur le droit d'auteur, SRC 1970, c. C-30, et ses amendements subséquents.

UNIVERSITY OF ALBERTA

A DESCRIPTION OF GLASS PHASES IN THE COLUMBIA RIVER BASALT GROUP

BY

IAN KENDRICK MARSH

A THESIS

SUBMITTED TO THE FACULTY OF GRADUATE STUDIES AND RESEARCH IN PARTIAL FULFILLMENT OF THE REQUIREMENTS FOR THE DEGREE OF MASTER OF SCIENCE

IN 

GEOLOGY

DEPARTMENT OF GEOLOGY

EDMONTON, ALBERTA

SPRING 1990

NOTICE

The quality of this microform is heavily dependent upon the quality of the original thesis submitted for microfilming. Every effort has been made to ensure the highest quality of reproduction possible.

If pages are missing, contact the university which granted the degree.

Some pages may have indistinct print especially if the original pages were typed with a poor typewriter ribbon or if the university sent us an inferior photocopy.

Reproduction in full or in part of this microform is governed by the Canadian Copyright Act, R.S.C. 1970, c. C-30, and subsequent amendments.

AVIS

La qualité de cette microforme dépend grandement de la qualité de la thèse soumise au microfilmage. Nous avons tout fait pour assurer une qualité supérieure de reproduction.

S'il manque des pages, veuillez communiquer avec l'université qui a conféré le grade.

La qualité d'impression de certaines pages peut laisser à désirer, surtout si les pages originales ont été dactylographiées à l'aide d'un ruban usé ou si l'université nous a fait parvenir une photocopie de qualité inférieure.

La reproduction, même partielle, de cette microforme est soumise à la Loi canadienne sur le droit d'auteur, SRC 1970, c. C-30, et ses amendements subséquents.

ISBN 0-315-60188-4

This one is for my mum and dad

ABSTRACT

The Mid-Miocene Columbia River Basalt Group (CRBG) of Washington, Oregon, and Idaho exhibits two phases that are, or once were, glasses. The colourless glass is granitic in composition: SiO_2 74%, Al_2O_3 14%, FeO+MgO <2%, Na_2O 1.9%, K_2O% 6.55 and $\delta^{18}O$ + 10‰. The amounts of colourless glass (CGL) ranges from traces in the Imnaha to roughly 25% in the Wanapum. The coexisting glass phase, mostly altered to smectite is ultramafic in nature: SiO_2 46%, Al_2O_3 4.5%, FeO+MgO >35%, CaO 1.5%, alkalies <2%, and, $\delta^{18}O$ +10%. The amount of brown glass (BGL) ranges from 2-3% in Grande Ronde to 7-10% in Wanapum units.

The occurrences of globules of <0.1mm BGL in a matrix of CGL, similar Fe/Mg ratios in BGL and CGL, and modelling in the systems K_2O-FeO-Al_2O_3, and Fo-Di-Qz suggest that an immiscible relationship existed between the two glass phases. The REE concentrations are in agreement with the preferential partitioning of Ti and to a lesser extent P into the granitic fraction which is contrary to experimentally determined partitioning coefficients where Ti and P are enriched in the unpolymerized basaltic melt.

Current petrogenetic theories concerning the generation of the CRBG are the fractionating sill model, with or without that of crustal contamination of the primary magma. In addition, a model utilizing the partial melt of eclogite as the magma source is discussed.

ACKNOWLEDGEMENTS

The author wishes to thank the following people for their invaluable assistance that aided the production of this thesis.

1) Dr. R. St J Lambert who provided many hours of discussion on the complexities of this project, without whose guidance this project would not have been completed.

2) Technical assistance was afforded by many talented individuals; S. Launspach and D.A. Tomlinson were invaluable in attaining the microprobe analysis, Dr. J.G. Holland carried out XRF analysis, Mr. A. Stelmach assisted in attaining AAS data, Mrs. E. Toth ran the oxygen isotope extractions, and, finally, M.J.M Duke carried out INAA analysis.

3) Many people provided useful insights into technical difficulties encountered throughout this study: Dr. D.G.W. Smith, and Dr. K. Muehlenbachs, M.J.M. Duke, P. Cavell, and M. Hirschman. Finally, thanks go to R. Pinckston who listened to an account of every problem encountered in this study.

4) Thanks also go to Tanya, my fiancee, for understanding what this meant to me and putting up with all the difficulties this year provided us.

5) An additional thanks is owed to Lt (N) Cowen, Bras d'Or Officer, at NOTC Venture who made it possible for me to return to Edmonton to finish this project.

6) Finally, to my mum and dad who provide never ending love, support and encouragement throughout my educational career, in addition to the much needed financial support.

TABLE OF CONTENTS Page.

LIST OF TABLES

LIST OF FIGURES

LIST OF PLATES

INTRODUCTION

During the field seasons of 1983 and 1984, R. St. J. Lambert collected a representative suite of samples covering all major units in the Columbia River Basalt Group (CRBG). During an initial study of these rocks and their chemistry in an undergraduate geochemistry course the immense complexities of the data surrounding these basalts became apparent. As such, finding a worthy thesis study project within the body of samples already collected was a simple matter. One such aspect was the lack of a quantitative description of the glass phases in these rocks. The scope of this research will be primarily in the area of petrography and chemical petrology, the major task being to describe the glass phases in the CRBG, and the behaviour and relationships between the glass phases as the extruded magmas cooled.

In the initial study of the many thin sections available the Columbia River Basalt Problem arose. This problem is to describe the coexistence of two glass phases which exhibit a texture suggestive of an immiscible nature between the two.

Another major unanswered question dealing with the CRBG concerns their origin and nature of emplacement. Waters (1961) first addressed this problem in order to explain differences between Picture Gorge and Yakima sequences. Waters (1961) noted a marked increase in phenocryst occurrence, and increased Al, Mg, and Ca in the Yakima with no apparent gradation between the two units. This led to the conclusion that Picture Gorge and Yakima represented separate units generated in different magmatic hearths. The influence of olivine, plagioclase and a Mg-rich pyroxene have been proposed as the possible differentiating phases in the magma genesis of these basalts. The lack of any transitional flows between the two major units led Waters (1961) to doubt that the Yakima was a late stage differentiate of the earlier Picture Gorge unit. He did not elaborate further on the physiochemical parameters that affected this process.

Cox (1980) provides a model for the generation of flood basalts based on studies of African examples, such as the Karoo basalts. This model involves the storage of primary magmas in deep crustal sills. In these sills removal of olivine, plagioclase and pyroxene is accomplished in order to account for the enrichment in incompatible trace elements. Extensional tectonics in the CRBG area during the Mid-Miocene (Tauenbeck 1969, Barrash *et al.* 1983, Ross 1983, Catchings and Mooney 1988) provide an alternate mechanism (to density decrease due to olivine removal in the sills) for tapping the deep seated magma in the sills.

In order to fully satisfy isotopic constraints, Carlson (1984) proposed another method of genesis involving crustal contamination of the primary magma. This model requires the mixing of up to five, distinct, separate isotopic and chemical components. By varying the amount of mixing, the components involved and the amount of fractionation which occurs after mixing, the order of the units and their chemical and isotopic signatures can be accounted for.

The final model to be discussed is that of partial melting of eclogite. This model accounts for trace elements and isotopic constraints by utilizing an enriched mantle derived by the addition of partially melted eclogite. Sediments associated with the slab may also influence the isotopic signature. Trace element abundances are controlled by a two stage enrichment process, first at the mid ocean ridge as the slab is produced, the second in the subcontinental wedge as a result of the partial fusion process. The large scale homogeneity within units is accounted for by partial fusion at a pseudo-invariant point as discussed by Presnall (1969). Variations between units are accounted for by large scale heterogeneity of the sub continental mantle similar to the model proposed by Morris and Hart (1983). The partial melt of eclogite does not require large scale fractionation as do other models. The majority of fractionation, which occurs as partial fusion, in this model occurs at the ridge environment where MORB is produced, not under the continental margin. However, the imprint of this 'fractionation' process is still seen in the later rocks derived by the partial fusion process. Hence the use of the term interfacing in later discussion to describe fractionation process

that occurred in a previous environment yet whose imprints are still seen in the rocks derived by a later partial fusion process.

The treatment of the CRBG problem follows the order:

1. Stratigraphy.
2. Petrology.
3. Geochemistry.

Having established the mineralogy, geochemistry, and petrology of this suite of rocks the problem of the glasses will be discussed in the context of immiscibility, supercooling, and the bearing these may have on petrogenetic theory.

STRATIGRAPHY

The CRBG is a well known representative of a continental flood basalt. Nearly 200,000 square kilometres of Washington, Oregon, and Idaho are covered by as much as one kilometre of lava (Swanson *et al.* 1979, Hooper 1982, Reidel 1983), Figure 1. These basalts were extruded from a series of NW trending dykes (Tauenbeck 1969, Barrash *et al.* 1983) likely associated with east-west extension at the time basaltic outpouring was Mid-Miocene, but continued over an 11 million year period from 17 - 6 Ma. (Dodds 1970, McDougall 1976, Goles 1980, Hooper 1982). The great majority of the extruded material was erupted in a three million year period from 16.5 - 13 Ma. (Holmgren 1970, B.V.S.P. 1981, Ross 1983). Extremely high rates of eruption, on the order of $10^8 m^3/yr$ (Baksi and Watkins 1973, Watkins and Baksi 1974, Swanson *et al.* 1975), facilitated the emplacement of such a large volume of basalt in such a short period of time.

Waters (1961) subdivided the CRBG into two major formations, the younger Yakima, and Picture Gorge, based on petrographic evidence. In the past 25 years the original groupings of Waters (1961) have been successively divided and redefined by many authors. Wright *et al.* (1973) divided individual members by chemical variation, listing eight subdivisions of the Yakima and two units within Picture Gorge. McDougall, (1976), using methods such as K-Ar dates, magnetic polarity and geochemical analysis, has added four divisions to the original Picture Gorge, and a further 22 subdivisions to the Yakima. B.V.S.P. (1981) summarizes all available information in 1981, including a further 7 erosional hiatuses in the stratigraphic sequence. Beeson *et al.* (1985), have further subdivided the Frenchman Springs member of the Wanapum basalt into six separate units. This division is based on chemical variations of Cr, P, Ti, Mg, palaeomagnetism, and stratigraphic relationships. The latest data reported by Mangan *et al.* (1987) subdivides the Grande Ronde into 5 chemically distinct subtypes with as many as 18 recognizable subunits. The vast amounts of work which have been done on the stratigraphy of these basalts has resulted in a greater understanding and a narrower definition of the individual units of the CRBG. Figure 2 shows the stratigraphy

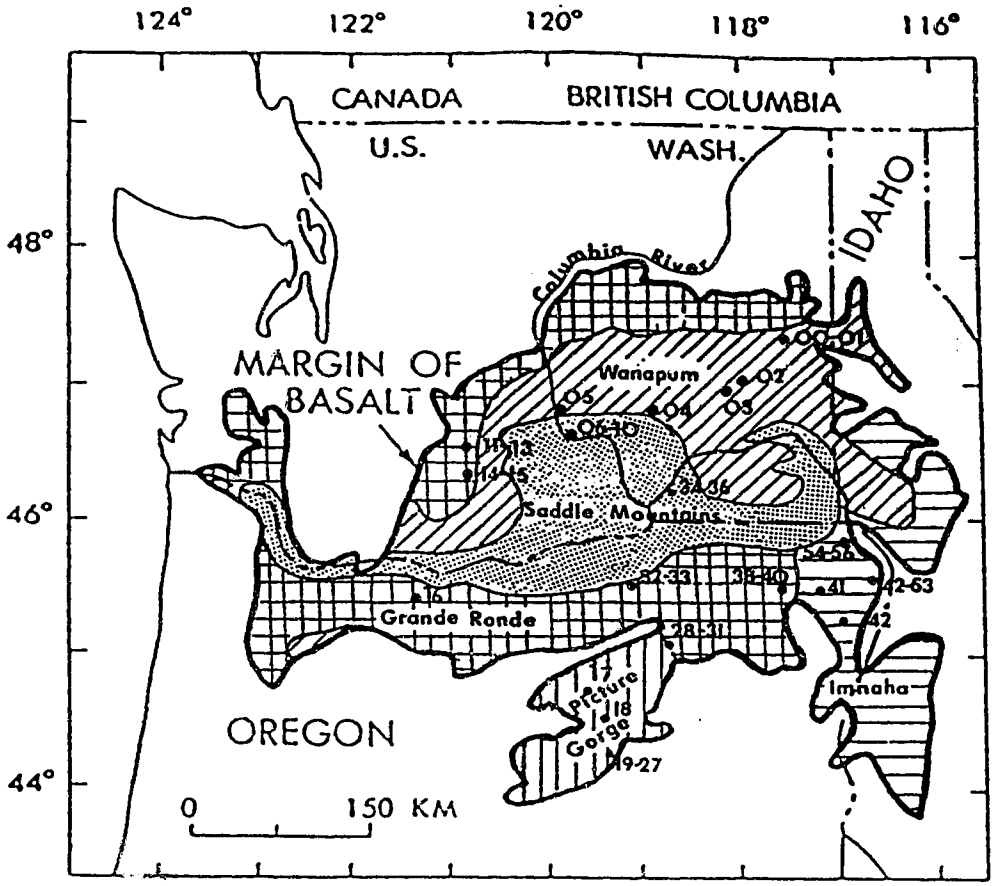

Figure 1. General map area of the Columbia River Basalt Group.(●) represents sample locations and the sample numbers (prefixed by 6900) collected at each location.

SERIES		GROUP	SUB-GROUP	FORMATION	MEMBER	THIS STUDY
MIOCENE	UPPER	COLUMBIA RIVER BASALT GROUP	YAKIMA BASALT GROUP	SADDLE MOUNTAINS BASALT	LOWER MONUMENTAL MEMBER	
					Erosional Unconformity	
					ICE HARBOR MEMBER Basalt of Goose Island Basalt of Martindale Basalt of Basin City	6935,36
					Erosional Unconformity	
					BUFORD MEMBER	
					ELEPHANT MOUNTAIN MEMBER	
					Erosional Unconformity	
					POMONA MEMBER	6915,39a,b
					Erosional Unconformity	
					ESQUATZEL MEMBER	
					Erosional Unconformity	
					WEISSENFELS RIDGE MEMBER Basalt of Slippery Creek Basalt of Lawton Orchards	
					ASOTIN MEMBER	
					Local Erosional Unconformity	
					WILBER CREEK MEMBER Basalt of Lapwai Basalt of Wahluka	
					UMATILLA MEMBER Basalt of Silkual Basalt of Umatilla	6932a,b, 33
					Local Erosional Unconformity	
	MIDDLE			WANAPUM BASALT	PRIEST RAPIDS MEMBER Basalt of Lola Basalt of Rosella	6906
					ROZA MEMBER	6900-05
					FRENCHMAN SPRINGS MEMBER Basalt of Lyons Ferry Basalt of Sentinel Gap Basalt of Sand Hollow Basalt of Silver Falls Basalt of Ginkoe Basalt of Paloume Falls	6908-10, 14 3AS7,8
					ECKLER MOUNTAIN MEMBER Basalt of Shomaker Creek Basalt of Dodge Basalt of Robinette Mountain	
				GRANDE RONDE BASALT		6942, 51-56 6937, 41 3AS4,6,12,13 3AS15a,b 6911-13
	LOWER			PICTURE GORGE BASALT	Basalt of Deyville Basalt of Monument Mountain Basalt of Twickenham	6916-27
				IMNAHA BASALT		6905, 43, 50

Figure 2. Stratigraphic cross section of the Columbia river Basalts. Altered from Beeson *et al.* (1985) to include sample numbers from this study.

of the CRBG and is based on the work of Beeson *et al.* (1985) but is further expanded to show where individual rocks in this thesis project fall in the overall stratigraphy. For the purposes of this discussion, a simple four-fold division of stratigraphy; Picture Gorge, Grande Ronde, Wanapum, and Saddle Mountain, will be sufficient.

GENERAL PETROGRAPHY

The rocks available for this study cover all the major units within the CRBG. Generally, these rocks are fine grained, with occasional phenocrysts and gas vesicles. The overall mineralogy of the units is simple: plagioclase, clinopyroxene, occasional olivine, opaque mineral phases, brown and colourless glass, clay alteration products and accessory apatite and rutile. This mineral assemblage is fairly consistent throughout the samples, differing only in modal abundances. Table 1 gives a modal analysis of seven representative samples from the major units within the CRBG.

Plagioclase

Plagioclase is most common as a groundmass phase in most units. Grain size is variable, and is a function of whole rock grain size. Commonly, grain size is 0.1 - 0.5mm. Plagioclase is also the most frequently occurring phenocryst phase, ranging from 0.5 - 1.5mm. Picture Gorge and Imnaha units have a higher occurrence of a phenocryst phase (5 - 10% modally) than do the Wanapum, (2 - 3%), Grande Ronde (0 - 2%), and Saddle Mountains units (0 - 5%).

Plagioclase determinations were made optically using the Michel-Levy method. Compositions are usually in the An_{40} - An_{50} range. Many other authors (Waters 1961, Hooper 1974, Reidel 1983) also describe plagioclase in these basalts as andesine. There are occasional occurrences of more calcic compositions, An_{50} - An_{60} (Holden and Hooper 1976, Schmincke 1967, Hooper 1974, Hoffer 1980). This more calcic composition is most commonly associated with samples from Picture Gorge unit. Larger phenocrysts commonly exhibit oscillatory zoning with more sodic rims around more calcic cores.

Plagioclase grains share common grain boundaries with all other minerals. The one relationship peculiar to plagioclase is the occurrence of swarms of brown glass bubbles, usually less

Table 1.

Wanapum	6900	6908	3AS7
Plagioclase	40.1	36.9	28.7
Pyroxene	29.0	28.4	28.7
Apatite	1.1	1.2	1.2
Brown Glass	6.9	7.1	3.4
Colourless Glass	10.1	18.9	23.2
Iron Oxides	12.8	7.5	4.5
Grande Ronde	**6911**	**6939b**	
Plagioclase	49.3	47.9	
Pyroxene	29.9	28.0	
Apatite	1.1	0.2	
Brown Glass	2.0	7.2	
Colourless Glass	11.7	2.7	
Iron Oxides	5.9	13.9	
Picture Gorge/ Imnaha	**6918**	**6945**	
Plagioclase	57.7	57.8	
Pyroxene	32.9	25.2	
Apatite	0.0	0.5	
Brown Glass	7.0	10.9	
Colourless Glass	trace	trace	
Iron Oxides	2.4	5.6	

Table 1. Modal abundances of major mineral phases in the various units within the Columbia River Basalt Group. Based on 1500 points counted on each thin section.

than 0.01mm diameter, within colourless glass adjacent to plagioclase boundaries. The bubbles of brown glass in colourless glass are more commonly found along plagioclase boundaries in the interstitially occurring colourless glass. Brown glass bubbles have not, to date, been found in association with any other mineral.

Clinopyroxene

Clinopyroxene is a major component in the groundmass of all units. Grains range form 0.1 - 0.5 mm in the groundmass and from 0.5 - 1.5 mm when in phenocryst form. Phenocrysts of clinopyroxene are always associated with a coexisting phenocryst phase of plagioclase, and occasionally olivine.

Pyroxenes in thin section are clear to light tan in colour with a medium, (40 - 50 degrees) positive 2V angle. This suggests a composition of augite which is consistent with results reported by Waters (1961) and Ridel (1983). Microprobe analysis shows that the composition is subcalcic with a slight enrichment in magnesium with respect to iron, with a composition of roughly Hd_{35} - Hd_{45} (Table 2). There is no evidence of zoning in phenocrysts of pyroxene as was the case with plagioclase. Pigeonite has been observed by Floyd Hodges of Rockwell Hanford, but its distribution is not yet fully documented outside of the Upper Grande Ronde units (pers. comm. 1987).

There are no definite mineral associations for the pyroxene phases. There is, however, an increase in pyroxenes and other mafic minerals in cases where the modal abundance of colourless glass is low.

Olivine

Olivine is a minor groundmass phase in a few of the CRBG units, ranging from 0.1 - 0.5

Table 2.

	Wanapum	Grande Ronde	Imnaha
	6908	6954	6944
SiO_2	51.5	51.5	51.3
Al_2O_3	1.2	1.2	0.9
FeO	15.1	14.9	18.6
MgO	13.4	13.5	13.2
CaO	17.3	17.3	14.7
Na_2O	0.2	0.2	0.2
TiO_2	0.9	0.9	0.9
MnO	0.2	0.3	0.4
Cr	0.2	0.1	0.1
Total	100.0	99.9	99.3
Hd	40.	40.	45.

Table 2. Three analysis of Columbia River Basalt Group clinopyroxenes showing a slightly Mg-rich Diopside-Hedenbergite composition. No further analysis were carried out as part of this study. The data from these three pyroxenes are consistent with those reported by other authors. Data are reported in oxides rather than elements for the sake of consistency with other data presented in this thesis.

mm. Rarely, olivine occurs as phenocrysts, from 0.5 - 1 mm. In this mode of occurrence it is always highly altered. As with plagioclase there is an increased occurrence of phenocrysts of olivine in Picture Gorge and Imnaha units. Also, as was the case with clinopyroxene, olivine is never the sole phenocryst phase, but always occurs in association with another phenocryst phase, usually plagioclase (Wright et. al. 1973).

The fine grain size of olivine makes optical identification of composition difficult. Microprobe analysis reveals a highly Fe rich, fayalitic composition, roughly Fo_{30}. Table 3. Similar olivine occurrences are noted by Waters (1961), Schmincke (1967), Hooper (1974), and Reidel (1983). Modal abundances of fayalite range from 0 - 3% in most units, but may be as high as 5% in Picture Gorge samples. This data is consistent with Waters (1961) data, 5% olivine in Picture Gorge, and <2% in Yakima units.

Opaque Iron and Iron-Titanium Oxides

Opaque minerals occur only as a groundmass phase, ranging in size from 0.1 - 0.3 mm. Wright *et al.*, (1973) describe microphenocrysts of iron oxides. However, this has not been seen in our samples. Modal abundances of opaque minerals are quite variable, ranging form 3 - 14 . As with other ferromagnesium a corresponding decrease in colourless glass phase in associated with a relative increase in mafic minerals.

Qualitative examination of opaque mineral phases using the electron microprobe revealed the major opaque mineral phase to be magnetite. Some iron-titanium oxides were also present. Titano-magnetite is often found as dendritic inclusions within the colourless glass phase. Similar dendritic occurrences of magnetite were reported by Schmincke (1967) in Upper Yakima flows.

Table 3.

	6908	6946
SiO_2	32.4	32.3
Al_2O_3	0.2	0.1
FeO	53.9	54.4
MgO	12.4	11.8
CaO	0.2	0.4
TiO_2	0.1	0.0
MnO	0.9	0.9
Total	100.1	100.0
Fo	30.	28.

Table 3. Two analysis of Columbia River Basalt Group olivines showing their highly fayalitic nature. No further analysis were carried out as part of this thesis as the data were consistent with that reported by other authors.

Alteration Products

Many of the samples show varying degrees of alteration, primarily of the mafic glass phase. Peacock and Fuller (1928), Waters (1961), Schmincke (1967), and Hearn *et al.* (1984) describe this alteration product as a mixture of clays, primarily smectite and chlorophaeite, and iron oxides. Walters and Ineson (1983) describe similar alteration products in basalts from the southern Pennines, England. Alteration of other phases in the rocks is apparent in some cases but to a much lesser extent. Plagioclase is altered to smectite in a small number of samples. Optically, other minerals and the colourless glass rarely appear altered.

The degree of alteration varies considerably from unit to unit. The highly altered brown glasses appear red-brown in both plane and crossed polarized light conditions, see plates 1 and 2. This characteristic colour is associated with concentric, alternating rings of red brown and black. A less altered sample shows only the red-brown colour. The least altered mafic glass is a light tan brown colour in plane polarized light and appears isotropic under crossed polars, see plates 3 and 4. The unaltered appearance of brown glass is much less common in the interstitial groundmass. However it is the usual appearance of the mafic globules within colourless glass.

Plate 1. Altered red-brown appearance of Columbia River Basalt brown glass or smectite from thin section 6908. Field of view is 0.55 mm, plane polarized light conditions.

Plate 2. Altered red-brown glass of smectite from 6908. Field of view is 0.55 mm, crossed polarized light conditions.

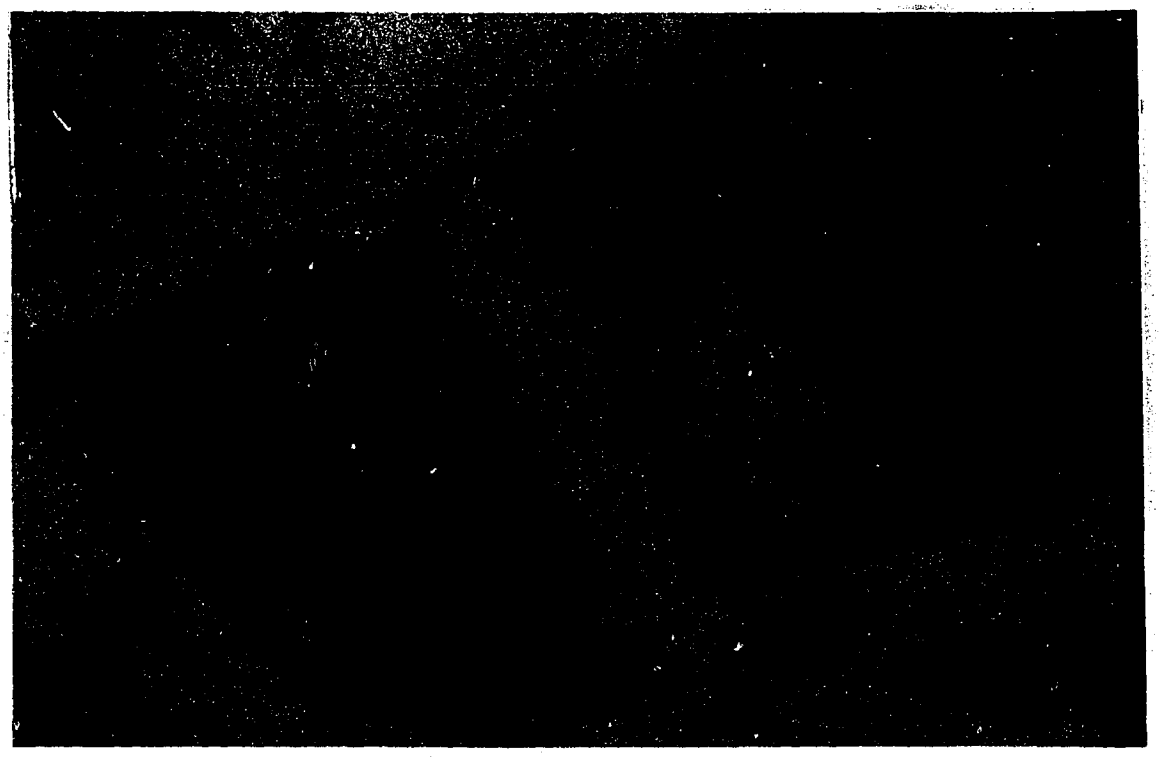

Plate 3. Bubble of relatively unaltered brown glass within a matrix of colourless glass in 6909. Field of view is 0.55 mm, plane polarized light conditions.

Plate 4. View of the same area of thin section 6909 as seen in plate 3. Field of view is still 0.55 mm, crossed polarized light conditions.

GLASS PETROGRAPHY

In thin section there are two readily visible phases that may be considered to be, or at one time to have been, glasses. These glasses are most often an interstitial phase in the ground mass and range in size from 0.1 - 2 mm. Based on their colour, glass phases have been designated as the brown, and colourless glasses. What is referred to as the brown glass in this discussion has been noted as altered mafic material by previous authors, (Waters 1961, Schmincke 1967, Holden and Hooper 1976), and is generally found in one of two habits.

The first, and most common, appearance of this glass is as an interstitial component in the ground mass. When in this form, especially when the rock is very coarse-grained, the mafic brown (glassy) material is commonly altered. The alteration in these samples is consistent with that described by Hearn *et al.* (1984) and is most likely to clay minerals such as smectite. Peacock and Fueller (1928), Waters (1961), and Schmincke (1967) also describe this alteration product as smectite. However, as will be discussed in greater detail it is likely that the smectite represents the alteration of a mafic glass. As such, in the context of the following discussion the term brown glass will be used to describe this phase. This is based on the supposed nature of its precursor, and in order to maintain consistency when comparisons to the colourless glass are drawn. Meyer and Sigurdsson (1978) describe a similar occurrence of smectite-like chlorophaeite in Icelandic basalts.

The second, much less common, occurrence is as small subspherical to spherical droplets in the colourless glass phase, or in bubble swarms along the boundaries of plagioclase phenocrysts. Again, Meyer and Sigurdsson (1978) describe a similar occurrence in the basalts from Iceland. Bubble size is quite variable in these swarms but is usually less than 0.0125 mm. Photographs of these bubbles rarely turn out as a result of the lack of sufficient depth of focus. A representative sketch of this relationship is provided in plate 5. The colourless glass in all cases is an interstitial phase. It has not to date been seen as a droplet in brown glass or anywhere else. Modal

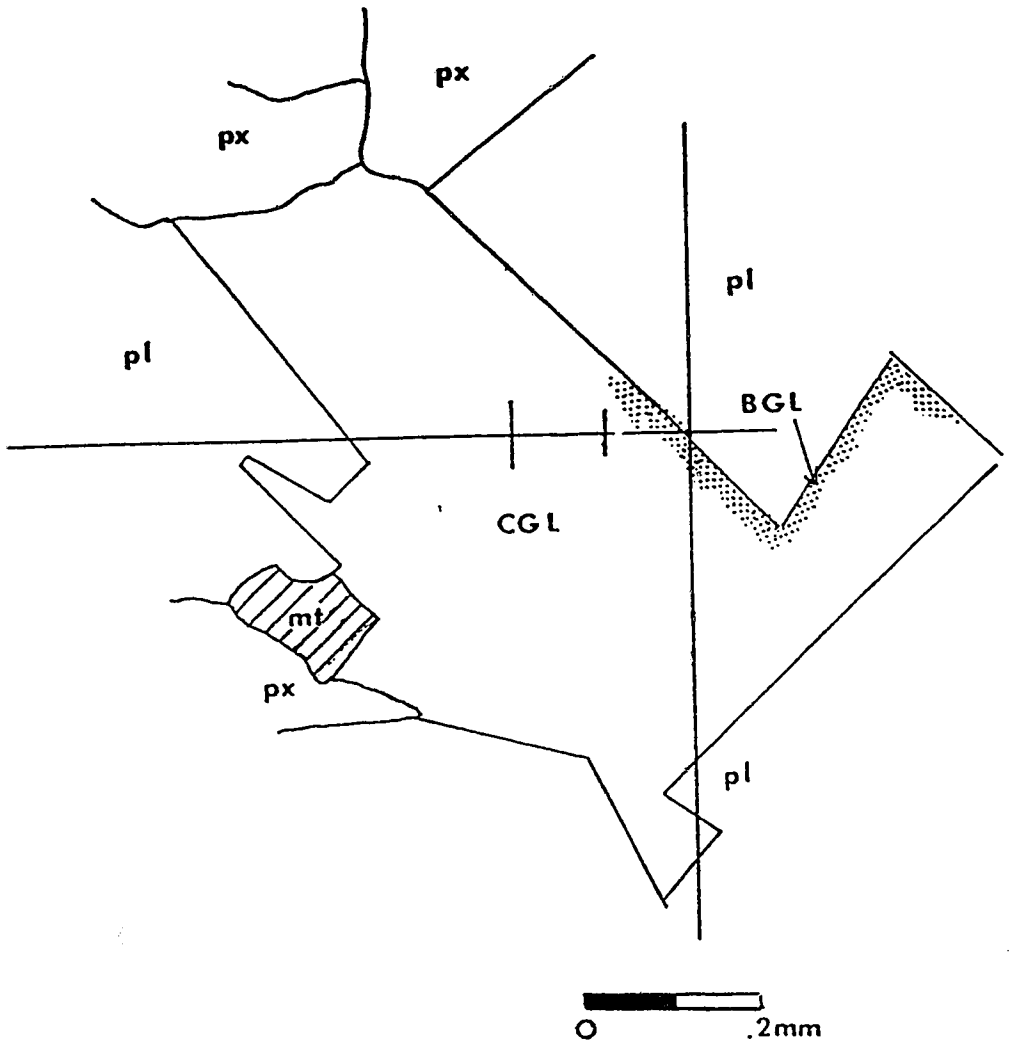

Plate 5. Sketch of a section of colourless glass surrounded by plagioclase. Bubbles of brown glass are roughly 0.01 mm in diameter. Such bubbles are more concentrated near plagioclase/glass boundary.

proportions of the two glass phases in most units of the CRBG are quite variable from flow to flow.

Following is a more detailed discussion of the variation of glass content in various units of the CRBG that will be covered in this discussion.

Saddle Mountains

The Saddle Mountains units are the most varied within the CRBG. These relatively small volume basaltic outpourings represent the last stages of the event that formed this entire flood basalt province. Chemistry and modal mineralogy of the individual members vary significantly from one unit to the next. Based on the data from Wright *et al.* (1973), the three units of the Saddle Mountains represented by the rocks in this study are the Umatilla, Pomona, and the Ice Harbor. The data in table 4 is used to compare whole rock chemistry from our samples, and the data used to subdivide the units of The Saddle Mountains Formation.

Ice Harbor

Ice Harbor, stratigraphically the youngest unit (Beeson, *et al.* 1985), shows a relatively constant occurrence of brown glass, roughly 10%. Most of the glass in this unit is altered, with less than 25% of it having escaped alteration to clay minerals, such as smectite (Hearn *et al.* 1984). The brown glass appears in both modes of occurrence. However, the interstitial phase is much more common, greater than 95% of brown glass occurring in this manner. The colourless glass is always present as an interstitial phase, but in varying proportions from unit to unit ranging from 10 - 25%.

Acicular apatite and rutile are associated with the colourless glass. These acicular crystals are not seemingly associated with the brown glass. Initially, it appears as though the apatite

Table 4

	UMATILLA				POMONA				ICE HARBOR			
	6932 (A)	6932 (B)	6933	SW19	6915	6934 (A)	6934 (B)	SW25	6935	E.M. 6936	I.H. SW26	SW29
SiO2	56.78	56.15	56.28	54.70	50.17	51.17	50.88	51.88	50.22	49.54	51.08	48.73
Al203	13.25	13.57	13.40	14.10	15.70	15.19	15.21	14.88	14.19	13.82	13.54	13.88
FeO*	11.51	11.66	11.54	12.63	11.14	10.54	11.05	10.55	14.54	14.86	14.75	14.41
MgO	3.26	3.08	3.07	2.71	6.12	6.06	6.30	6.96	4.05	4.26	4.28	5.88
CaO	5.81	6.00	6.14	6.14	11.18	11.02	10.89	10.67	8.72	8.90	8.34	9.72
Na2O	2.85	3.02	2.98	3.20	2.58	2.52	2.60	2.36	2.50	2.59	2.45	2.42
K2O	2.81	2.72	2.77	2.88	0.60	0.65	0.63	0.64	1.15	1.44	1.25	0.73
TiO2	2.34	2.32	2.42	2.80	1.76	1.75	1.73	1.62	3.38	3.54	3.52	3.30
MnO	0.16	0.19	0.19	0.17	0.20	0.19	0.19	0.19	0.21	0.21	0.20	0.20
P2O5	0.90	0.95	0.88	0.88	0.21	0.21	0.21	0.25	0.57	0.39	0.59	0.73
Total	99.67	99.67	99.77	99.11	99.68	99.30	99.69	98.70	99.53	99.55	100.00	100.00

Table 4. Chemical analysies of rocks from this study (6900's) and those used by Swanson *et al.* (1979) to subdivide the Saddle Mountains Member of the Columbia River Basalt Group. 6934a,b are supposedly Pomona, but are somewhat dissimilar to the Swanson *et al.* (1979) sample #19 (SW19), the Pomona chemical type. 6935,36 have been designated to the Ice Harbor flow but are also similar to the Elephant Mountain flow.

*** FeO expressed as FeO + .9 x Fe_2O_3**

nucleates and grows in both the CGL and BGL often extending into adjacent minerals. However, upon close investigation, and later chemical evidence, it is apparent that in the case of BGL this is a three dimensional affect. Apatite needles, in fact, do not originate in the brown glass.

Pomona

The Pomona unit is 1.5 million years older than the Ice Harbor, (Beeson *et al.* 1985) and is a single member representative unit of the Saddle Mountains formation. Glass occurrences in this unit are more inform than in the previous unit. Brown glass ranges from 1 - 3%, and the colourless glass fraction if 20 - 25%. In relation to the Ice Harbor there is an overall decrease of both glasses. The brown glass is commonly seen as droplets, usually along the edges of plagioclase crystals. The interstitial brown glass is highly altered to smectite (Peacock and Fuller 1928, Waters 1961, Hearn *et al.* 1984). The colourless glass is an interstitial phase in the groundmass in this flow. There is no associated apatite and rutile in the colourless glass as seen in the Ice Harbor. However, dendritic titano-magnetite, is commonly present. Overall decrease of the brown glass phase in this unit may be due to a 5% increase in the modal abundance of pyroxenes, olivine, and opaque minerals with respect to that seen in the Ice Harbor.

Umatilla

The Umatilla flows are the oldest in the Saddle Mountains formation, overlying the Wanapum formation, 14.5 Ma., and separated above by an erosional unconformity (B.V.S.P. 1981). All thin sections from the Umatilla show considerable alteration, not only of the brown glass, but also of the plagioclase, olivines, and pyroxenes. The mafic glass phase is altered to smectite. The modal proportion of brown glass is 10 - 20%, with less than 3% in the droplet phase.

Colourless glass is interstitial, and associated with accessory apatite and rutile, and the

dendritic form of titano-magnetite. The colourless glass and its associated minerals the only phases of the Umatilla units that seem to have completely escaped the effect of weathering, appearing fresh and unaltered.

Wanapum

Below the basal unconformity of the Saddle Mountains Formation is the Wanapum, ranging in age from 14.5 - 15.5 Ma. This unit is well represented by numerous samples. From the data of Beeson *et al.* (1985), it is apparent that six of the samples are from the Roza, and five from the Frenchman Springs. The Roza flows show a modal variation of 3.3 - 3.4% brown glass, and 19.5 - 23.3% colourless glass, while the Frenchman Springs show variations from 5.2 - 7.1% brown glass and 7.8 - 18.8% colourless glass, Table 5. In all cases the colourless glass is unaltered and associated with acicular apatite and rutile. Brown glass is altered in the interstitial phase but shows far less alteration in the droplet phase.

Variable glass contents in the Wanapum seems to be related to the modal amounts of mafic minerals. The general relationship is an increase in colourless glass accompanied by a corresponding decrease in mafic minerals and brown glass. The converse of this relationship is also seen. It is noticeable that the modal proportion of colourless glass in the upper members of the CRBG, the Saddle Mountains and Wanapum, is far higher than that of any of the lower stratigraphic members, Table 6.

Grande Ronde

The Grande Ronde members show variable modal glass proportions. Colourless glass is significantly less abundant than in the higher units, ranging from 2 - 11%. The 11% is an exception, since most of the Grande Ronde thin sections show no colourless glass at all. Those

Table 5.

Sample #	Wanapum unit	BGL	CGL
6900	Roza	6.87	18.87
6908	F. Springs	7.13	18.07
6909	F. Springs	5.27	7.80
6983	F. Springs	3.27	19.47
3AS7	F. Springs	3.40	23.27

Table 5. Modal analysis of glass proportions in the Frenchman Springs (F. Springs) and Roza members of the Wanapum unit of the Columbia River Basalt Group.

Table 6.

Sample #	%BGL	%CGL
Saddle Mountains		
6932a	20.00	20.03
Wanapum		
6900	6.87	10.07
6908	7.13	18.87
6909	5.27	7.81
6983	3.27	19.47
3AS7	3.41	23.27
Grande Ronde		
6911	2.00	11.73
6939b	7.21	2.73
6954	3.67	6.37
Picture Gorge		
6918	7.00	trace
Imnaha		
6945	10.93	trace

Table 6. Comparative modal abundances of brown and colourless glass from the major units within the Columbia River Basalt Group. With the exception of 6911 there is a marked decrease in colourless glass in the units below the Wanapum Member.

that do exhibit this glass phase contain much less, averaging 2 - 4%. The brown glass modal distribution is bimodal, depending on whole rock MgO content. Nathan and Fruchter (1974) divided the Grande Ronde into separate high and low Mg types. Rocks classified as High-Mg Grand Ronde, >6% MgO, show modal abundance of brown glass ranging from 7 - 11%. the low Mg rocks, 4 - 6% MgO, show a lower range of brown glass content, ranging from 2 - 5%.

Both phases are primarily an interstitial component in the groundmass. Again, the brown glass is commonly altered to clay minerals. Apatite and rutile are associated with the colourless glass but are rare due to the diminished content of colourless glass. Brown glass droplets are commonly found in the colourless glass in heavy concentration where colourless glass meets the plagioclase crystals. As the amount of brown glass decreases, the occurrence of the droplet phase in the plagioclase decreases, relatively.

Picture Gorge

Picture Gorge units show entirely different modal abundances of glass phases. In the 16 thin sections described only six showed any sign of colourless glass, modally less than 1%. Correspondingly, there is a lack of the accessory apatite and rutile. Brown glass is less common than in other units, ranging from 3 - 10%. The brown glass in Picture Gorge units is occasionally larger than the phenocryst phases, but usually is an interstitial phase. Again, alteration of the mafic glass is common, with smectite being the major clay mineral present.

Imnaha

The Imnaha units again exhibit the two glass phases with highly variable modal abundances. Colourless glass ranges from trace - 6% and brown glass ranges from 10 - 20%. The brown glass is again highly altered to smectite in the interstitial phase. In the droplet phase the brown glass

is a much lighter colour, tan, and is nearly always isotropic. Meyer and Sigurdsson (1978) similarly describe isotropic smectite-like globules of chlorophaeite in Icelandic basalts. The droplets of brown glass are found in both plagioclase and colourless glass. Due to the diminished occurrence of the colourless glass finding the droplets phase in colourless glass and accessory apatite and rutile is rare.

It is apparent that in most instances the brown glass in these samples is indeed altered to clay minerals such as chlorophaeite or smectite. However, once again, the term brown glass used to describe this material need not be construed as a misnomer. It merely refers to the precursor material that has subsequently been altered to smectite.

CHEMICAL ANALYSIS

Chemical analysis of whole rock and glass samples were obtained using a number of analytical techniques. Major and trace element data for whole rock samples were obtained by X-ray fluorescence and atomic absorbtion methods. Major element data for glass samples were obtained using a SEMQ electron microprobe and the EDATA-2M software programme (Smith and Gold 1979). Some whole rock trace elements and all those reported from glasses were obtained using instrumental neutron activation analysis. More detailed descriptions of analytical techniques accompany data tables in the associated appendices.

A set of whole rock chemical analysis which are representative of the CRBG are given in table 7. Silica values are generally <60%, MgO 3 - 7%, alumina 13 - 16%, combined alkalies 3 - 5%. Enrichment with respect to MORB occurs in total iron, expressed as FeO. In addition, the enrichment in Fe results in a very high Fe/Mg ratio ranging from 0.65 - 0.80 in various units of the CRBG. This phenomenon of enrichment in Fe with corresponding high Fe/Mg ratios, is not confined to the CRBG, but is common to all continental flood basalts (B.V.S.P. 1981).

The glasses within these basalts exhibit an entirely different chemical signature from the parental whole rocks, Table 8. Colourless glasses show high SiO_2 values, 68 - 75%, combined alkalies, Na_2O 2 - 7% and K_2O, 4 - 7%. Conversely, these glasses exhibit low Al_2O_3, 11 - 14%, FeO, 0.8 - 4%, and MgO, 0.4 - 1%, values (Lambert *et al.* 1988 in press). Kuo *et al.* (1988) report similar chemical composition of a granitic glass believed to host an immiscible basaltic component from the Umtanum flow of the Grande Ronde Formation. Even with the extremely low quantities of FeO and MgO in the colourless glass the corresponding Fe/Mg ratio remains high. The brown glasses are considerably more variable than the colourless glasses (Table 9). This is most likely a result of alteration processes affecting the mafic phases in the rocks to a greater extent than other phases. Silica values are very low, 46 - 47%, as is alumina, 3 - 6%, and combined alkalies, <1%.

Table 7.

	Saddle Mtns U.	Saddle Mtns I.H.	Grande Ronde		Picture Gorge		Wanapum		Imnaha	
SiO_2	56.15	49.54	55.86	56.49	49.28	50.07	50.37	50.11	52.31	51.25
Al_2O_3	13.57	13.82	13.56	13.89	16.32	15.27	13.22	13.52	13.47	13.71
Fe_2O_3	2.97	3.88	2.98	2.84	2.78	2.79	3.74	3.79	3.39	3.47
FeO	8.93	11.37	8.94	8.71	8.44	8.43	11.63	11.49	10.26	10.29
MgO	3.02	4.26	3.41	3.31	6.32	7.43	4.43	3.97	4.38	4.75
CaO	6.00	8.90	7.13	6.87	10.95	0.62	8.27	9.00	8.19	8.81
Na_2O	3.02	2.59	3.13	3.28	3.11	2.94	2.76	2.37	3.32	3.26
K_2O	2.72	1.44	2.11	2.06	0.46	0.48	1.14	1.18	1.21	1.08
TiO_2	2.37	3.54	2.16	1.98	1.77	1.47	3.44	3.72	2.81	2.71
MnO	0.19	0.21	0.22	0.19	0.20	0.22	0.23	0.21	0.21	0.21
P_2O_5	0.96	0.39	0.48	0.28	0.36	0.26	0.74	0.59	0.45	0.48
H_2O	-	-	-	-	-	-	-	-	-	-
Total	99.90	99.74	99.98	98.98	99.89	99.99	100.18	99.98	100.00	100.02

Table 7. Representative set of whole rock analyses for the major units of the Columbia River basalt Group. The abbreviations below the Saddle Mountains member U., and I.H. stand for Unatilla, and Ice Harbor respectively.

Table 8.

	6908			6944		
	BGL	CGL	W.R.	BGL	CGL	W.R
SiO_2	46.3	74.4	51.60	49.3	75.4	54.21
Al_2O_3	5.2	14.0	13.69	3.4	13.3	14.03
Fe_2O_3	na	na	3.53	na	na	3.25
FeO	26.6	1.7	10.47	25.4	1.0	9.63
MgO	8.3	0.3	4.52	10.9	0.4	4.37
CaO	2.1	0.4	8.53	10.1	0.2	8.60
Na_2O	0.0	1.8	2.63	1.4	3.4	3.18
K_2O	0.5	6.1	1.36	0.4	5.7	1.12
TiO_2	0.5	0.8	2.87	0.3	0.2	2.75
MnO	0.2	0.0	0.22	0.0	0.0	0.20
P_2O_5	0.0	0.0	0.52	0.0	0.0	0.46
H_2O	10.4	1.5	0.00	8.9	0.0	0.00
Total	99.6	101.5	99.94	100.1	99.6	102.00

Table 8. Representative chemical analysis of whole rock, brown, and colourless glasses for the samples 6908 and 6944.

Table 9.

	AVERAGE BGL	RANGE	AVERAGE CGL	RANGE
SiO_2	46.80	46.00 - 49.30	74.84	72.20 - 76.96
Al_2O_3	3.85	2.20 - 5.20	13.02	11.81 - 14.37
FeO	27.33	25.40 - 30.50	1.31	0.91 - 1.64
MgO	8.68	5.61 - 10.90	0.39	0.32 - 0.48
CaO	1.58	1.40 - 2.10	0.37	0.18 - 0.85
Na_2O	0.33	0.00 - 0.70	2.57	1.84 - 3.48
K_2O	0.35	0.20 - 0.40	6.63	1.70 - 7.43
TiO_2	0.03	0.00 - 0.30	0.77	0.20 - 1.29
MnO	0.27	0.00 - 0.30	na	na
P_2O_5	0.00	0.00 - 0.00	0.04	0.00 - 0.20
H_2O	10.80	8.90 - 13.20	0.00	0.00 - 2.11
Total	100.10		99.90	

Table 9. Average values of the oxides in the two glass phases. The range shows that the brown glass chemistry is somewhat more variable than that of the colourless glass.

na Element not analyzed.

Total FeO values are high, 26 - 30%, and MgO values are moderately high ranging from 3 - 11%, Mafic glasses analyzed by Kuo *et al.* (1988) have SiO_2 contents of 30%, FeO approximately 35 - 47%, and MgO roughly 1 - 3%. Even with the relative enrichment of both FeO and MgO the high Fe/Mg ratio is preserved. The high iron contents of the brown glasses, and to a lesser extent the whole rock iron enrichment trend are easily seen in Figure 3.

CIPW norm calculations of whole rock as well as glass phases of the CRBG data show varying modal abundances of: quartz, albite, anorthite, hypersthene and diopside, (Table 10). The Picture Gorge unit is the only one to show a consistent minor occurrence of normative olivine. Due to the extreme iron enrichment the brown glasses show very high ferrosilite contents, almost 80%. Colourless glasses exhibit lesser amounts of normative hypersthene but never exhibit the co-occurrence of normative diopside common seen in the brown glass. Colourless glasses conversely show very high quartz, 25 - 35%, and albite, 15 - 60%, values. Both glasses in many cases show minor normative corundum contents. Corundum does not occur as a modal mineral in any of the sixty whole rock calculations.

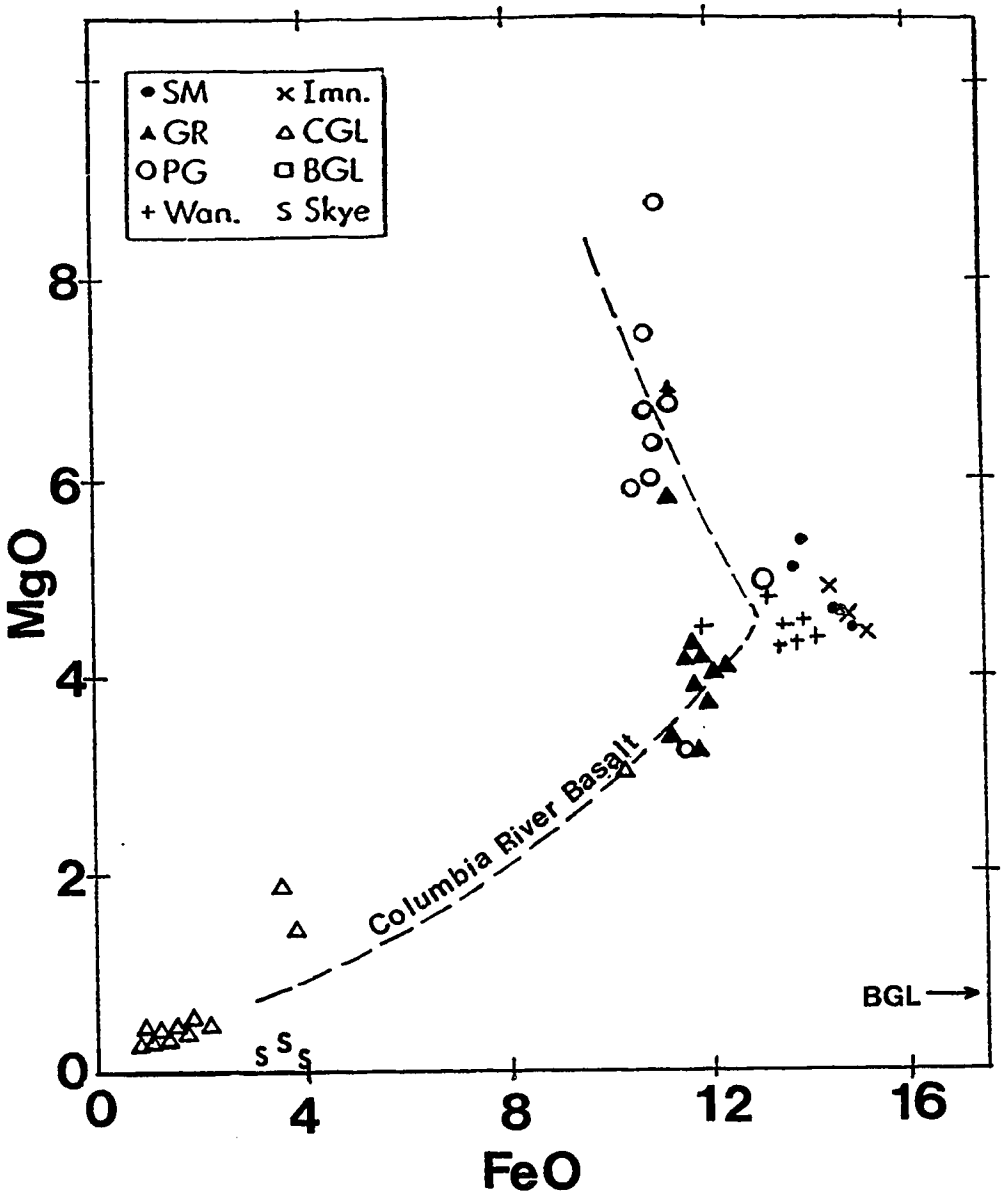

Figure 3. MgO - FeO variation diagram. The majority of points cluster around the magnetite crystallization corner. Explanation of abbreviations: SM = Saddle Mountains, GR = Grande Ronde, PG = Picture Gorge, Wan = Wanapum, Imn = Imnaha, CGL = colourless glass, BGL = Brown glass, and S = Isle of skye granites.

Table 10.

	6908				6944	
	BGL	CGL	W.R.	W.R.	CGL	BGL
Qz	5.84	23.01	5.54	5.13	31.14	5.61
Ap	1.13	0.00	0.00	1.00	0.00	0.00
Il	5.45	2.16	0.00	5.26	0.38	0.00
Or	8.02	28.03	3.54	6.61	34.10	1.18
Alb	22.23	31.36	0.00	26.88	29.40	4.22
An	2.52	6.58	11.89	20.68	1.28	7.23
Cor	0.00	0.00	5.15	0.00	1.40	0.00
Ol	0.00	0.00	0.00	0.00	0.00	0.00
Hy	16.05	7.62	75.75	13.51	2.65	80.29
Diop	14.42	1.06	0.00	15.69	0.00	1.58
Mt	5.12	0.00	0.00	4.68	0.00	0.00
Total	99.78	99.82	101.87	100.36	100.45	99.12

Table 10. Hand calculated CIPW norms (calculations as described by Best 1982) for samples where whole rock, brown glass, and colourless glass data are all available from the same sample. Analyses are reported with all Fe as FeO, no attempt was made to account for Fe_2O_3: this value was entered into the CIPW norm calculation as 0.

MAJOR ELEMENT VARIATION DIAGRAMS

Once formed, the liquids that became the individual units of the CRBG may be acted on by a number of processes. The most likely process is: fractional crystallization with or without contamination or quenching and crystallization with the entrapment of residual liquids. The fractionation model is related to such petrogenetic theories as Cox's (1980) sill model, or Carlson *et al.* (1983), and Carlson's (1984) models of fractionation of mantle material, affected by the addition of crustal material as a contaminant. The alternative process involving cooling and crystallization, without great amounts of fractionation, implies that the composition of the parent magma and the bulk composition of the whole rock units in the stratigraphic sequence are virtually the same. Such a process is consistent with models such as partial melt of eclogite where the highly evolved chemical nature of the rock is determined in the initial derivation of the magma from material other than the typical upper mantle source.

The liquid as erupted, roughly a ferrobasalt, sometimes a ferroandesite in composition, must cool to give the assemblage: clinopyroxene(s), occasional olivine, plagioclase, magnetite and titano-magnetite plus colourless and mafic glass phases, minor apatite and rutile. Major element variation diagrams play a major role in determining which mineral phases interacted with the bulk liquid during the cooling process to produce the present crystalline assemblage.

Chemically, the CRBG are much more evolved than MORB, the standard primary partial melt product of depleted upper mantle. Figure 4 shows the relative positions of the CRBG units on an AFM diagram. Whole rock compositions plot near the compositional deflection caused by the start of magnetite crystallization in tholeiitic differentiation series. Similar evidence on the FeO/FeO+MgO vs SiO_2 variation diagram, Figure 5, which shows that units of the CRBG have increasing Fe/Mg ratios at relatively constant SiO_2 values. The individual CRBG whole rock points do not extend past the magnetite bend seen on the trend line established by rocks from Thingmuli

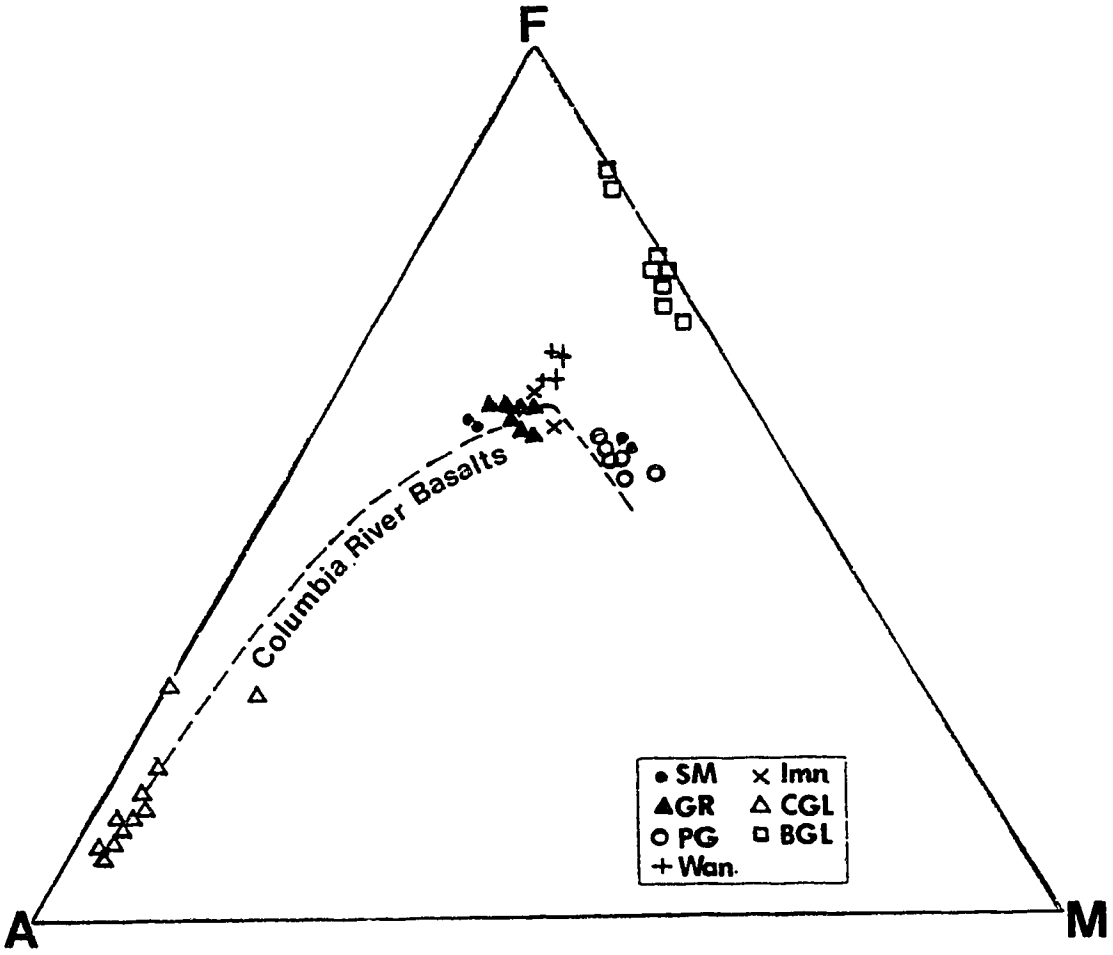

Figure 4. AFM variation diagram. The majority of points cluster around the corner defined by the commencement of magnetite crystallization.CGL points cluster around those of the skye granites. Explanation of abbreviations: SM = Saddle Mountains, GR = Grande Ronde, PG = Picture Gorge, Wan. = Wanapum, Imn. = Imnaha, CGL = colourless glass, and BGL = brown glass.

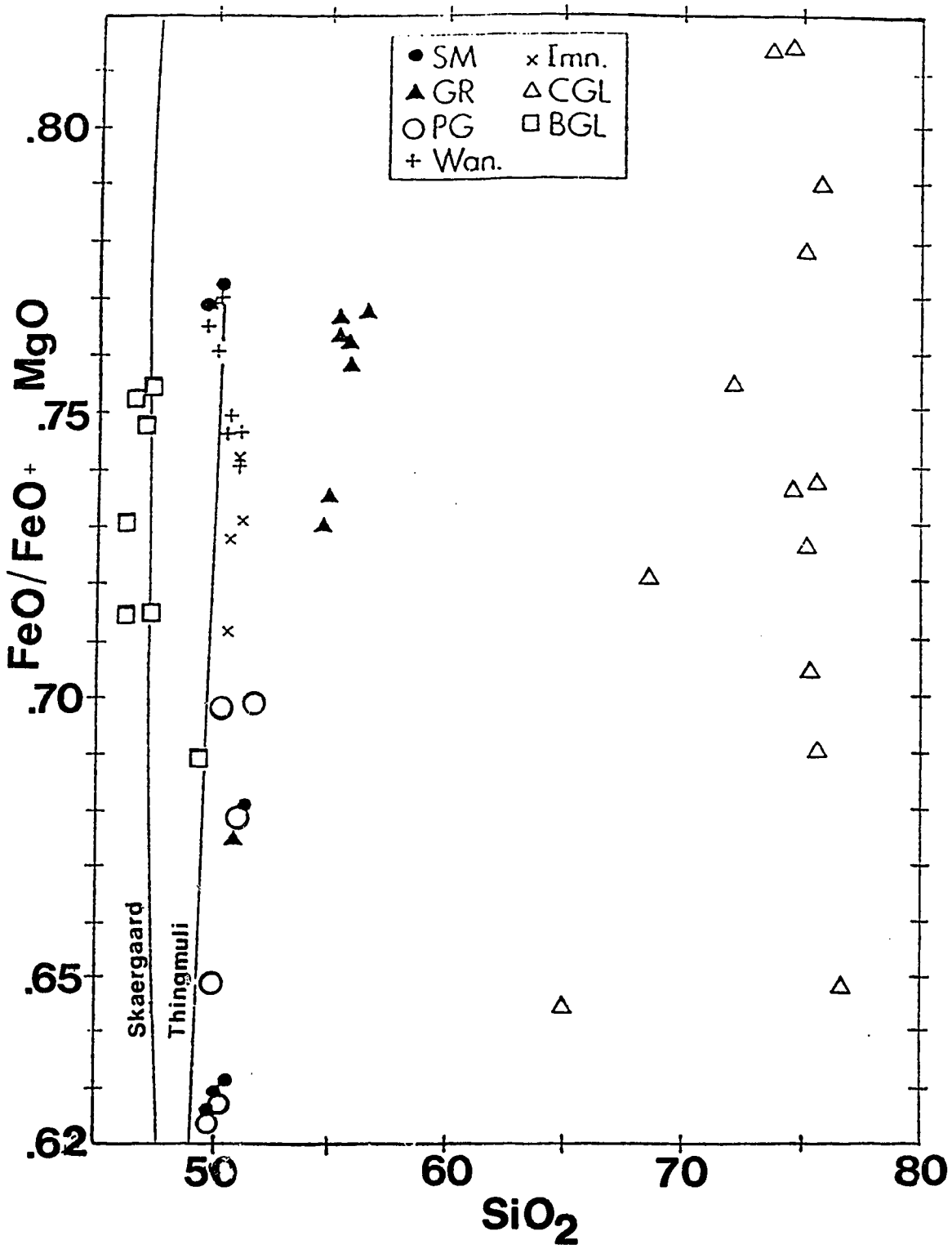

Figure 5. FeO/FeO+MgO vs SiO_2 variation diagram. Thingmuli trend is after Carmichael (1964) and Skaergaard trend is after Wager and Brown (1967). Again CRBG data shows displacement from the Thingmuli trend but mimics it closely. Explanation of abbreviations: SM = Saddle Mountains, GR = Grande Ronde, PG = Picture Gorge, Wan. = Wanapum, Imn. = Imnaha, CGL = colourless glass, and BGL = brown glass.

volcano, Iceland, Carmichael (1964). The extruded Columbia River Magmas were not affected by pre-extrusive magnetite crystallization. Chemically this is supported by the lack of any whole rock plots along the trend lines in locations that require their having been affected by magnetite crystallization. However, CGL points show that magnetite crystallized as a subliquidus phases. This point is further shown physically in the texture of the individual rocks. Although Waters (1961) reports the presence of microphenocrysts of magnetite in the CRBG, this phenomenon has not been found in the body of about 100 thin sections available for this study. The presence of microcrystalline magnetite in a rapidly cooling liquid would indeed be expected if magnetite were a crystallizing phase which affected the subliquidus path of the residual liquid shown in this variation diagram.

When plotted on the ternary plane defined by quartz, albite and orthoclase from the FeO apex (defining the quaternary system) relative groupings of the individual units of CRBG are easily discernable, (Figure 6). Due to the high amounts of iron in these rocks, this variation diagram is useful only to show relative position of individual units as these points are projected down to the base from planes representing 9 - 15% FeO. The diagram shows a general increase in K_2O values, from the very primitive units such as Picture Gorge to the highly derived units similar to the Saddle Mountains, and further yet to the highly derived nature of the residual colourless glasses. This is direct evidence that there is no mineral phase in the CRBG, nor was any ever present, that preferentially removes K from the extruded melt. Chemically this is supported by low K_2O contents in whole rock analysis, 1 - 1.5%, and K enrichment in residual glasses 4 - 7%. This K-enrichment in the colourless glass is represented by the calculated 30 - 40% normative orthoclase.

In a similar fashion P_2O_5 was concentrated in the residual liquid as crystallization occurred, Figure 7. From the plot of FeO/FeO+MgO vs P_2O_5 it is evident that the whole rock composition reached a point where apatite began to crystallize as seen in Wager and Brown's (1967) diagram see Figure 8. Figure 7 also shows that the glasses contained in these basalts have P_2O_5 contents

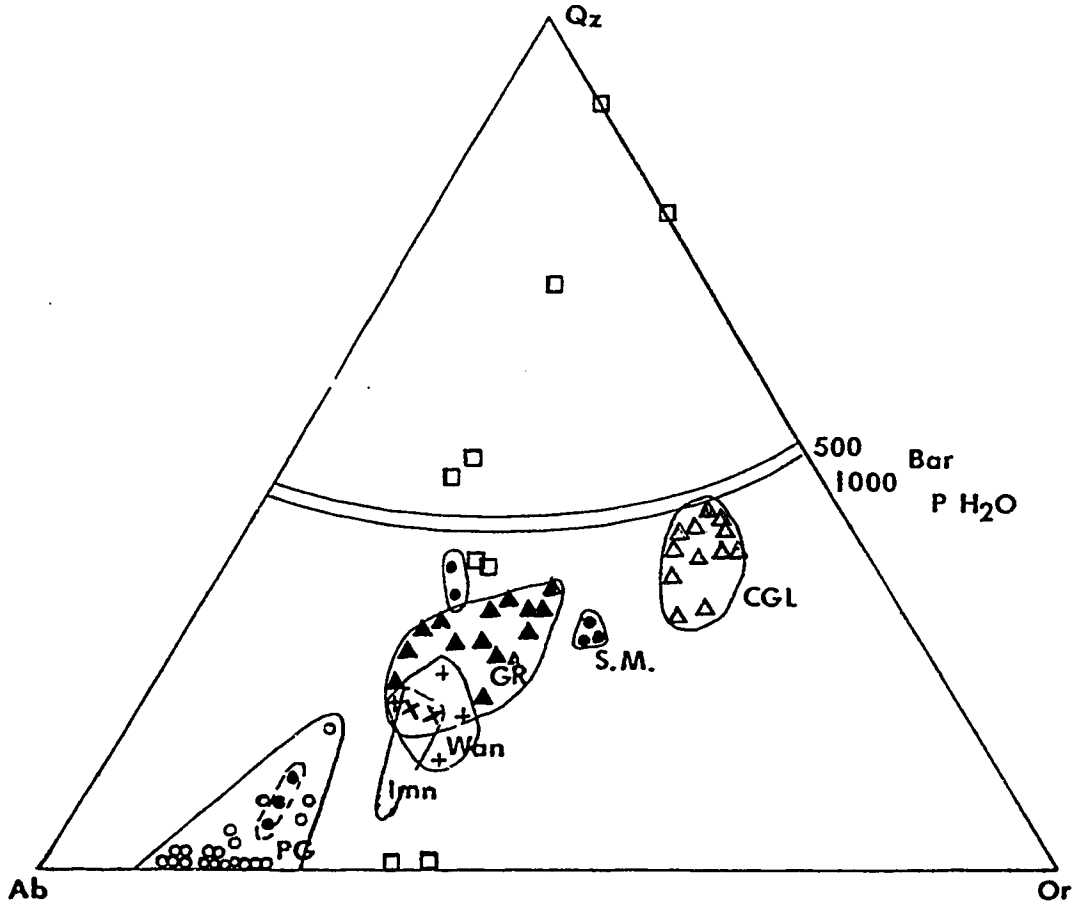

Figure 6. Qz-Ab-Or variation diagram. When plotted down to this plane from Fe-rich compositions relative groupings and separation of the individual units can be seen. The wet melt curves of granite show the proximity of CGL points to that of melted granite.

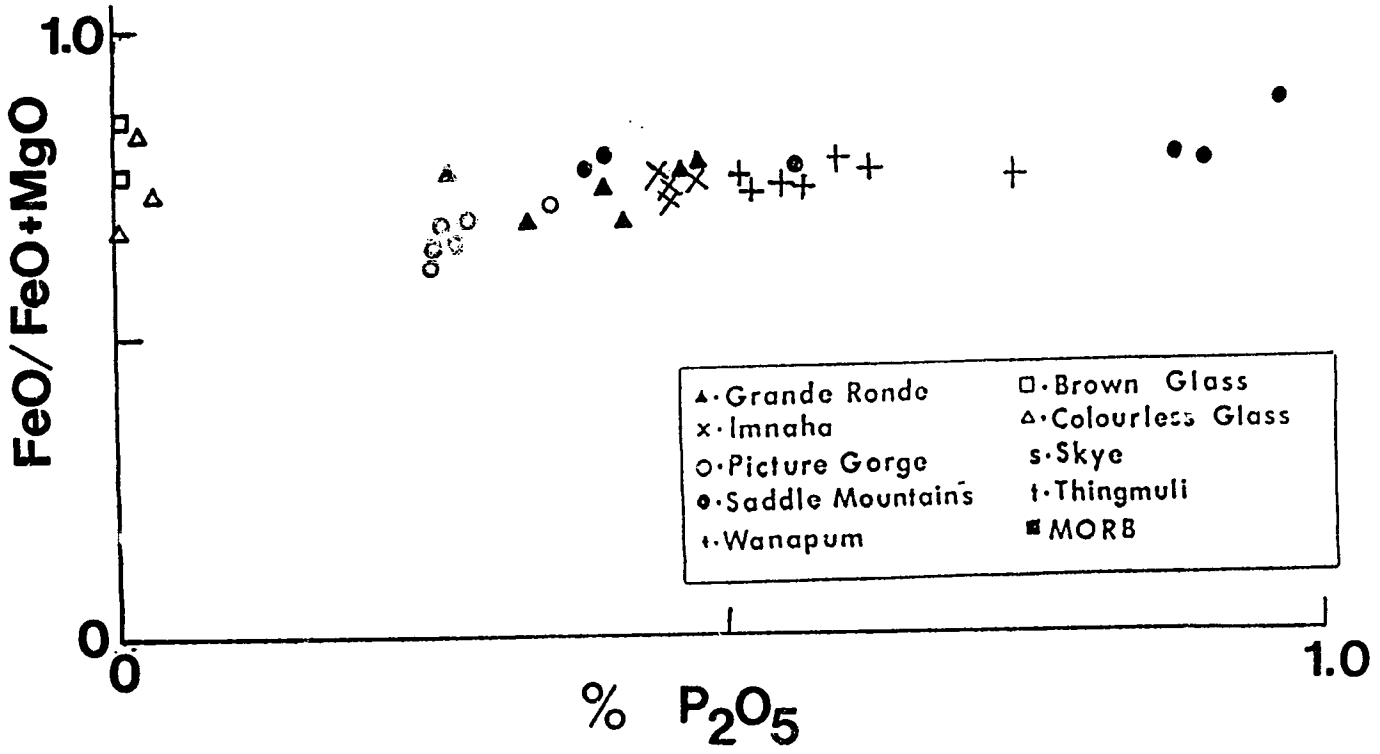

Figure 7. FeO/FeO+MgO vs P_2O_5 variation diagram. Trend shows clearly that apatite had crystallized beforethe glass phases were frozen with their present chemistry. The pronounced drop in P_2O_5 content is a function of apatite crystallization.

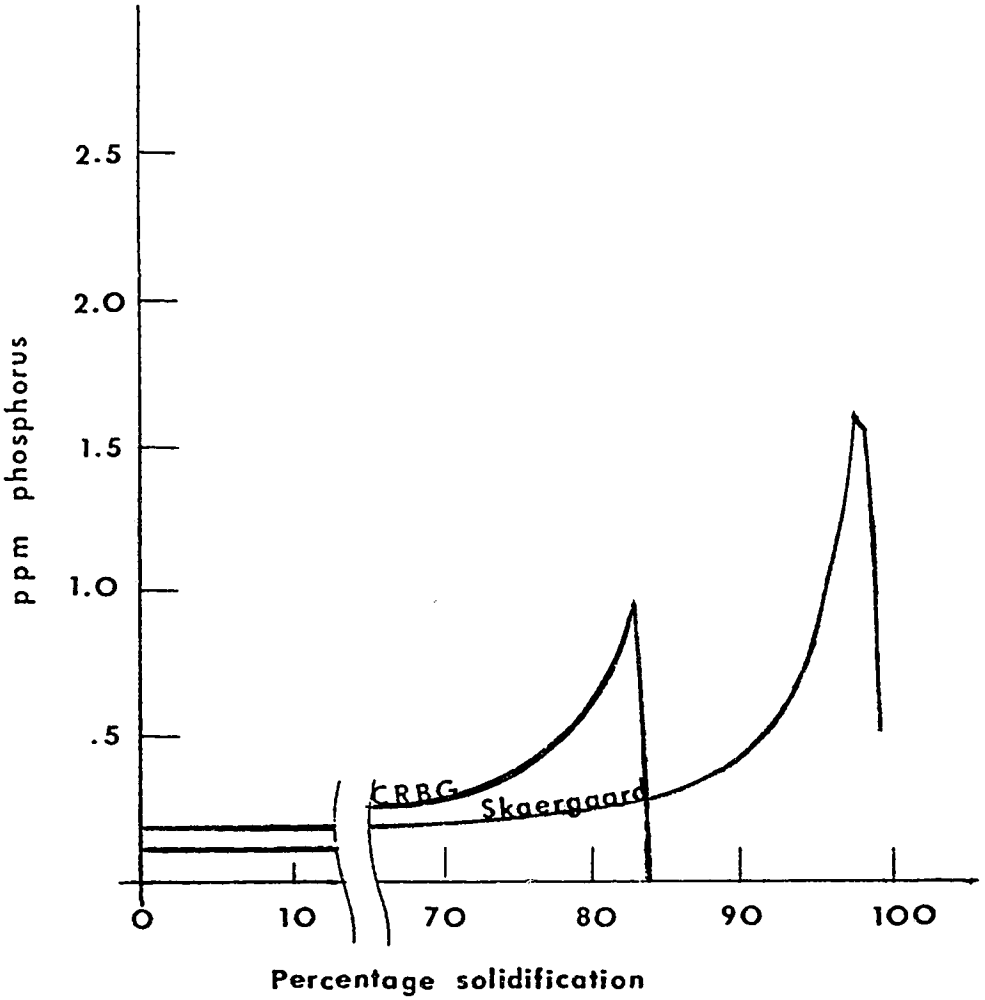

Figure 8. P_2O_5 vs % crystallization diagram after Wager and Brown (1967). The CRBG samples crystallized apatite before the glass phases, which represent roughly 15 - 25 modal percent of the rock composition, hence the rapid drop in P_2O_5 content 10% sooner than in Skaergaard.

below the analytical detection limits. This indicates that apatite crystallization occurred prior to the final cooling event that froze the glasses with their present chemistry.

As will be discussed in greater detail later, this is likely due to rapid cooling: in some cases supercooling may be involved. As initial nucleation of plagioclase is suppressed 20 - 40 degrees below its solidus, the eventual onset of crystal growth is accompanied by extremely rapid cooling and fine grained crystal habit (Gibb 1974). In this manner the fine grained acicular apatite crystals were the final mineral to crystallize from the cooling magma before solidification froze the present mineral/glass assemblage into the rocks as seen today.

Using modal analysis of individual Wanapum rocks (and assuming that apatite was the last mineral phase to crystallize) it is apparent that apatite crystallization occurred at a point when roughly 70 - 75% of the liquid had crystallized. This corresponds to the modal abundance of the two glasses ranging from 25 - 30% in Wanapum units and is also based on the assumtion that the brown mafic material is, or was, at one time glass. If BGL is not an altered magma. glass, then apatite crystallization occurs roughly 5 - 10% later, corresponding to approximately 80% solidification of the magma.

The remaining phases that are available to control bulk chemistry as the flow cools are pyroxene, olivine, and plagioclase. Figure 3, the MgO/FeO variation diagram, would suggest that the trend of the bulk liquid as it cools is controlled by pyroxene. At a large stage an iron rich material begins to crystallize, which could be magnetite or fayalitic olivine. We know that olivines in these basalts are fayalitic in composition: therefore olivine interfacing or crystallization can only affect the later stages of the system as it cools. This does not imply that olivine interfacing did not play a major role in controlling the remaining bulk liquid as the system cooled.

Figure 9 shows the various locations of mineral and glass phases as well as whole rock

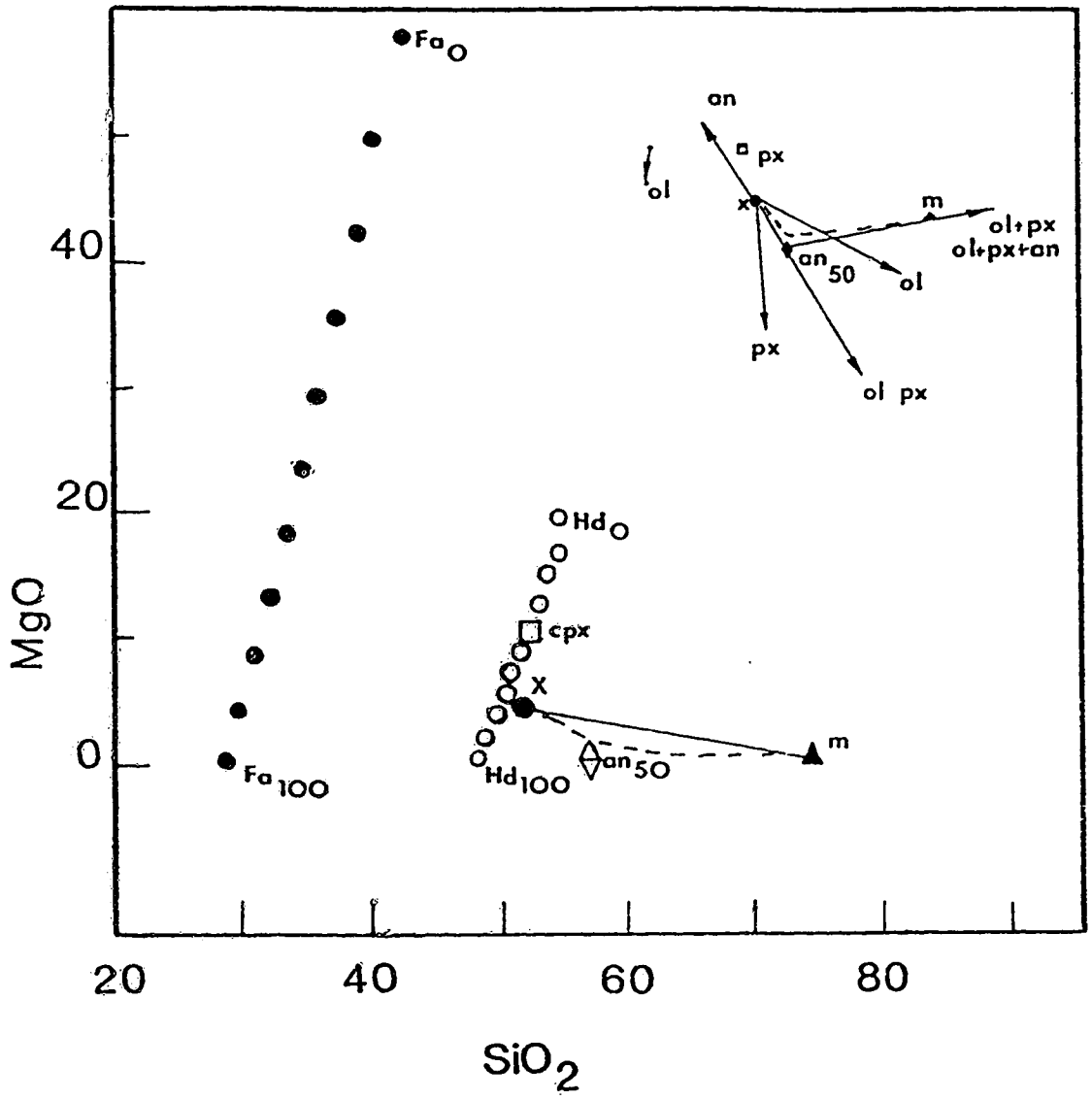

Figure 9. MgO-SiO_2 variation diagram. Compositions of the major minerals in the CRBG are shown. Dashed line is a possible path of liquid composition from bulk composition to the residuum MWGM (m). The inset shows a possible crystallization sequence that would produce the shift from bulk (X) to MWGM (m). Initial crystallization of olivine and pyroxene drives the composition towards that of andesine, whose subsequent crystallization drives the remaining liquid towards m. Due to ranges of compositions in the flows of olivine and plagioclase this is likely an oversimplification of the actual process.

compositions on a MgO-SiO_2 variation diagram. In addition the various members of the olivine series and diopside-hedenbergite series are plotted. The extreme proximity of the whole rock composition to that of the Hd_{70} member of the pyroxene series makes it unlikely that crystallization of average CRBG pyroxene (Hd_{40} - Hd_{45}) alone caused the residual liquid's path to deflect to the point m (MWGM). Mean Wanapum Glass Mixture is an attempt to recreate the composition of the final liquid in this system by mixing the compositions of CGL and BGL in a ratio of 3:1 CGL:BGL (see appendix 3). The result, in the two axis system MgO-SiO_2, of removing pyroxene will push the residual liquid's path well below m (MWGM). Similar arguments may be applied to the sole crystallization of olivine (average CRBG olivine is Fo_{70}), or a combination of olivine and pyroxene. The removal of plagioclase (An_{50}) will cause large increases on the MgO axis while SiO_2 remains relatively unaffected. This process alone is also incapable of deflecting the path of the residual liquid from its bulk composition (X) to m (MWGM). It can therefore be shown that the major process controlling the path of the cooling liquid was the crystallization of olivine (Fo_{70} - Fo_{80}) associated with clinopyroxene (Hd_{40} - Hd_{45}). The onset of andesine crystallization will serve to deflect the trend of the residual liquid's path flattening the descent on the MgO axis while simultaneously increasing SiO_2 content towards the point m (MWGM), as shown in the inset in Figure 9.

Another variation diagram that shows the extent of olivine fractionation is Ab+Or/Ab+Or+An vs FeO+Fe_2O_3+MnO/ FeO+Fe_2O_3+MnO+MgO, Figure 10. This diagram shows the effect of two simultaneous fractionating trends. To discuss this diagram in detail some nomenclature must first be clarified.

Water and Brown (1967) in a discussion of the Skaergaard layered intrusion uses the terminology lower, middle, and upper zones and finally the upper border group to describe the broad divisions of this intrusion. These groups are abbreviated LZ, MZ, UZ, and UBG respectively. Earlier, Wager (1956) uses arbitrarily defined lines based on the fractionation of a

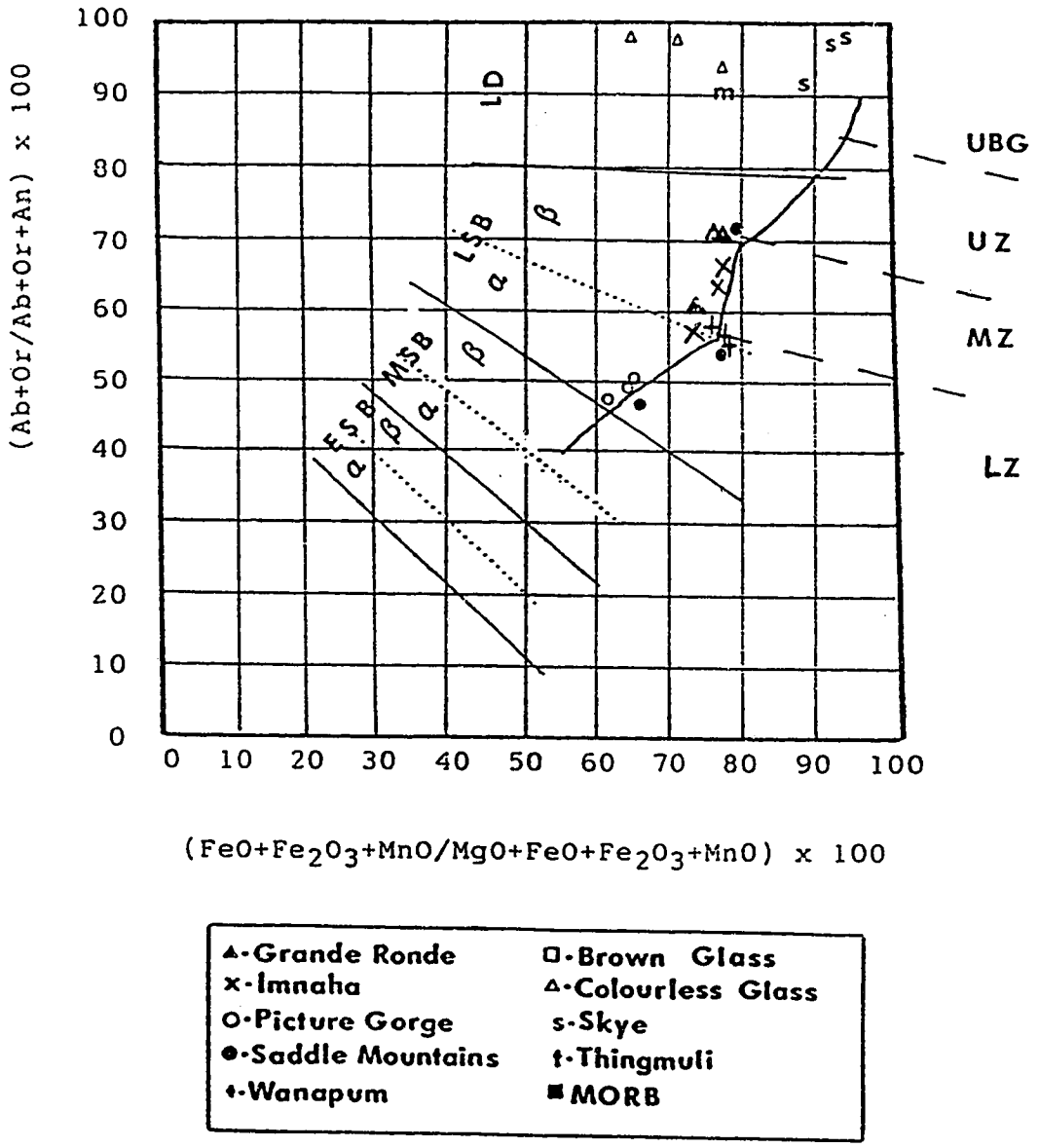

Figure 10. Ab+Or/Ab+Or+An vs. $FeO+Fe_2O_3+MnO/FeO+Fe_2O_3+MnO+MgO$ variation diagram. The trend line from Thingmuli is from Carmichael (1964), the divisions along the line represent divisions in the Skaergaard and are from Wager and Brown (1967). Most CRBG rocks plot along the kink in the Thingmuli trend, within the middle zone, MZ, defined as the olivine gap in the Skaergaard.

basaltic liquid to subdivide the sequence. In this nomenclature the divisions are early, middle, and late stages and finally late differentiates. These subdivision are abbreviated ESB, MSB, LSB, and LD respectively. Additionally, each of these units are further subdivided into alpha, early, and beta, late stages. There is no correlation between the corresponding stages in the two types of nomenclature. These divisions are seen in Figure 10 which is modified after Carmichael (1964) to include CRBG data from this study. In Figure 10 the trend line of Thingmuli is also shown. It is therefore necessary to determine where this unit plots with respect to the original and current zones defined for the Skaergaard if the three units are to be compared. Samples 1 - 3 from Thingmuli contain olivine and labradorite, (Carmichael 1964). This corresponds to LZ compositions of Wager and Brown (1967). Samples 4 - 10 from Thingmuli contain no olivine and labradorite, (Carmichael 1964), which corresponds to the MZ, olivine gap, in the Skaergaard, (Wager and Brown 1967). Samples 16 - 24 from Thingmuli contain fayalitic olivine and andesine, and are generally rhyolitic in composition, (Carmichael 1964). Wager and Brown (1967) defines the beginning of UZ with the first occurrence of fayalitic olivine. Plagioclase compositions from UZ(c) (Wager and Brown 1967) best corresponds to LD rocks from Wager's (1956) earlier data.

With a common reference between the two units in Figure 10, comparison can now be drawn with the CRBG. The division in the various stratigraphic units can be clearly seen. Picture Gorge units plot along the early trend MSB (Wager 1956, Carmichael 1964), more accurately LZ, (Wager and Brown 1967). LZ rocks contain olivine in the Skaergaard, similarly, higher modal percentages of olivine occur in Picture Gorge units of the CRBG, 5 - 10%. The bulk of the CRBG units plot in the area defined as LSB, (Carmichael 1964, Wager 1956), or MZ, (Wager and Brown 1967), corresponding to the olivine gap in the Skaergaard. Physically this is shown by the general lack of olivine in CRBG units. This zone is the pronounced kink in the trend on the variation diagram.

The kink in this trend can be attributed to a sudden increase in the Ab+Or/Ab+Or+An

ratio, as a result of a sudden increase in the plagioclase fraction. The other possibility is the cessation of a crystallizing phase that concentrates Fe in the melt, or the crystallization of a phase that will preferentially remove Fe from the melt.

Given that this kink is surrounded by the lines defining MZ (Wager and Brown 1967) the most likely cause is the cessation of olivine as a crystallizing phase. This is supported by the general lack of olivine phenocrysts in most
units of the CRBG. Carmichael (1964) attributes this kink in the Thingmuli series to the beginning of magnetite fractionation. Evidence from this phase diagram suggests that the extent of magnetite crystallization as a pre-extrusive process was not extensive in the case of the CRBG.

Once past the kink in the LD zone (Carmichael 1964, Wager 1956) or UZ (Wager and Brown 1967), the trend continues along a similar path as in the LZ. The lack of CRBG points in this part of the trend line was reached.

Another significant observation that can be made from major element variation diagrams is in the process that forms the CRBG. Figure 11, the AFM diagram and Figure 12 the MgO-FeO diagram are both expanded to include the trend of Thingmuli and late stage differentiation products such as Skye Granites. An interesting similarity arises in the similar yet displaced trends of the two systems. This suggests that the process of formation is similar, but that the original bulk material differs.

There is a strong similarity between the colourless glasses in the CRBG and the granites of Skye (Thompson 1969, Dickin 1981) and a series of fractionated liquids from Thingmuli (Carmichael 1964). This similarity to classic fractionating trends poses a petrogenetic problem with the CRBG in that there is no evidence of fractionation occurring as a post eruptive event. Minerals are distributed evenly throughout flows, with no evidence of cumulate mineral phases or

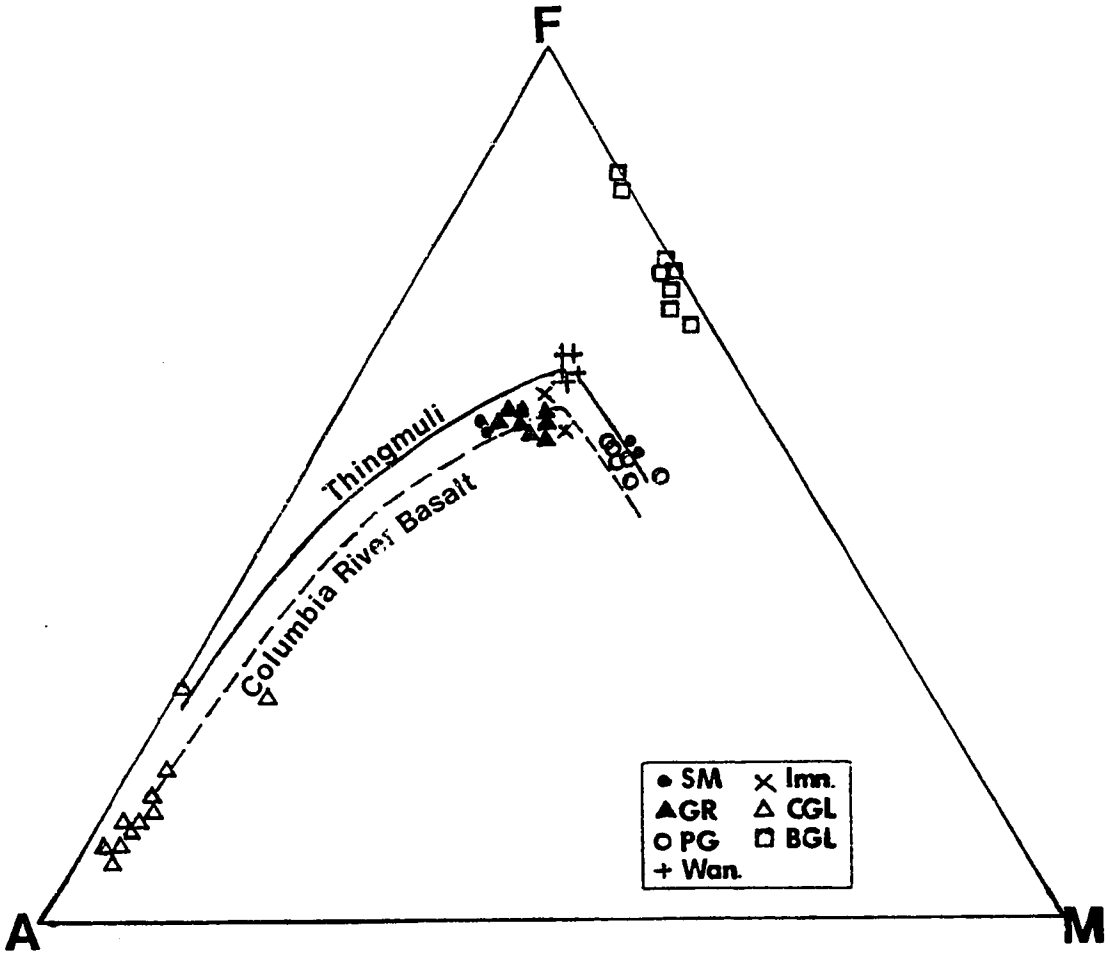

Figure 11. AFM variation diagram replotted to include a trend line from Thingmuli. The trends of the two lines are identical, but displaced, an indication of similar process.

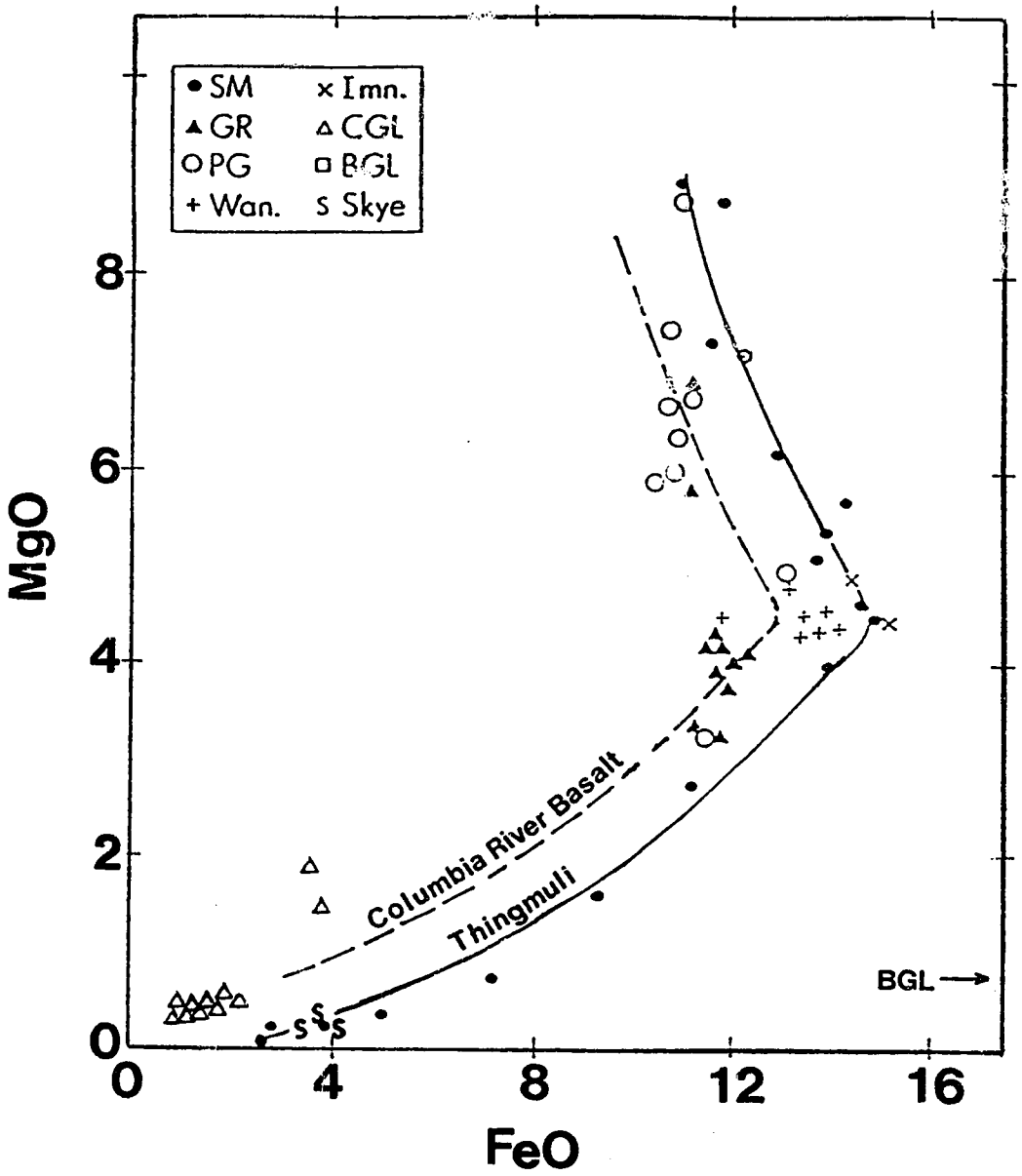

Figure 12. MgO - FeO variation diagram replotted to include Thingmuli trend line, again the two lines are similar yet displaced indicating similar process.

any layering. The production of the glass phases is therefore not due to fractional crystallization as a post eruptive event, but is a result of crystallization removing material from the bulk melt producing less refractory residual liquids which are finally frozen as glasses.

TRACE ELEMENT VARIATION DIAGRAMS

Trace element geochemistry is used to determine processes which affected pre-extrusion, bulk magma formation. Data concerning trace element abundances of CRBG glasses are not available, and hence cannot be used to support processes proposed using major element data. Trace element data also establish that the CRBG units are fractionated with respect to the MORB composition. The results of fractionation are clearly seen, with CRBG units being strongly enriched in both LIL and HFS elements. A major problem posed by the model involving fractionation is the observed sequence of the units. Ideally, the order of occurrence should be; Imnaha, Picture Gorge, Grande Ronde, Wanapum, and finally Saddle Mountains. The Saddle Mountains units should evolve in the following order; Umatilla, Pomona, and lastly, Ice Harbor. This is the expected order of occurrence if the CRBG was produced by a single large fractionating magma unit that periodically extruded the various flows that comprise this flood basalt province. The older, lower stratigraphic units should appear in a more primitive form than the later units as a result of lesser amounts of fractionation. None of the trace element variation diagrams show this ideal ordering of the units. Almost uniformly, the Picture Gorge unit is the least evolved composition, Wanapum and Grande Ronde chemistry is nearly reversed, and Saddle Mountains units are extremely variable, ranging from primitive to very highly fractionated.

At first glance olivine interfacing seems to be the predominant factor in producing whole rock chemistry. The variation diagram MgO-Ni, Figure 13, shows decreases in both Mg and Ni in the CRBG with respect to MORB. This is a result of both elements preferentially moving into the olivine structure, thereby depleting the liquid in these elements as olivine is removed. This evidence is mirrored in the SiO_2-Ni variation diagram, Figure 14. Conversely to MgO, SiO_2 is preferentially enriched at a ratio of 2:1 in the remaining liquid as a result of olivine removal. The observed trend of decreasing SiO_2, accompanied by decreasing MgO and Ni is an indication of olivine interfacing.

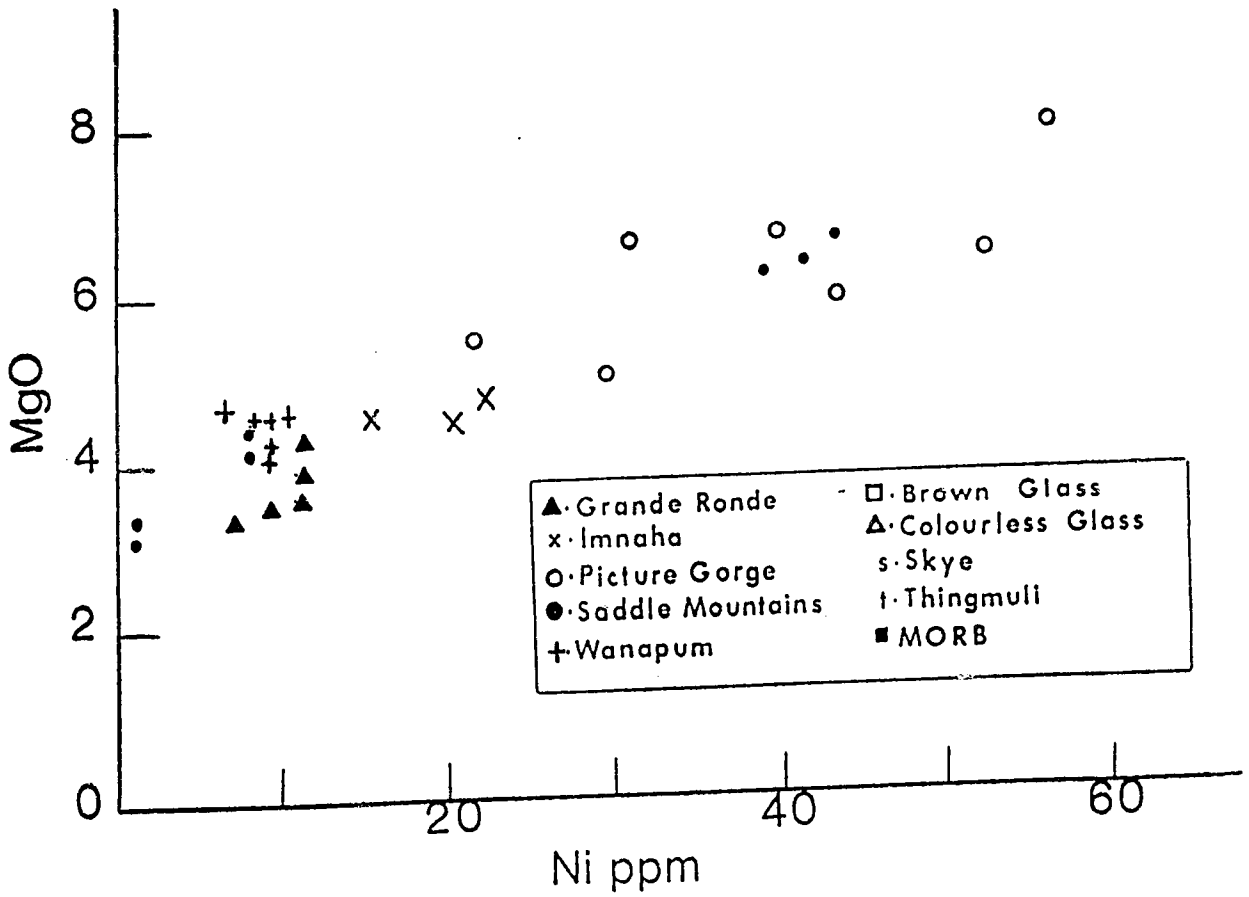

Figure 13. MgO-Ni variation diagram. Increasing Mg and Ni contents are indicative of olivine fractionation having occurred in the system.

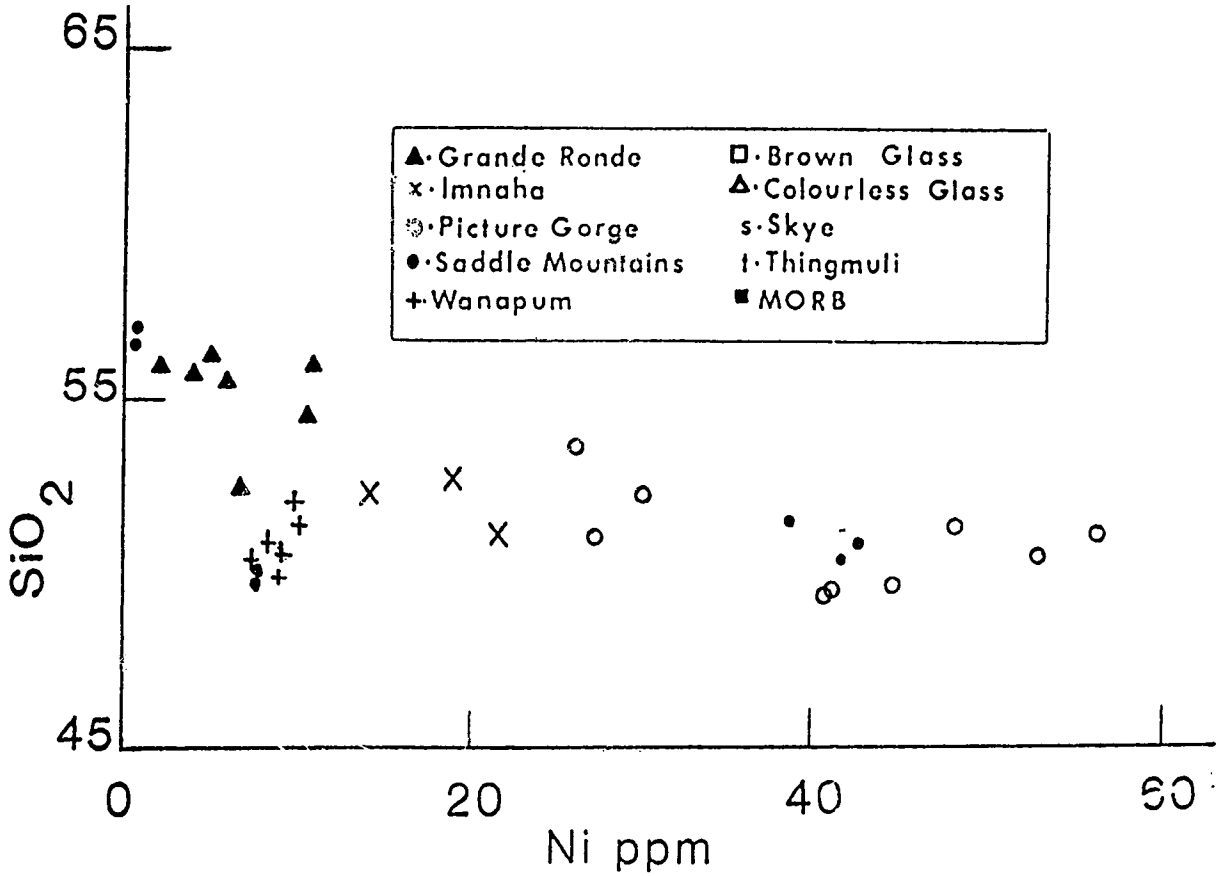

Figure 14. SiO_2-Ni variation diagram. Decreasing Si and increasing Ni are again indicative of olivine fractionation.

The lack of any large scale effects on pre-extrusion bulk chemistry by the removal of a pyroxene phase are again evident in the FeO-Zn variation diagram, Figure 15. Fe and Zn are controlled by pyroxene chemistry in the crystallizing melt (Rankama and Sahama 1966, Vlasov 1966). The pyroxene structure incorporates both Fe and Zn in roughly constant proportions. Interfacing of pyroxene with the melt will produce a trend marked by a general decrease in both FeO and Zn. As is clearly seen in Figure 15 this is not happening in the CRBG. Zn is being enriched in the remaining liquid by the mineral/melt interface, a strong indication that pyroxene was not the primary mineral phase interfacing with the original bulk material. Plagioclase controlled major element variation diagrams indicate at first that interfacing of this phase is likely. Data from B.V.S.P. (1981) and Hooper *et al.* (1984) show no evidence of a negative Eu anomaly in any of the whole rock data which is strongly indicative of there having been no large-scale plagioclase removal. Similarly, examining the behaviour of K_2O vs Rb, and K_2O vs Ba it is immediately apparent that the interfacing phase has enriched the melt in all of these large incompatible elements. (Figures 16 and 17) The predominant plagioclase phase in the CRBG is andesine/labradorite (Waters 1961, Schmincke 1967, Hoffer 1980). There are very few suitable substitution sites available for K, Rb, and Ba in the plagioclase structure based on Goldschmidt's rules (Goldschmidt 1937, Henderson 1982). Smaller, more highly charged ions such as Ca, Na, and Sr will compete more successfully for the plagioclase sites. K, Rb, and Ba will preferentially move into the K-feldspar lattice. However, no K-feldspar is present in the CRBG but there is 30% normative orthoclase contained in the colourless glasses. It is therefore very likely that the K, Rb, and Ba reside in the colourless glass phase. The occurrence of K in the colourless glass is clearly demonstrated in the 6 -7% modal K_2O content of the colourless glasses. Data obtained from instrumental neutron activation analysis indicates that Ba and Rb contents in the colourless glass are enriched by a factor of 2 - 5 with respect to the whole rock analysis. This trend can be associated with plagioclase removal. However, it also can be attributed to the removal of olivine or clinopyroxene.

The opposite trend is not readily observed when elements that are preferentially enriched

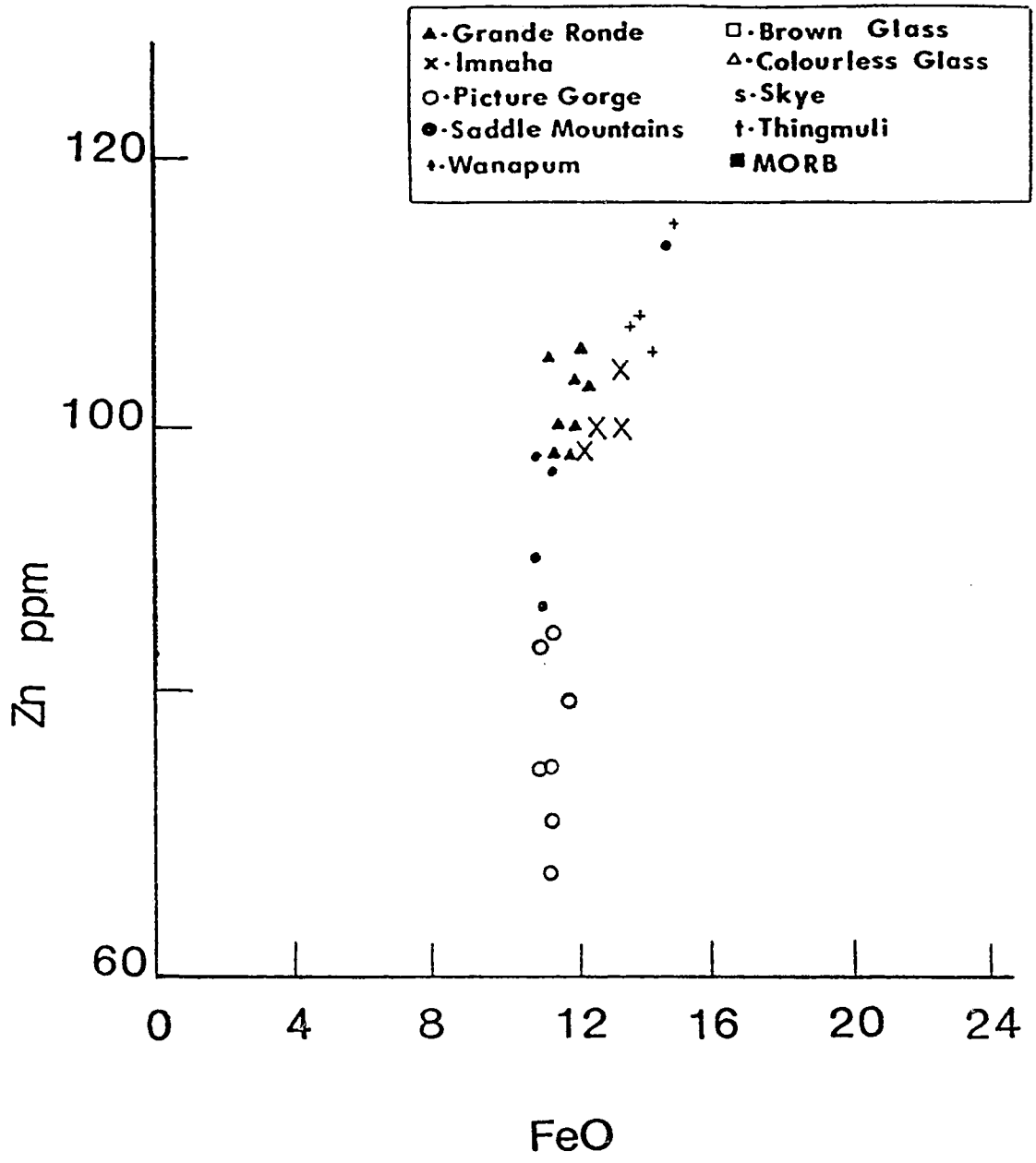

Figure 15. FeO - Zn variation diagram. Relatively constant Fe content with rapidly rising Zn content indicates that pyroxene removal has not greatly affected this system.

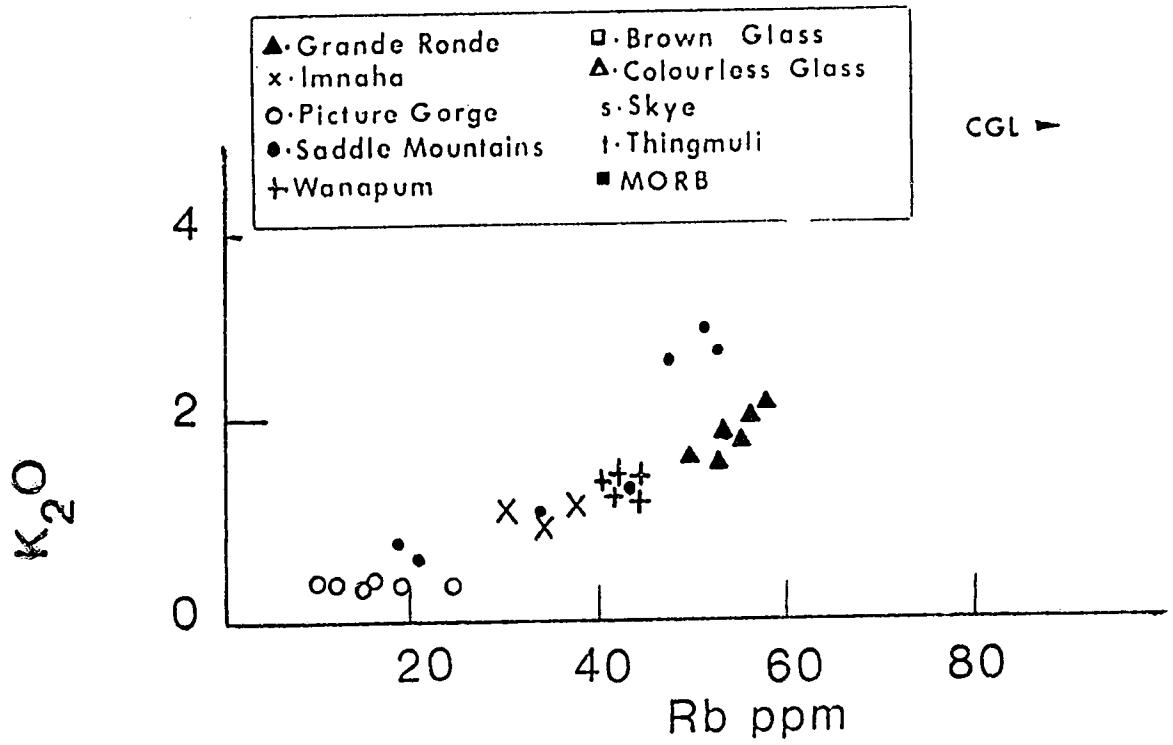

Figure 16. K_2O-Rb variation diagram. Increasing K and Rb again indicate that K-feldspar was not removed from this system.

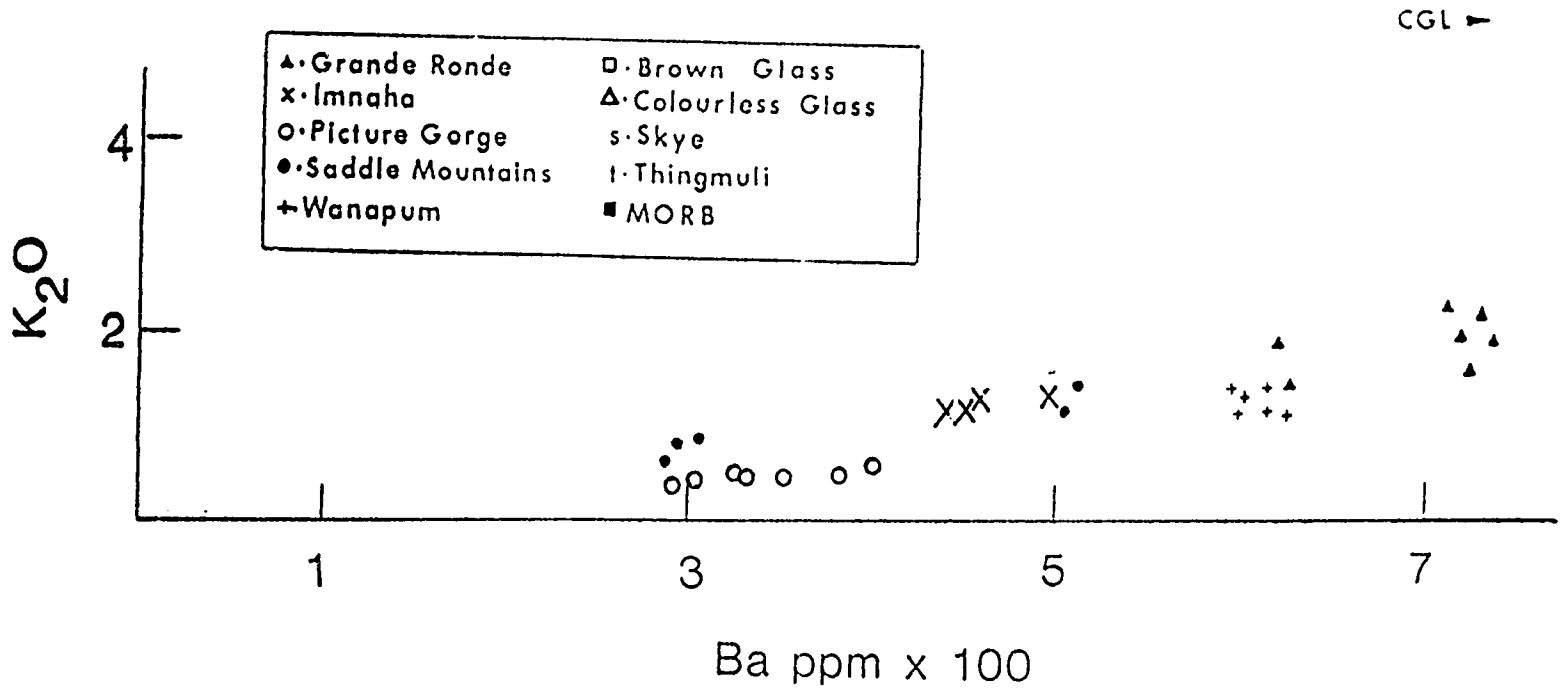

Figure 17. K_2O-Ba variation diagram. Increasing K and Ba again indicate that K-feldspar was not removed from this system.

in plagioclase are examined. The Sr - Rb diagram (Figure 18) does not show the expected negative correlation. Sr contents should decrease as plagioclase is removed, while Rb contents, ignored should be increased. Similarly the variation diagram CaO vs Sr, Figure 19, does not show the expected trend of mutually decreasing Ca and Sr that would be expected if plagioclase interfacing had occurred, and further suggests that the enrichment of K, Rb, and Ba is a result of olivine or clinopyroxene removal. These data may also indicate a late stage crustal contamination process.

The plagioclase related information also serves to shed light on another problem associated with the CRBG. Crustal contamination by a granitic host rock or sedimentary unit should be readily discernable in Sr, Rb, Ba trace element geochemistry. These large ion lithophile elements are all enriched in the continental crust and sediments with respect to the mantle and mantle derived products. Granites range in abundances of Sr (75 - 213 ppm), Rb (100 - 488 ppm), and Ba (260 - 705 ppm) (Glikson 1976, Pearce el al. 1984). Basalt values are much less, with values ranging from typical MORB; Sr (150 ppm), Rb (2.3 - 75 ppm), Ba (70 - 200 ppm) (B.V.S.P.). (1981), Hess and Poldervaart 1967). Therefore, if crustal contamination has occurred there should be a corresponding increase in these elements. Highly variable values for flood basalts from B.V.S.P. (1981) Sr (2 - 50 ppm), Rb (254 - 385 ppm), and Ba (1800 - 3000 ppm) from the CRBG are somewhat inconsistent with data from this study Sr (190 - 370 ppm), Rb (10 - 70 ppm) and Ba (230 - 3600 ppm). Excluding Saddle Mountains Ba contents for the remainder of the CRBG units range from 230 - 850 ppm. The small enrichment of incompatible elements in the flood basalts may be an indicator of late stage contamination of the liquid by a crustal component, but seem to indicate that the amount of contamination was small.

The final phases in the CRBG that may interface with the melt are the opaque phases, magnetite, titano-magnetite, and ilmenite. The variation diagram Y vs Zr (Figure 20) shows a strong positive correlation, indicating concentration of both these elements during melt evolution. Zr is found commonly in magnetite structures so magnetite removal should deplete the remaining

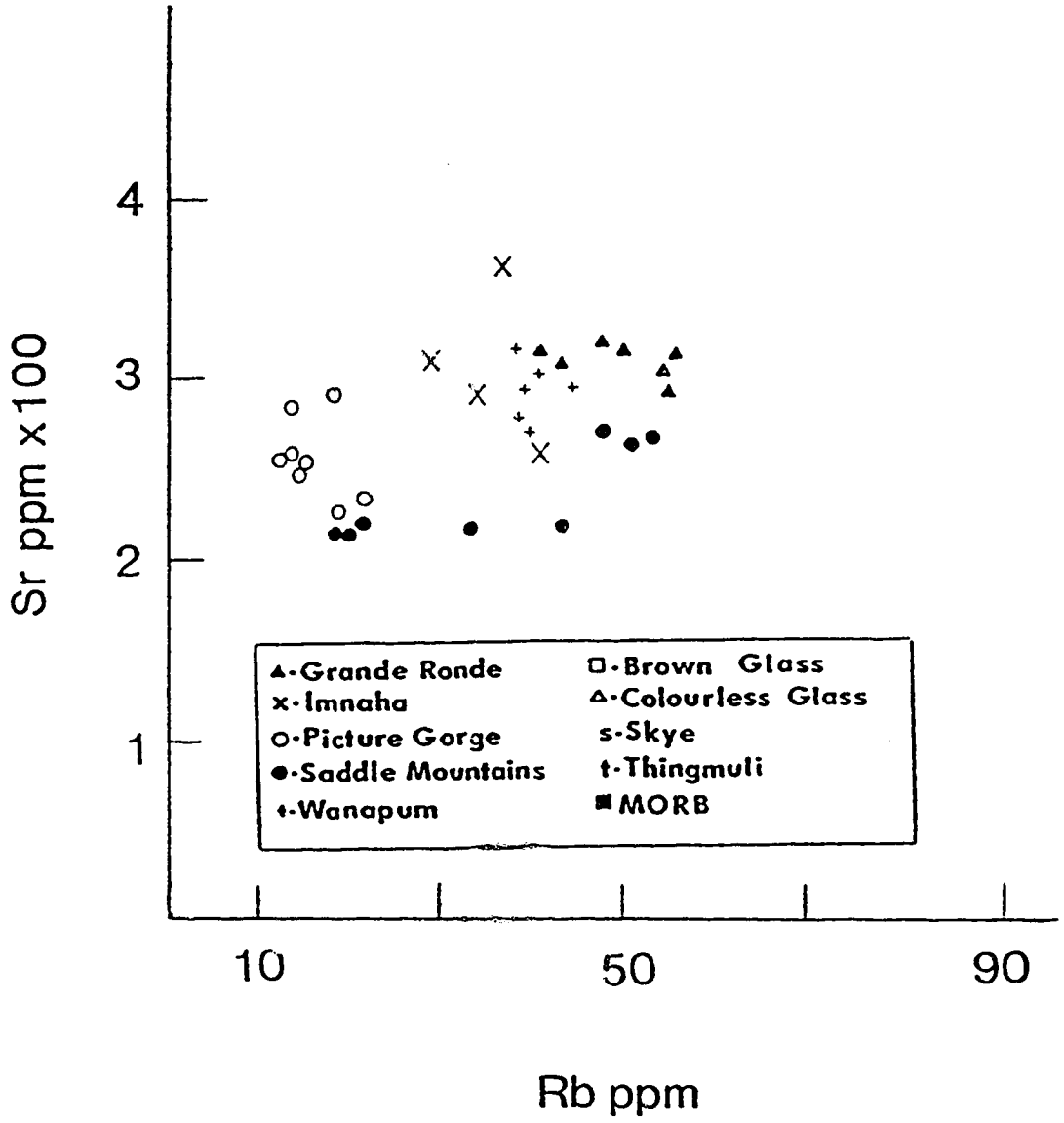

Figure 18. Sr vs Rb variation diagram. The expected trend of increasing Rb with decreasing Sr associated with plagioclase removal is not evident in this system.

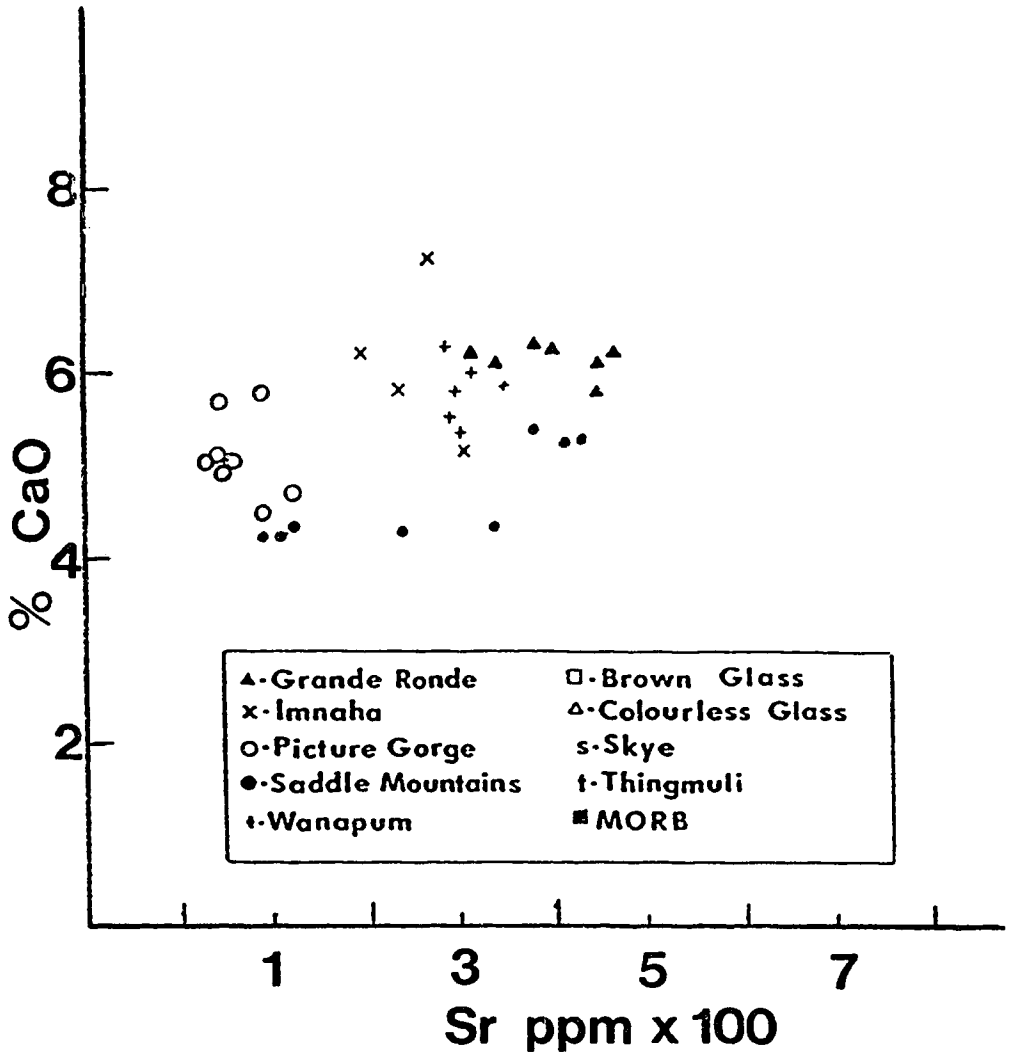

Figure 19. CaO vs Sr variation diagram. The expected increase in both CaO and Sr associated with plagioclase removal are not evident in this diagram.

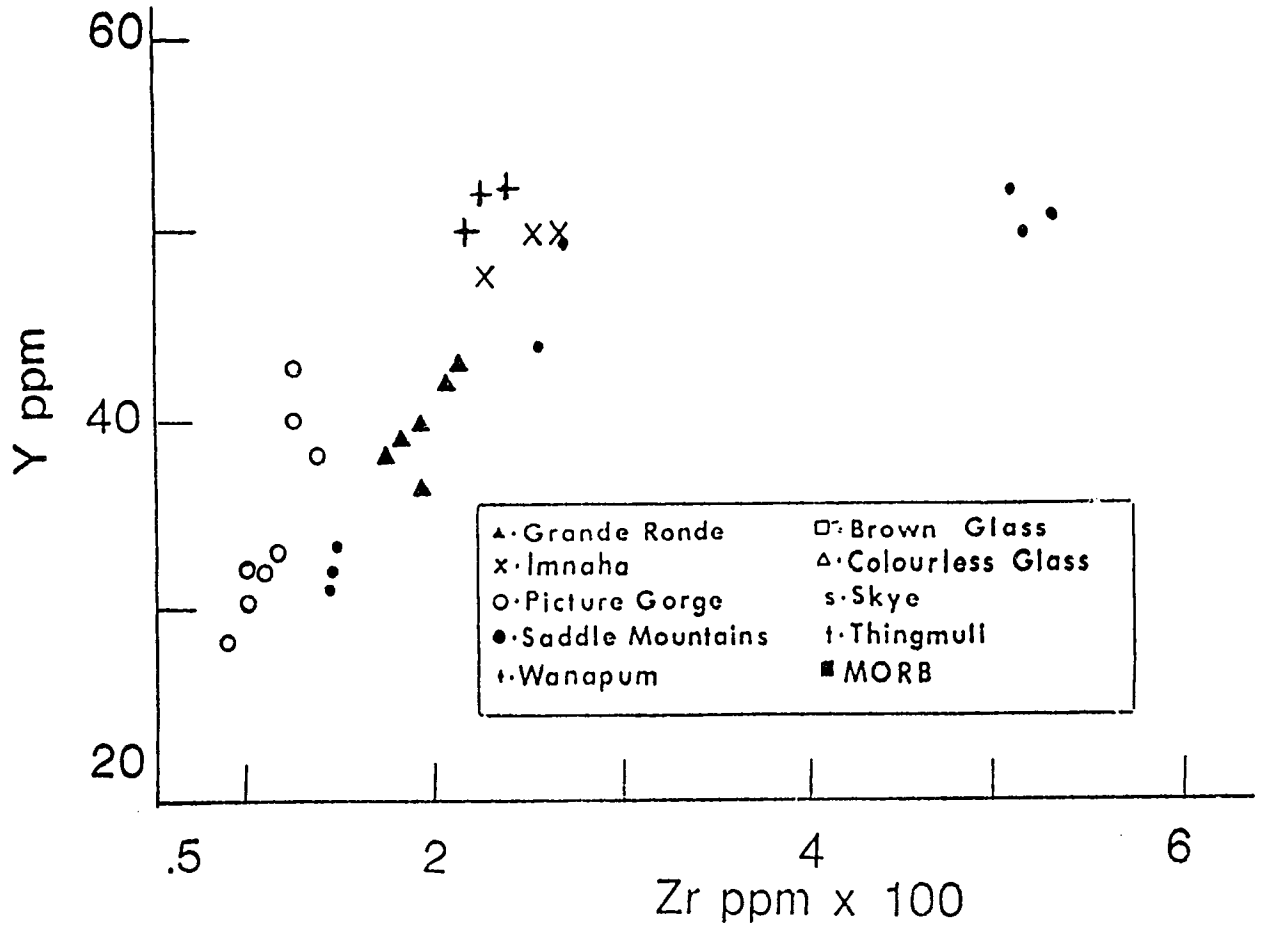

Figure 20. Y-Zr variation diagram.The enrichment of Zr in the residual melt is evidence that magnetite removal did not affect this system.

liquid in Zr. The lack of Zr depletion, when coupled with FeO major element data, strongly supports the lack of any magnetite/melt interfacing with pre-erupted liquids.

Trace element geochemistry reconfirms that an olivine/melt interface was the controlling influence on the generation of the CRBG. The evidence also suggests that some amounts of plagioclase interfacing may have occurred. Pyroxene removal, viewed on the basis of major element variation diagrams, has occurred as a post-eruptive process. However, trace element variation diagrams indicate that pyroxene interfacing was not a major process involved with pre-eruptive bulk liquid formation as none of the expected enrichments or depletions associated with pyroxene removal are evidence in the whole rock chemistry. Finally, trace element data does not suggest an active role of magnetite interfacing in CRBG magma genesis.

GENERAL LIQUID IMMISCIBILITY

One perplexing problem concerning the glass phases in the CRBG is a suitable explanation of the textural relationships between glasses, plates 6 and 7. This apparent suspension of brown glass in a matrix of colourless glass is suggestive of an immiscible relationship existing between the two phases. The existence of immiscible liquids in basalts of both lunar and terrestrial origin is well documented in the literature (Greig 1927, Roedder 1951, Dixon and Rutherford 1977, Philpotts 1979, 1982, Kuo *et al.* 1988). Hess (1980) describes the typical composition of immiscible liquids as being: granitic, containing normative quartz and feldspar on the one hand, and ferrobasaltic with high amounts of normative pyroxene on the other. These compositions are very similar to those calculated for the CRBG glasses. The only study of immiscible liquids in the CRBG to date known by this author is that of Kuo *et al.* (1988), where a series of 1 - 3 micron sized basaltic globules suspended in a granitic matrix were concluded to be the result of the liquid immiscibility.

Liquid immiscibility is favoured when melt fractions are enriched in SiO_2 preferentially to FeO (Hess *et al.* 1975, Rutherford *et al.* 1976). This is facilitated by the enrichment of Fe in the increasingly polymerized Si-rich melt. Once the critical point has been reached the melt splits into an Fe-rich unpolymerized fraction and a highly polymerized Si-rich fraction. Wood and Hess (1977) suggest that addition of Al_2O_3 to the system will depress the temperature of stability of the two liquid field, possible to a metastable state below the liquidus. Wood and Hess (1977) go on to suggest that if the melt is very rich in Al_2O_3 a relatively early fractionation of plagioclase is required to facilitate Al_2O_3 removal from the melt in order not to significantly depress the temperature of the two liquid stability field. Minor Al_2O_3 modification is consistent with data in major and minor element diagrams affected by plagioclase removal.

Whole rock analysis from the CRBG show a general 1 - 2% enrichment of Al_2O_3 when compared to the remaining glass phase MWGM (mean Wanapum glass mixture). Figure 9 showed

Plate 6. Large single bubbles of brown glass within colourless glass from thin section 6909. The "bent" bubble appears to have been deformed by the plagioclase crystals as they grew. These isolated individual bubbles are larger than those found in the bubbles swarms as seen in plate 5. Field of view is 0.55 mm, plane polarized light conditions.

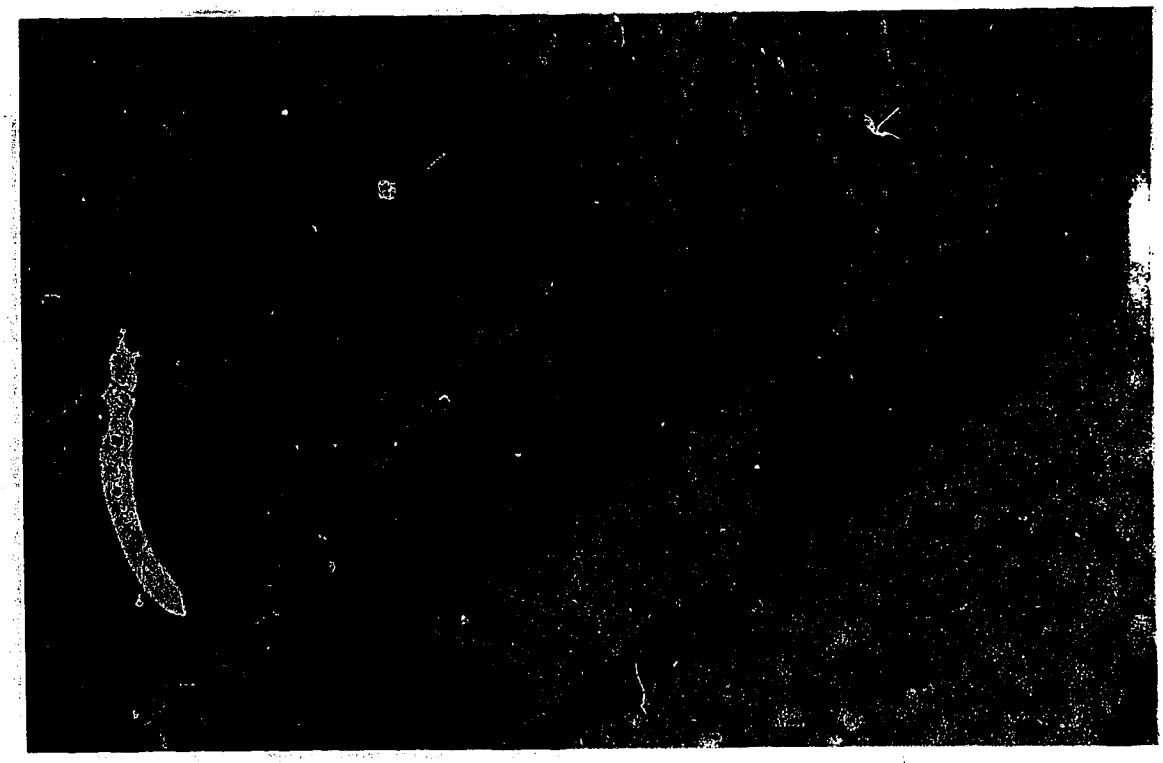

Plate 7. Isolated individual bubble of brown glass in colourless glass from 6909. the bubble seems to have wrapped itself around a crystal of magnetite. Field of view is 0.55 mm, plane polarized light.

that plagioclase fractionation possibly played a minor role in the late stages of crystallization moving the bulk composition of the magma towards that of the remaining liquid, MWGM. This evidence suggests that there was in fact a small degree of Al_2O_3 modification that prevented the depression of the two liquid stability field (Wood and Hess 1977) in the crystallization process that affected these basalt units.

The immiscible or unmixed nature of these two phases can be further demonstrated chemically. A series of bubble boundaries were analyzed by the electron microprobe by setting the crystal spectrometers in positions to detect Si, K, Fe, and Mg. The automated stage was then driven in steps of 1 μm from an area of colourless glass into an area of brown glass. The computerized scalars recorded the number of counts for each element at every point along the traverse. Plate 8 and Figure 21 clearly show the sharp well-defined "step-like" boundary between the glass phases. It is obvious that the two phases are not in any state in mixing or exchange at their respective boundaries. See appendix (4) for further data collected across bubble boundaries.

Glass separates were obtained for the purpose of attained rare earth elemental abundances in the individual glasses. The purity of the glass separates is vital in attaining reliable data. The purity of the separates can be argued on a basis of their chemistry and physical properties. The brown glass is obviously not contaminated by colourless glass or plagioclase due to the extremely low values of Na_2O and K_2O (BGL Na_2O = 0.5% K_2O = 0.65%, CGL Na_2O = 2 - 7% K_2O = 4 - 7%, plag Na_2O = 9%). Olivine and clinopyroxene are effectively removed from brown glass in density separation, olivine and clinopyroxene sink in dilute acetylene tetrabromo ethane (TBr_4) while the brown glass floats. The BGL fraction was collected after three successive dilutions of TBr_4 and recycling of the floating component. Similarly, colourless glass does not seem to be significantly contaminated by BGL, olivine, or pyroxene by the very low FeO contents in the glass (CGL FeO = 2%, BGL = 25%). Contamination by phases such as plagioclase are much more difficult to avoid due to similar density. If data were available Sr and Ca contents (both enriched

Plate 8. Secondary electron image of a bubble of brown glass within colourless glass. Automated stage was traversed along the line form A to B. Magnification is roughly 2000X. Probe conditions were 15 kV accelerating voltage, 0.6 nA probe current, count times were 20 seconds at each point.

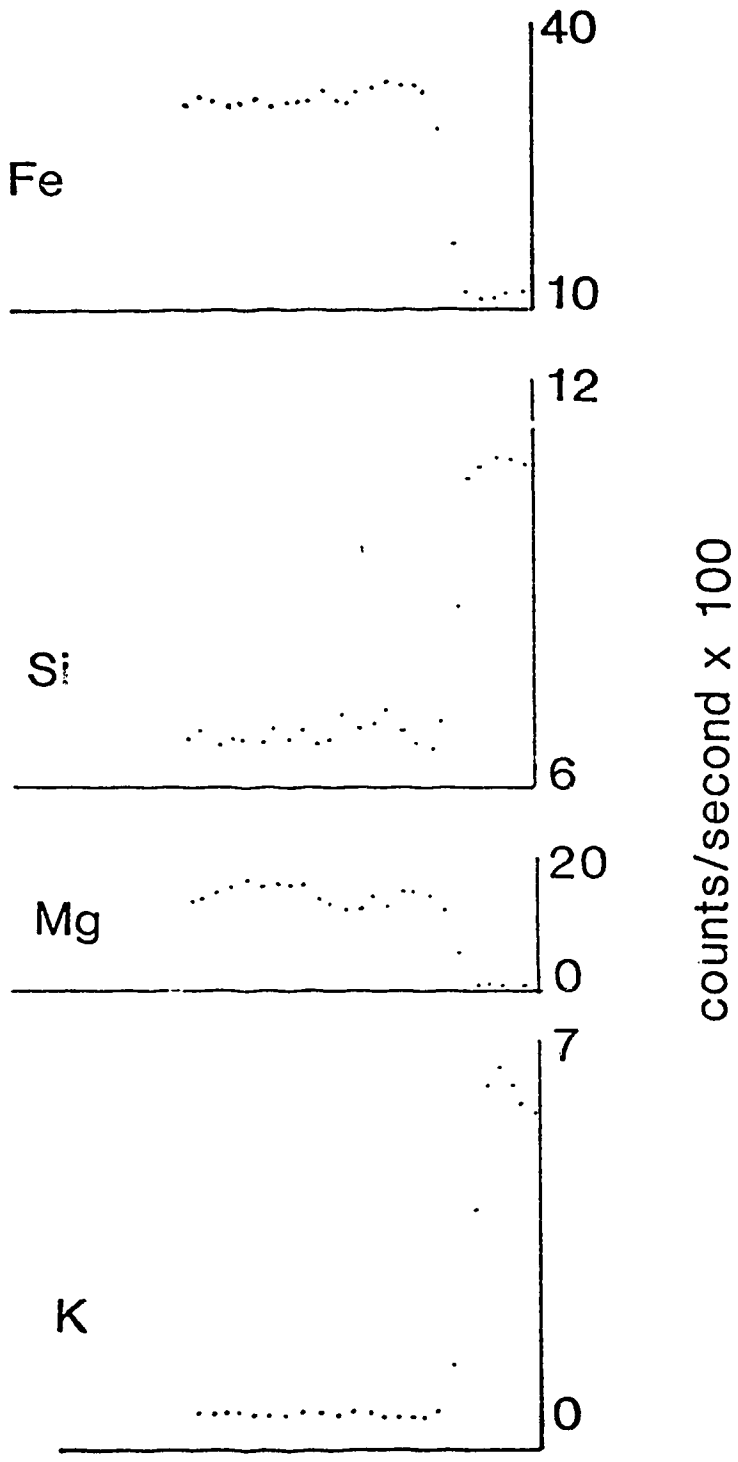

Figure 21. Bubble boundaries are sharp, well defined contacts as is clearly seen in the count rates encountered by the crystal spectrometers as the automated stage was driven from A (in CGL) to B (in BGL).

in plagioclase) of the separated colourless glass would give an indication of the limits of plagioclase contamination. In this light the purity of colourless glass separates remains somewhat problematic. Na values of 6983 colourless glass are 0.7% where as microprobe data is 1.21%. The 0.7% Na_2O is less than the average colourless glass figure which is 2.2% Na_2O. Average plagioclase Na_2O content is roughly 9%, this would indicate that substantial plagioclase contamination of the glass separate is unlikely.

Rare earth elemental abundances provide another line of evidence which supports the immiscibility theory. Both the colourless and brown glass phases exhibit similar REE patterns: the individual rock/chondrite patterns are displaced yet parallel, Figure 22. The negative Eu anomaly is evident in both of the BGL/CGL pairs analyzed and is roughly of the same magnitude. This is indicative of a state of equilibrium between the glass phases. If the brown glasses, chlorophaeite, represents the alteration of olivine then the brown glass REE patterns should not exhibit the same negative Eu anomaly seen in the colourless glass phase. The negative Eu anomaly is a result of plagioclase crystallizing in the system which occurs subsequent to olivine formation, hence neither the olivine or its alteration products will exhibit the large Eu depletion seen in the glass phases. This is another line of evidence that the brown glass was in coexistence with the colourless glass and attained its trace elemental composition after plagioclase crystallization had occurred. A further argument along this line is the similarity of Fe/Mg ratios in the coexisting glass pairs which is also indicative of immiscibility (Naslund 1983).

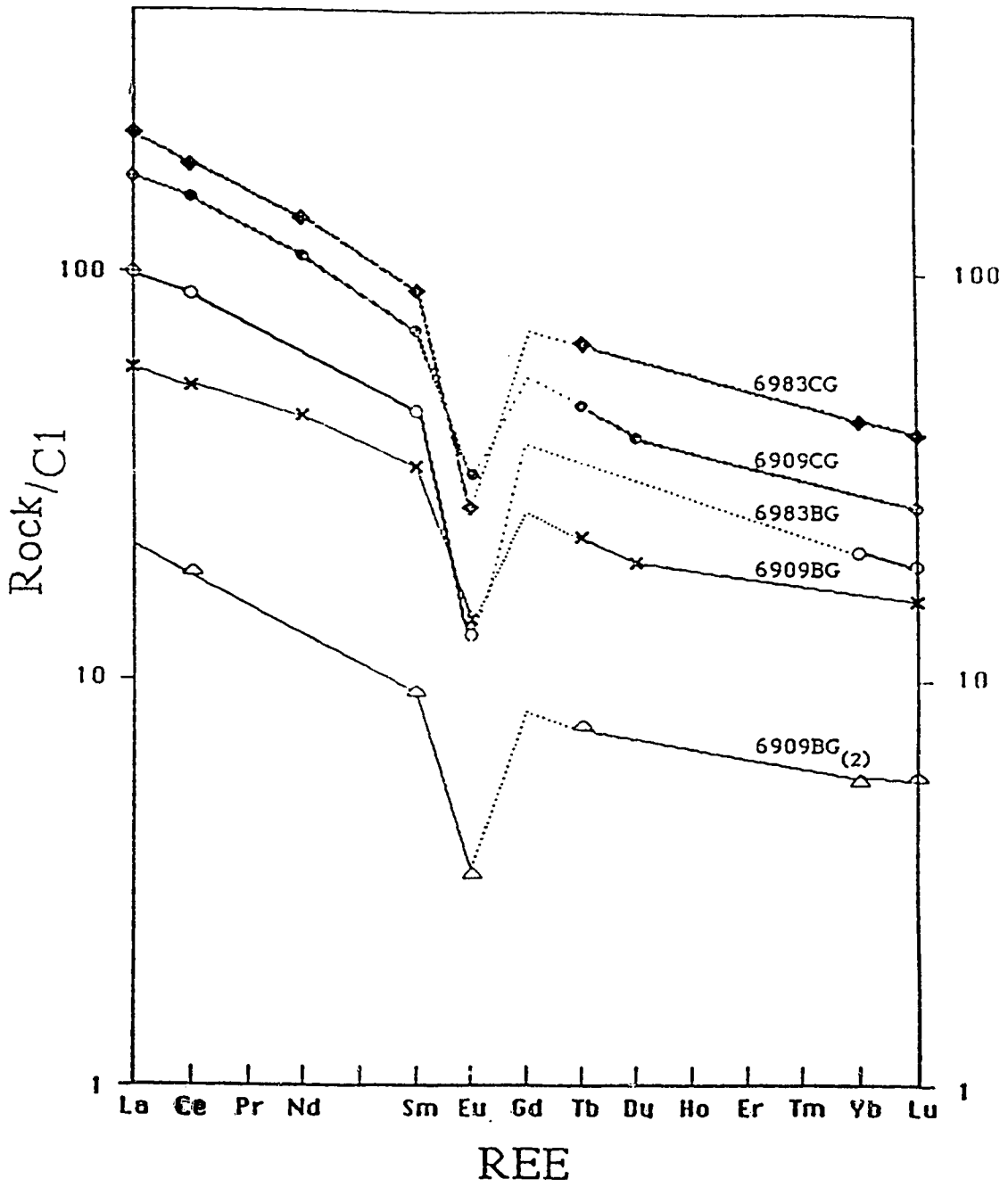

Figure 22. REE patterns of Columbia River glasses. REE data was obtained by INAA at the University of Alberta's SLOWPOKE reactor facility.

IMMISCIBILITY IN THE SYSTEM K_2O-FeO-Al_2O_3-SiO_2

Roedder (1978) describes the occurrence of liquid immiscibility in the experimental system K_2O-FeO-Al_2O_3-SiO_2 at temperatures relevant to geological environments. Figure 23 is an amalgamation of Roedder's description of the system at various FeO contents expanded to include CRBG points. Although not directly within the fields of liquid immiscibility, the CRBG points are very close to these fields. If the system of Roedder (1978) is expanded to include MgO and Na_2O it would include greater than 98% of the chemical components of CRBG units. In Figure 24 Roedder's (1978) system has been expanded. The FeO apex is now FeO-MgO and the K_2O apex is now K_2O+Na_2O. The result of this expansion is that the CRBG points now plot on the edge or within the defined field of liquid immiscibility. Notably the brown glasses plot near the top of the miscibility gap at high FeO contents while the colourless glasses plot near the bottom of the volume at low FeO contents. MWGM plots within the immiscible volume, this is a function of being an average mixture of two glasses that plot on the edge of the immiscible volume. However, if these compositions were significantly removed from the volume where two liquids coexist then MWGM would not have fallen within this volume. The expansion of this diagram is done on a purely theoretical basis by reviewing the phase diagrams and systems of the original oxides and the added oxides along the joins of the ternary system.

The representative phase diagrams for the systems MgO-SiO_2 (Bowen and Anderson 1914, Ol'shanskii 1951), and FeO-SiO_2 (Bowen and Schairer 1932) are very similar (Figures 25 and 26). Immediately obvious is the presence in both cases of a field of two liquid immiscibility occurring at approximately 1700°C, at a SiO_2 content of 60 - 90%. The overall phase geometry of the two systems are also very similar. Therefore it is likely that the addition of MgO to the FeO apex will not affect the behaviour of this system.

Similarities also exist when the two phases are compared along the Al_2O_3 join of this

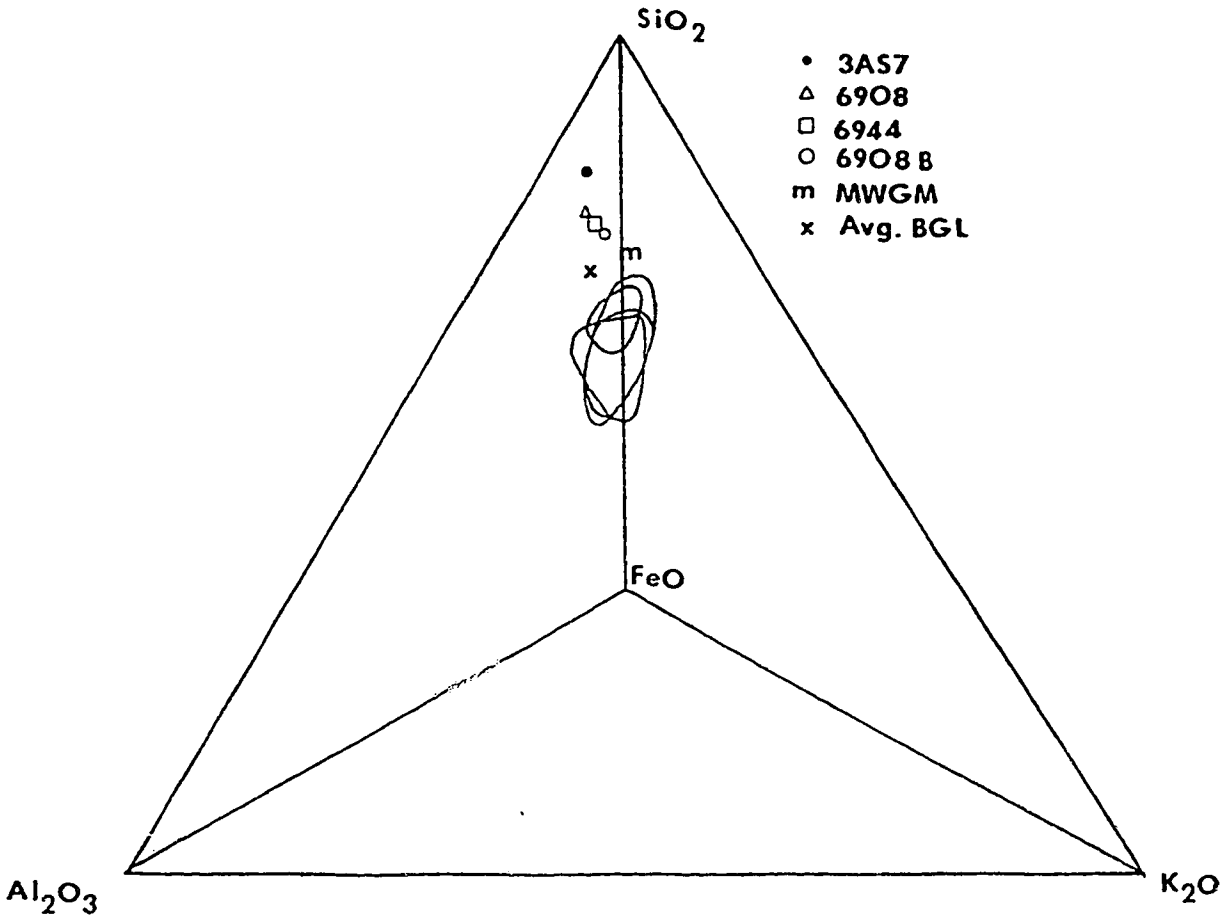

Figure 23. Liquid immiscibility in fields in the system K_2O-FeO-Al_2O_3-SiO_2 modified after Roedder (1978). The four fields 10, 20, 30, and 40 represent increasing FeO contents. The four labelled samples are all colourless glasses, in addition a mean BGl composition and MWGM (m) have been added. The BGL appears quite close to the others but it is on a higher FeO plane, 37%, whereas the others are on FeO planes much closer to 10%.

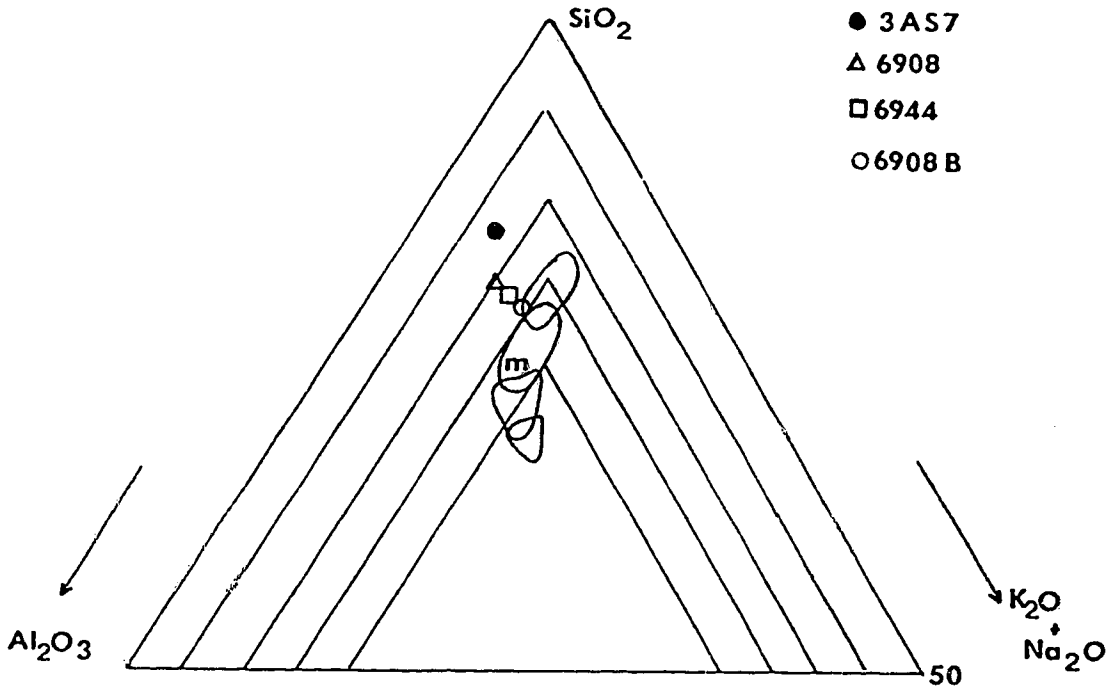

Figure 24. The system K_2O-FeO-Al_2O_3-SiO_2 with the addition of Na_2O and MgO these additions now account for greater than 95% of the CRBG wholerock chemistry. It can be seen that the composition of MWGM (m) is now within, although near the edge, of two liquid stability.

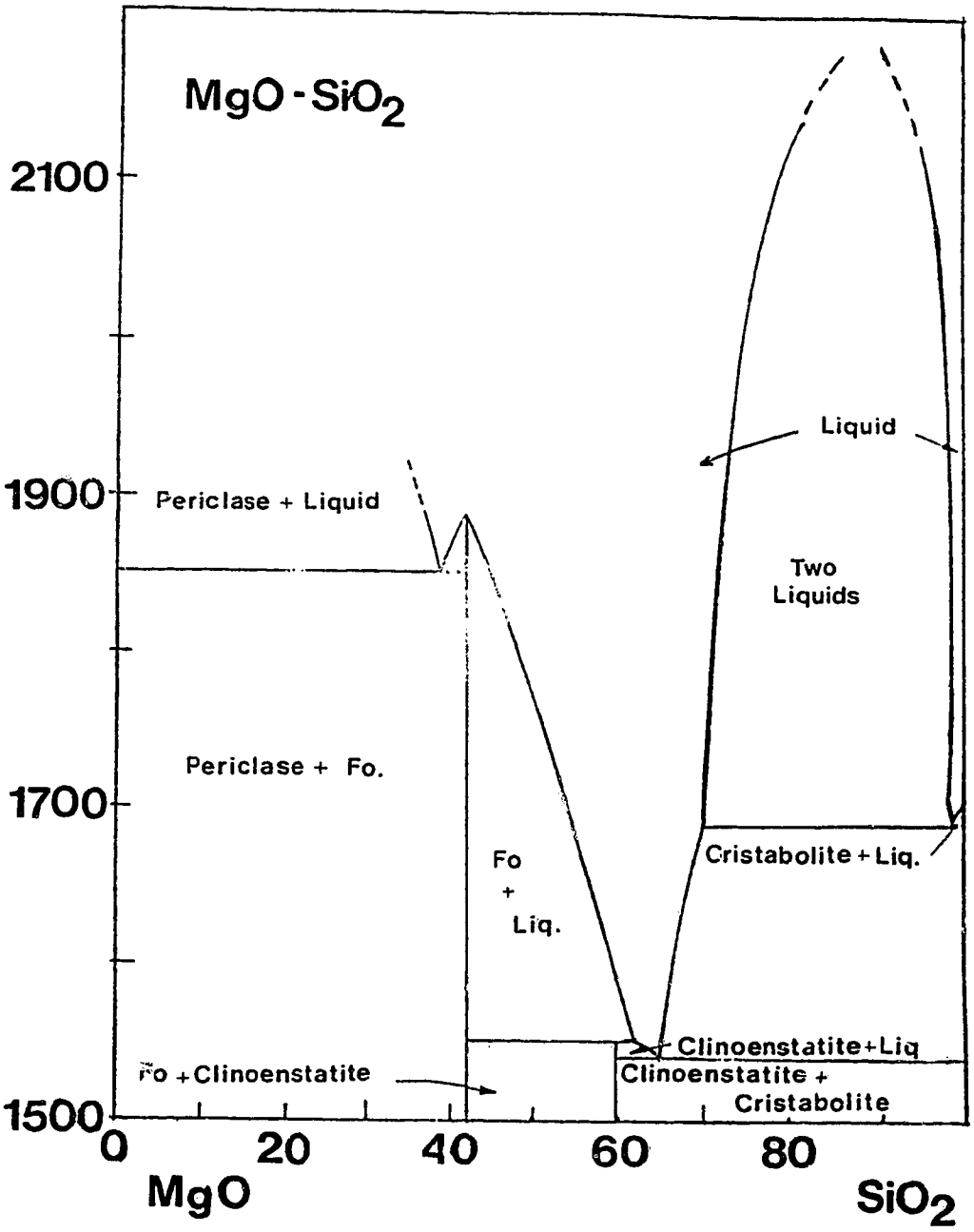

Figure 25. Phase diagram for the system MgO - SiO_2, modified after Bowen and Anderson (1914) and Ol'Shanskii (1951). The stable fields of two liquid immiscibility is associated with high SiO_2 contents.

Fe–Si–O

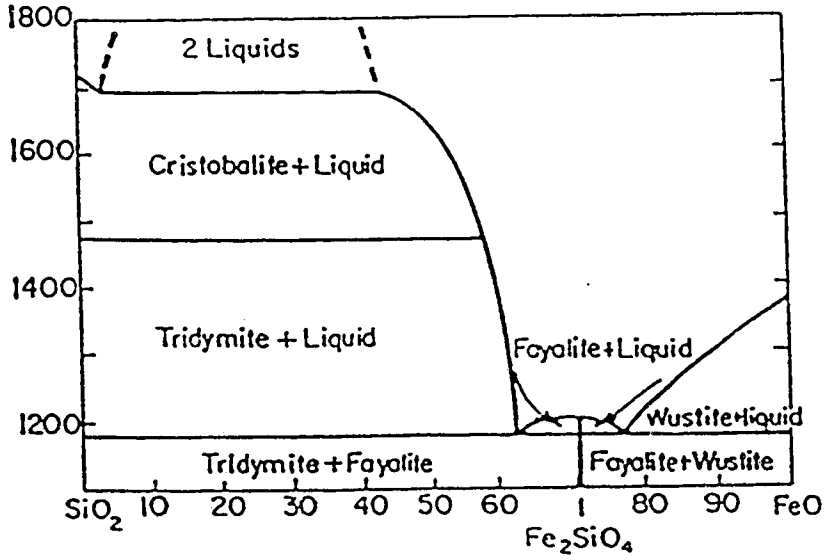

Figure 26. Phase diagram for the system FeO - SiO_2, modified after Bowen and Schairer (1932). Again the fields of stable two liquid immiscibility is associated with high SiO_2 contents.

system. The representative phase diagrams for the systems MgO-Al_2O_3 (Rankin and Merwin 1916) and FeO-Al_2O_3 (McIntosh *et al.* 1937, Novohatski *et al.* 1965) are reproduced in Figures 27 and 28. The temperature is much higher in the MgO-Al_2O_3 system, but the overall phase geometry is similar. Another difference is the displacement of the eutectic towards Al-rich compositions in the MgO-Al_2O_3 system, whereas the FeO-Al_2O_3 system has the eutectic displaced towards Fe-rich compositions. The important similarity is that neither of these Si-free systems show a field of immiscibility, and both systems will cool via a series of liquid/solid reactions until the solidus is reached. Again, addition of small quantity of MgO to the FeO rich system will not change the argument.

The effects of substitution of Na_2O for K_2O can be seen in the systems Na_2O-SiO (Kracek 1930, 1939) and K_2O-SiO_2 (Kracek *et al.* 1937, Wollast 1961). These systems, (Figures 29 and 30) are again very similar.

Due to the lack of availability of two component phase diagrams for the systems Na_2O-FeO and K_2O-FeO three component systems including SiO_2 will be examined. The systems $K_2O.2SiO_2$-FeO-SiO_2 (Roedder 1952) and Na_2O-FeO-SiO_2 (Carter and Imbrahim 1952) show minor phase differences in their phase relationships, Figures 31 and 32. This may be due to a lack of detail in the extreme SiO_2 compositions in the Roedder diagram, which represents a further extension towards the pure Na_2O composition (right side of the diagram) than the diagram presented by Carter and Imbrahim (1952). The K_2O system shows a very small field of liquid immiscibility at high temperatures, 1690±10°C, very high SiO_2 values and correspondingly low K_2O values. The extreme temperatures associated with this field of liquid immiscibility may not affect materials under normal geological conditions. However, the effect of the addition of components to this system is the depression of the temperatures demarcing the field of two-liquid stability. As such, the field of immiscibility in the K_2O rich system may be depressed to temperatures more consistent with those associated with CRBG volcanism. There is no corresponding immiscibility field in the Na_2O system. The effects of addition or replacement of either of these two oxides to

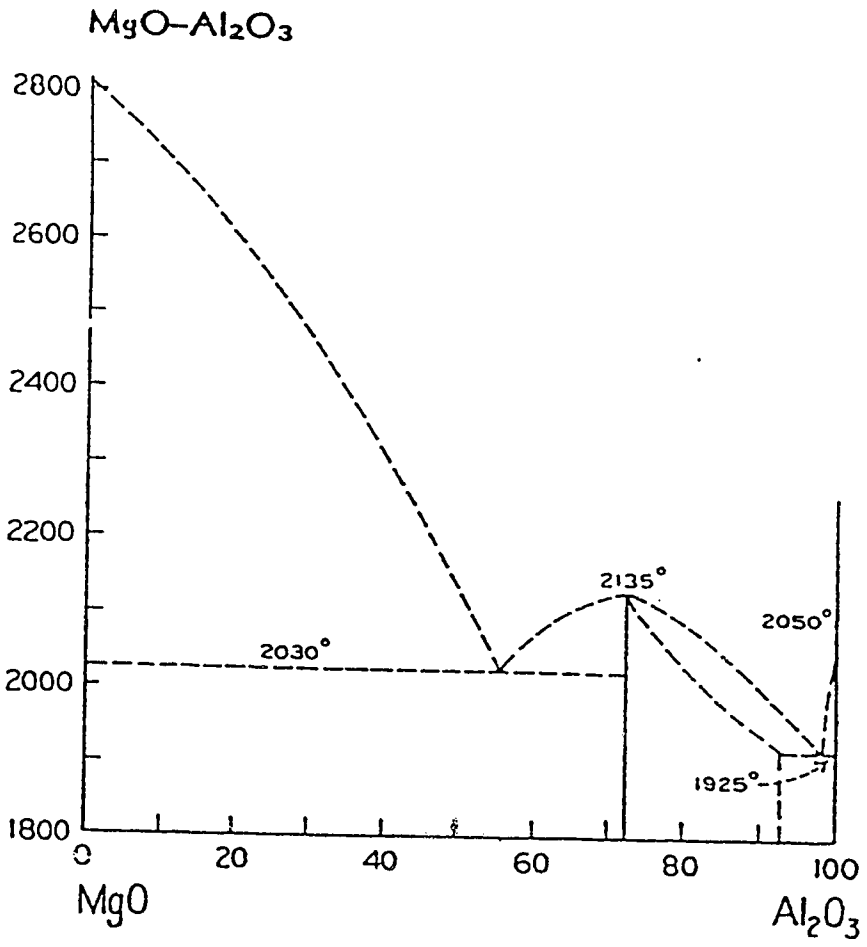

Figure 27. Phase diagram for the system MgO- Al_2O_3 modified after Rankin and Merwin (1916). There is no associated field of two liquid stability in this system.

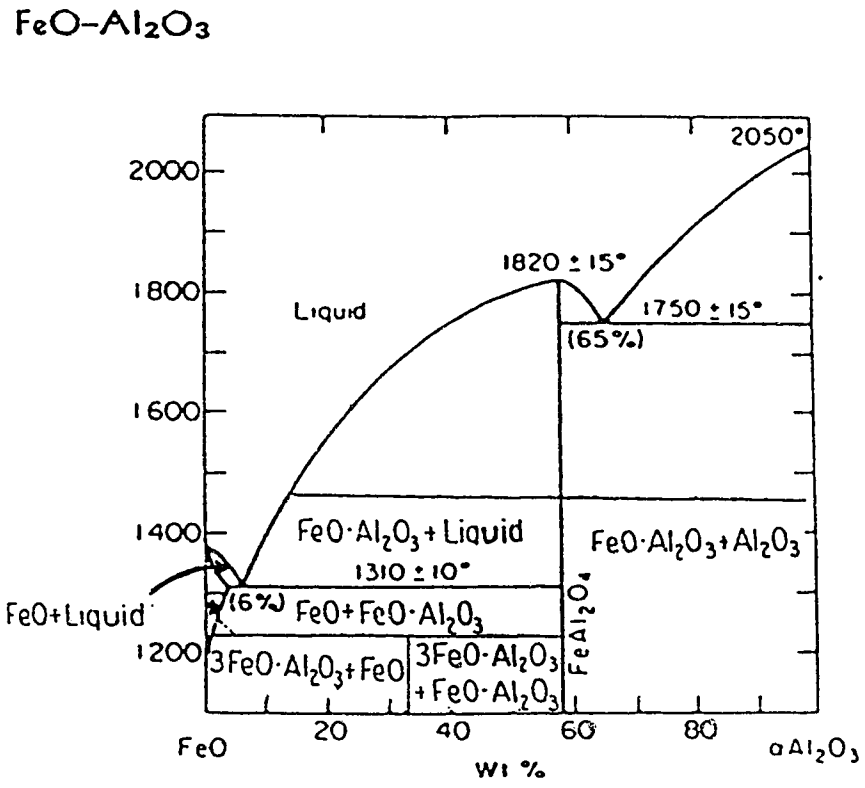

Figure 28. Phase diagram for the system FeO - Al_2O_3 modified after McIntosh *et al.* (1937) and Novohatski *et al.* (1965). Again there is no field of two liquid stability.

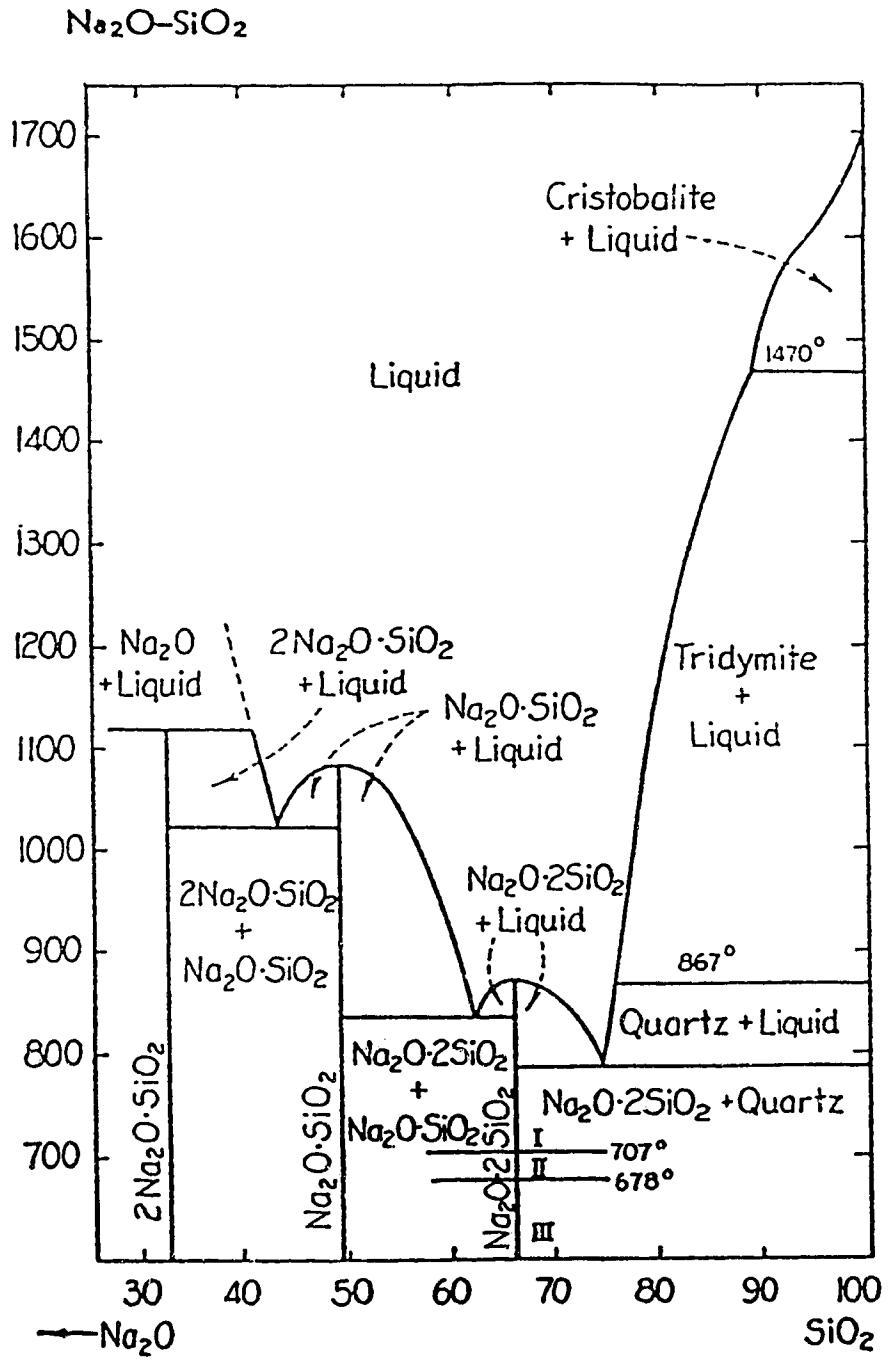

Figure 29. Phase diagram for the system Na_2O - SiO_2 modified after Kracek (1930,1939). There is no field of two liquid stability.

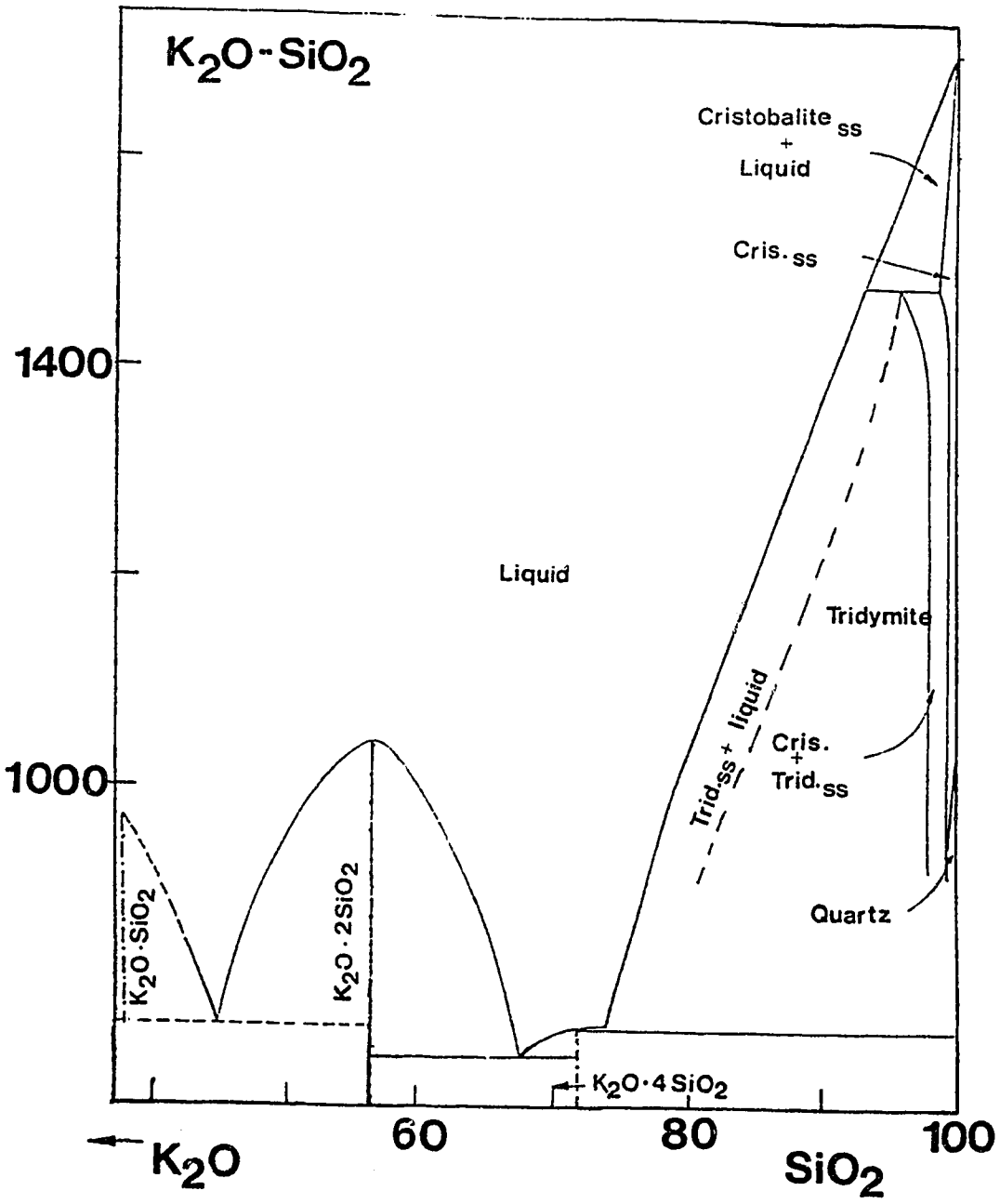

Figure 30. Phase diagram for the system K_2O - SiO_2 modified after Kracek *et al.* (1937) and Wollast (1961). Again, there is no field of two liquid stability

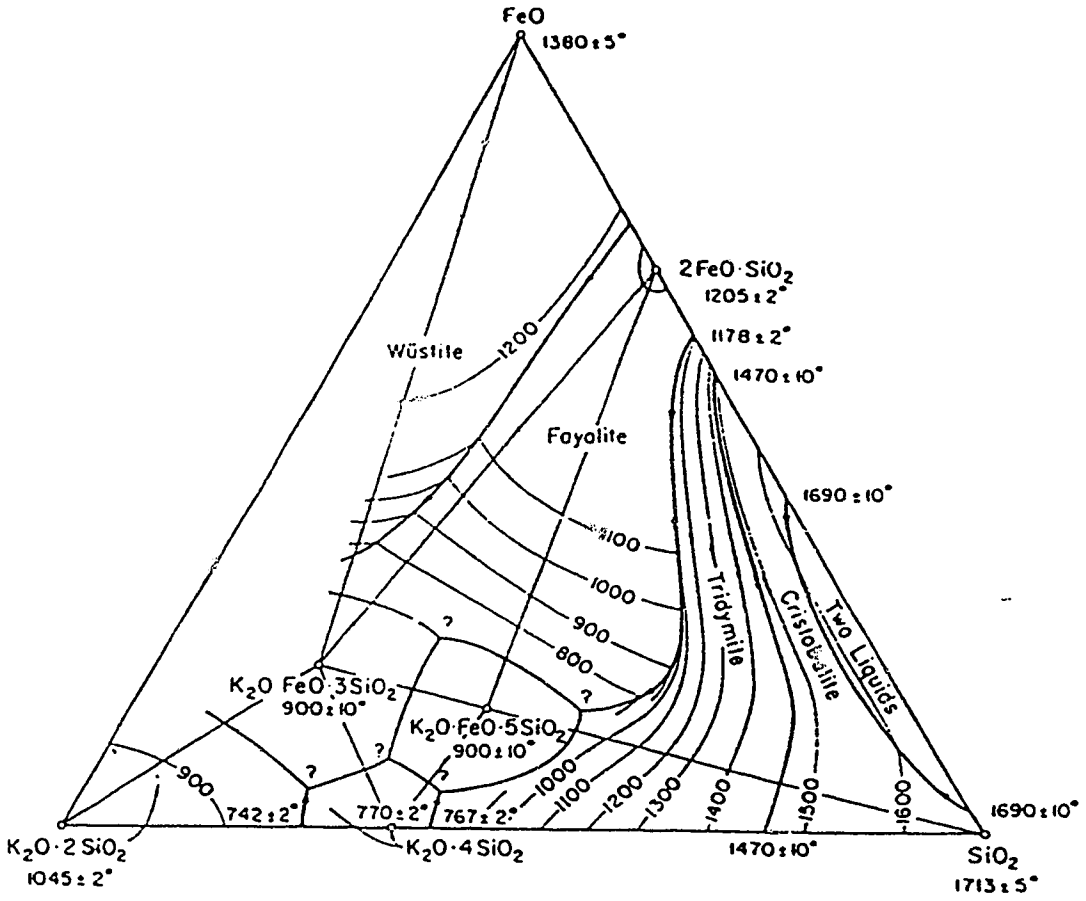

Figure 31. Phase diagram for the system $K_2O.2SiO_2$ - FeO - SiO_2 modified after Roedder (1952). No field of two liquid stability exists at high SiO_2 contents

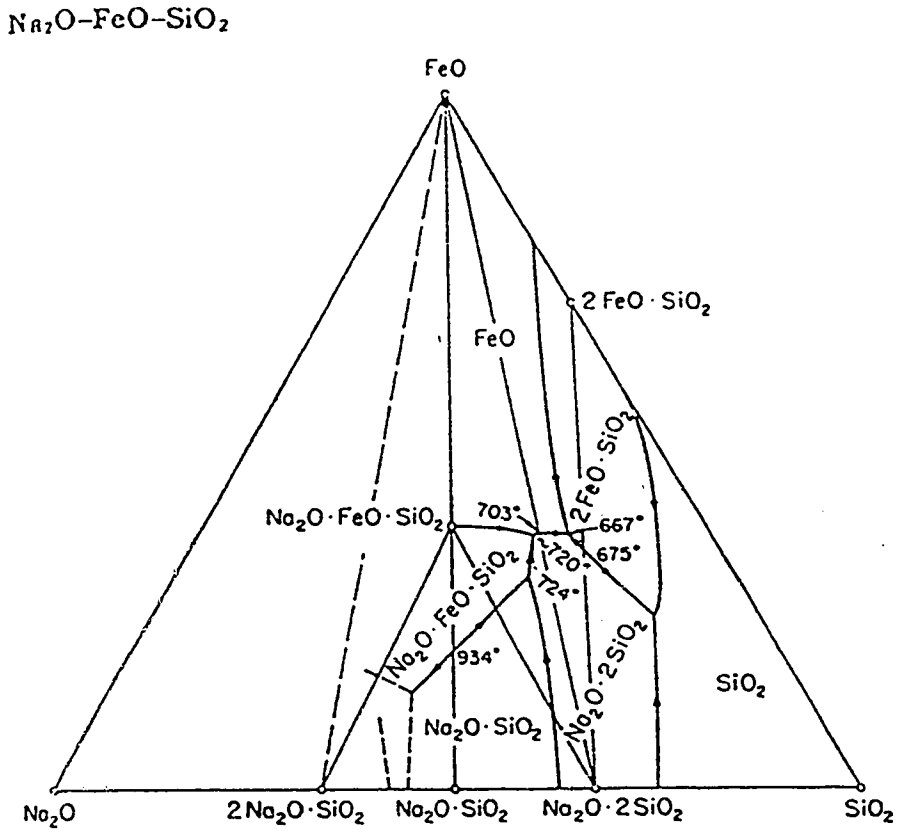

Figure 32. Phase diagram for the system Na_2O - FeO - SiO_2 modified after Carter and Imbrahim (1952). A small field of two liquid stability exists within this system at high SiO_2 contents.

the system are obviously somewhat different. However, the glasses in the CRBG have $K_2O > Na_2O$ and the K-rich systems are more relevant.

The effects of the addition of Na_2O to K_2O in this system may cause minor changes to the region of stability of a mineral or liquid phase. However, the impact of this extra component in the residual Wanapum glass phase (MWGM) will be slight. Without the added Na_2O the K_2O content of MWGM is 5.9% of the oxide sum $SiO_2+Al_2O_3+K_2O$. When the combined alkalies are considered they account for only 8.0% of the total of $SiO_2+Al_2O_3+K_2O+Na_2O$. The lateral translation of the point will be negligible in the context of the ternary system (SiO_2-Al_2O_3-(Na_2O+K_2O)) represented by a horizontal section through either the SiO_2-Al_2O_3-(Na_2O+K_2O)-FeO or SiO_2-Al_2O_3-(Na_2O+K_2O) - (FeO+MgO) system.

The final systems that should be considered as Na_2O-Al_2O_3 and K_2O-Al_2O_3. Unfortunately, adequate phase diagrams for these systems do not exist. Given the previous evidence or differences in the Na_2O-SiO_2 and K_2O-SiO_2 systems and the reverse nature of the systems FeO-Al_2O_3 and MgO-Al_2O_3 it is quite likely that there will be differences in the phase diagram geometry of these two systems. However, it is not likely that the addition of Na_2O will affect the field of immiscibility as this seems to be a function, in all systems, of high SiO_2 content. The Al_2O_3-(Na_2O+K_2O) join on this diagram, opposite the SiO_2 apex, corresponds to a very low SiO_2 content and can probably be ignored as a factor affecting the existence of the field of immiscibility. However, it may depress its temperature of stability.

The examination of the various phase diagrams of the subcomponents of the quaternary system K_2O-Al_2O_3-SiO_2-FeO supports the addition of the phases MgO and Na_2O. This addition to the model now accounts for greater than 98% of the components of MWGM. The component phase diagrams support immiscibility being dependant on enrichment of SiO_2 in the melt to a level above 70%. This is coincident with an enrichment of FeO relative to MgO in the residuum (Hess *et al.*

1975, Rutherford *et al.* 1976). The low Al_2O_3 content in MWGM agrees with the suggestion by Wood and Hess (1977) that a degree of Al_2O_3 modification is required to facilitate immiscibility. (Table 11).

Table 11.

	Average Wanapum Wholerock	MWGM+/-
SiO_2	51.36	69.98 + 17.62
Al_2O_3	13.86	11.21 - 2.65
Fe_2O_3	3.52	
FeO	10.54	8.41 - 2.13
MgO	4.30	4.56 - 1.83
CaO	8.56	0.43 - 7.62
Na_2O	2.75	1.95 - 0.80
K_2O	1.32	5.06 + 3.74
TiO_2	2.96	0.64 - 2.32
MnO	0.22	0.02 - 0.20
P_2O_5	0.54	0.02 - 0.52
H_2O	0.00	0.84 + 0.84
Total	100.02	101.69

Table 11. Relative enrichment and depletion of elements as crystallization produced the final residual liquids. Only Si and K are enriched in the final melt, all others are depleted. Average Wanapum wholerock was attained by averaging all Whanapum wholerock analyses (as determined by XRF methods). MWGM was attained by combining 75% of the average CGL composition with 25% of the average BGL composition (as determined by electron microprobe analysis).

THEORETICAL LIQUID IMMISCIBILITY AND THE SYSTEM Di-Fo-Qz

The presence of liquid immiscibility can be further modelled, theoretically, in the system diopside-forsterite-quartz, although for the CRBG the system would be augite-Fa-'granite'. Figure 33 shows the phase relationships in the MgO system (Schairer and Yoder 1962) with the addition of the CRBG points.

To account for the amount of iron, represented by fayalite in the rocks, the minimum temperatures must be shifted somewhat towards the forsterite corner as seen in Figure 34. This is based on examination of the various phase diagrams that occur along this join. Comparison of eutectic temperatures of Fe and Mg rich systems such as those seen in Figures 25 and 26, show marked increases in the temperatures in Mg-rich systems. Low temperatures associated with Fe rich systems will therefore tend to shift stability fields towards the low temperatures associated with the FeO apex. Similarly, in the natural system the quartz end-member is more accurately represented by granite, (the colourless glass is 75% SiO_2), rather than the pure SiO_2 end member composition. This change is necessitated by the lack of quartz as a mineral phase in the rocks. There are no documented occurrences of quartz as a mineral phase in the CRBG. However, the 30% normative quartz content in the colourless glass component can be deemed to be the quartz representative in the system. The addition of alkalies to this system will tend to shift the system towards the quartz corner, Figure 35, as dry granite melts at 900°C, 300°C lower than the minimum temperature in the three component system. Low temperatures associated with Fe rich systems will tend to shift phase boundaries towards that apex. Similarly, low temperatures in the Si (granite) corner will tend to will tend to shift phase boundaries towards the Si corner.

The overall effects of adding Fe and alkalies is to shift the stability fields towards the quartz corner. The general position of the CRBG bulk composition is shown in Figure 36. Bulk chemistry will be affected by cooling and crystallization of olivine in some samples, and clinopyroxene in

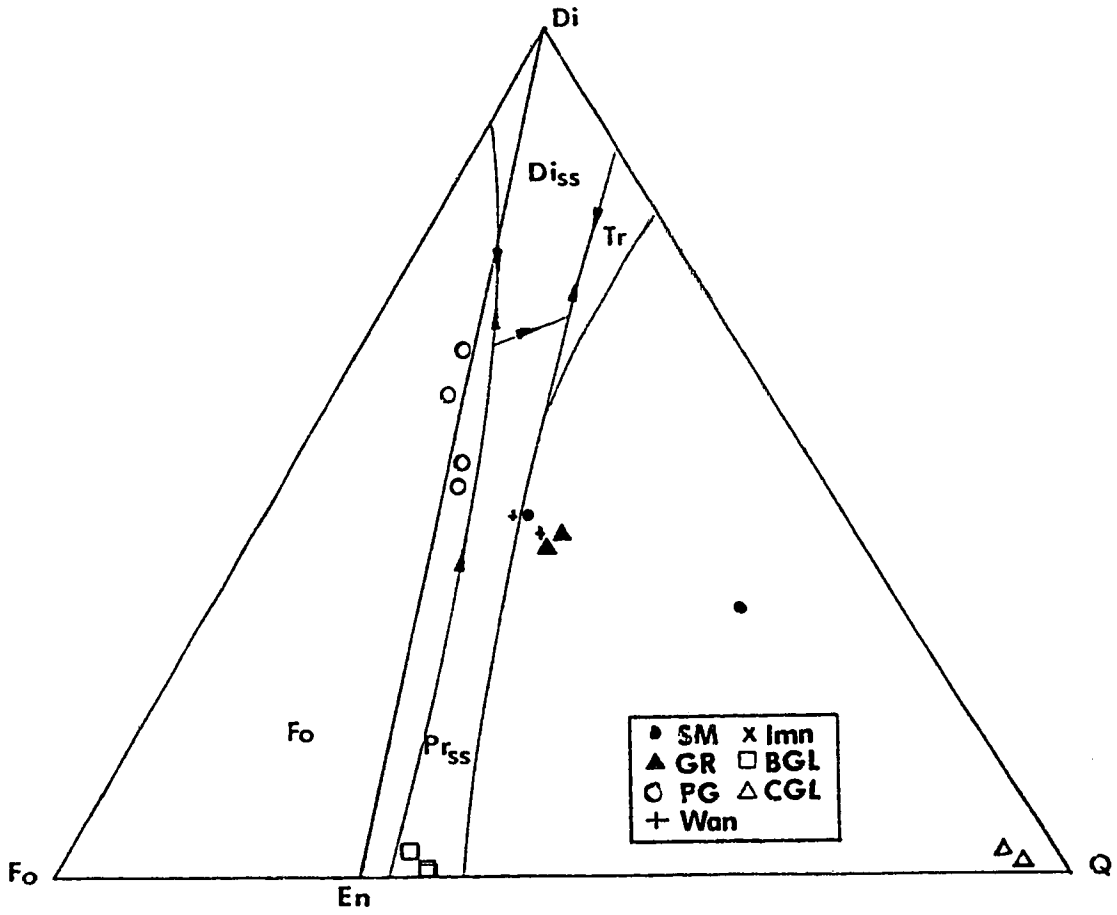

Figure 33. Phase ralationships in the system Di-Fo-Qz, modified after Schairer and Yoder (1961).

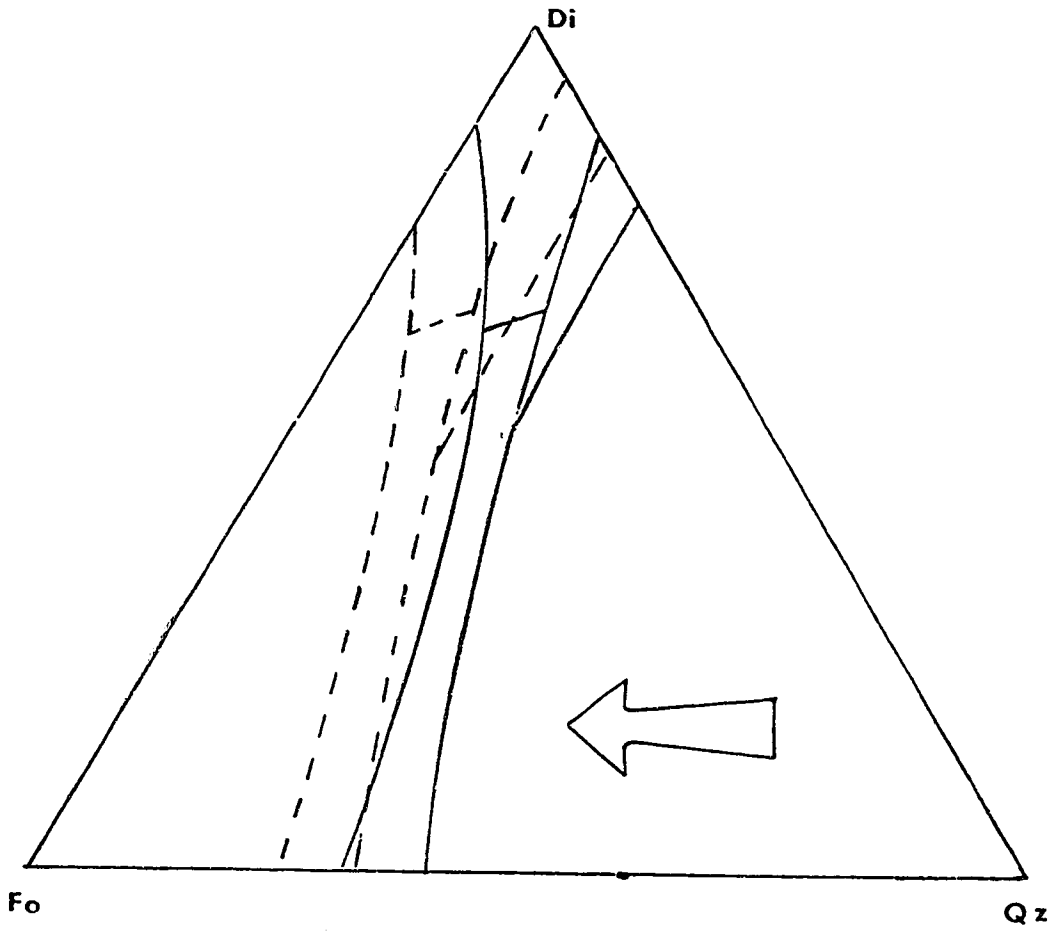

Figure 34. Expected shift direction of phase boundaries in the system Di-Fo-Qz in the presence of an iron-rich system.

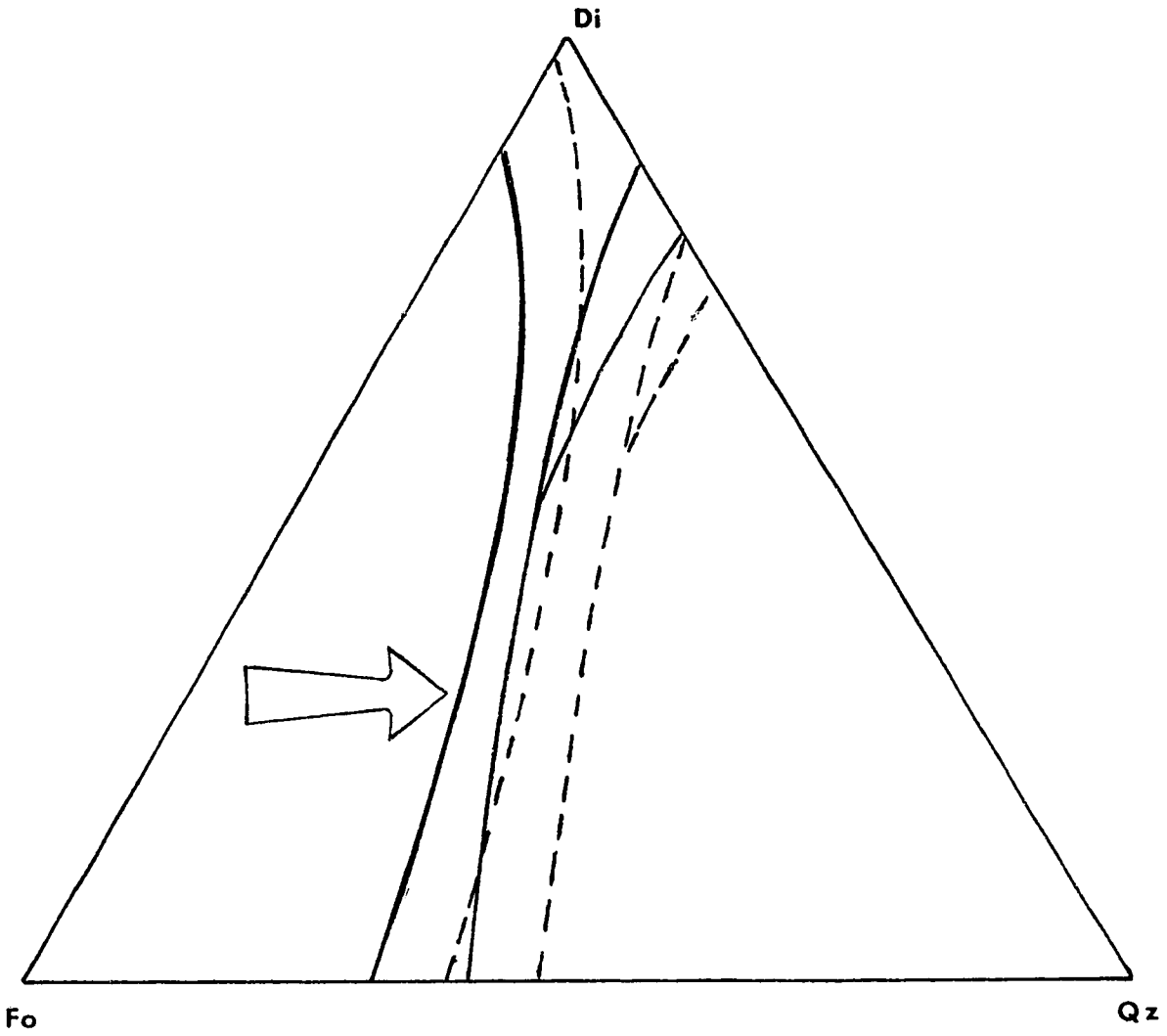

Figure 35. Expected shift direction of the phase boundaries in the system Di-Fo-Qz if the SiO_2 end member is represented by granite having a lower melting temperature than pure end member SiO_2.

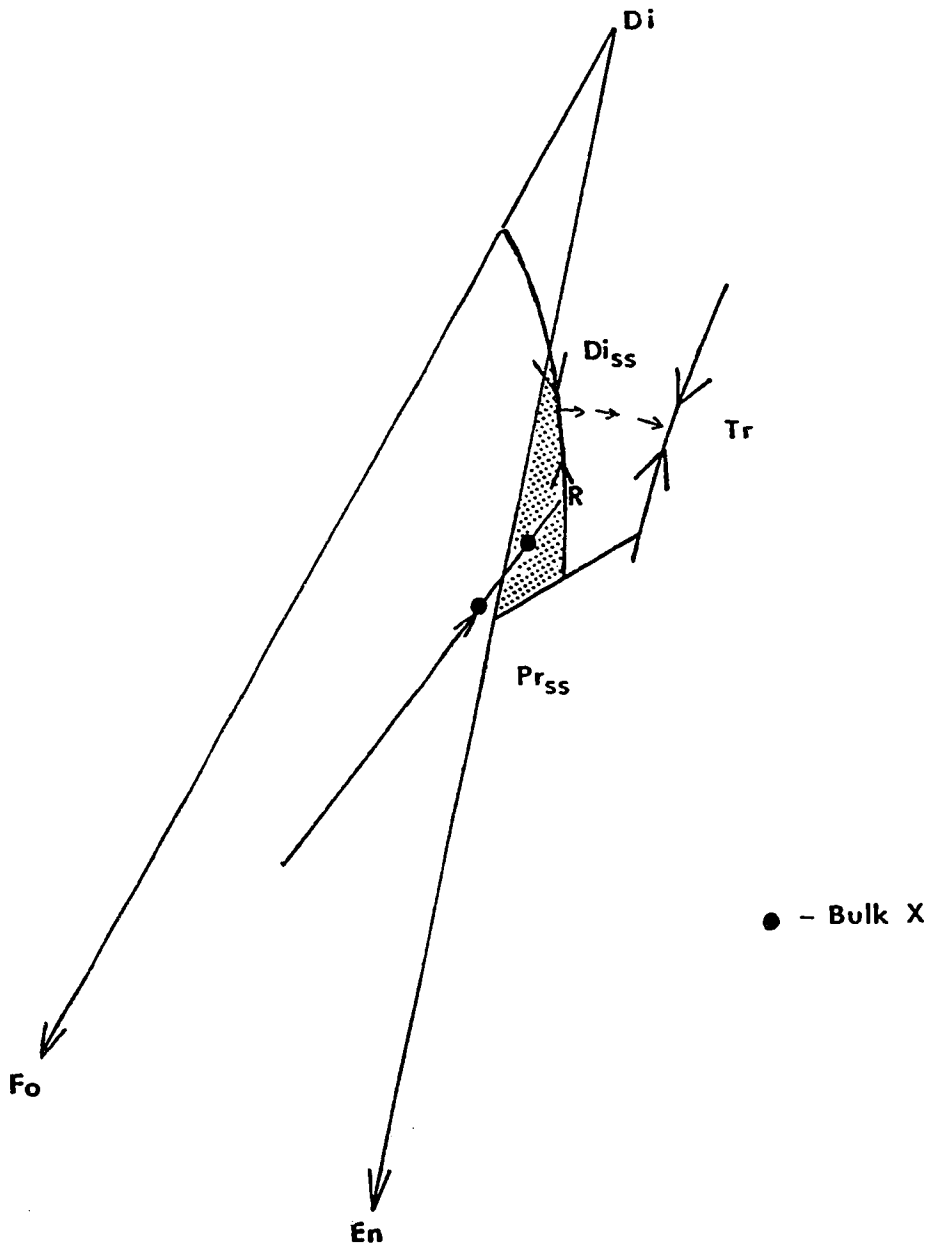

Figure 36. General position of bulk chemistry once the phase boundaries have been shifted (cross hatched area), and the suspected crystallization path taken by the liquid under equilibrium conditions.

others. This depends on whether the compositions plots lie within the stability field of olivine, to the left of the diopside-enstatite join, or to the right of the join in the stability field of enstatite. Crystallization will drive the remaining liquid towards the point R on the cotectic line. At R olivine begins to react with the liquid to produce Di_{ss}, (clinopyroxene), by the reaction Ol+liq Di_{ss}. As cooling continues this reaction continues until the point R", a local minimum on the cotectic. At R" the remaining liquid will move across the field of Di_{ss} by a unique path until it reaches the system minimum at R'". At R'" tridymite will begin to crystallize.

This reaction at the minimum will have zero degrees of freedom; a phase must be lost before further cooling can occur. Due to the very minor occurrence of olivine in CRBG units, it is likely that solidification took place just before these reactions had gone to completion. This would account for minor occurrences of olivine in most units.

Thus, this model of the system Fo-Di-Qz can be used to model the CRBG in a rather simplified manner. Evidence provided by the phase diagram ($MgO-SiO_2$ Figure 25) shows that olivine plays a minor role in displacing the bulk chemistry to the point MWGM, the residual phase in the natural system. This simple system, Fo-Di-Qz, supports the argument that the first phase to crystallize was olivine. Clinopyroxene, due to its proximity to the bulk composition, is not likely to produce the required shift of bulk composition during cooling. Essentially clinopyroxene removal will have the effect of removing crystals of the same composition as the melt from the melt with no real change in overall melt chemistry in terms of Ca, Fe, Mg, and Si.

At the point R in Figure 36, pyroxene crystallization begins as a result of the reaction Ol+liq Di_{ss}. This step is important in the CRBG, as nearly 35% of the mass is clinopyroxene. At the point R'" four phases exist; liquid (BGL) of protoenstatite composition, olivine (nearly exhausted in the reaction ol+liq tr at R'"), Di_{ss} (clinopyroxene) and tridymite (CGL as a result of the reaction Di_{ss}+liq tr at R'"). This corresponds with roughly 80% solidification of the magma

if both brown and colourless glasses are presumed to be liquid.

This model of the cooling history is more accurate than that proposed if the fields are not shifted to the left as a result of considering the granite component. If the bulk composition X is located in the primary field of Pr_{ss} stability shown in figure 37, the crystallization of olivine or enstatite will drive the composition to a point R on the univariant line separating Pr_{ss} and tridymite, thereby crystallizing tridymite (granitic colourless glass) before pyroxene. From a petrographic analysis of rocks in this study it is apparent that final glass formation must have occurred very closely after apatite crystallization, which is determined to be at roughly 75 - 80% solidification. This is not consistent with the model where a primary crystallizing phase is tridymite.

The modelling of complex natural systems by simpler three component systems can be misleading. However, as an approximation liquid immiscibility in this system is supported by the predicted residual phases tridymite, and Pr_{ss}. Tridymite is represented by CGL a liquid of granitic composition containing 30% normative quartz. The Prss is represented by BGL a liquid with roughly 80% normative protoenstatite (hypersthene). These natural components are fairly consistent with those predicted by the phase petrology of the diopside-forsterite-silica system.

However, examination of the phase relationships along the diopside-enstatite join indicates a departure in the natural system from the expected final compositions. In studies of this system Boyd and Schairer (1962), Kushiro (1969), and Morse (1980) indicate that the final crystalline composition should exhibit both clinopyroxene Pr_{ss}, and clinopyroxene, Di_{ss}. This final composition will be expressed over 80% of the possible bulk compositions ranging from $MgSiO_3$ (enstatite) - $CaMgSi_20_6$ (diopside). Similar examination of the system hedenbergite-ferrosilite (Lindsley 1967) also indicates that unless the system is extremely iron rich and calcium deficient the final assemblage will be coexisting ferrosilite and hedenbergite.

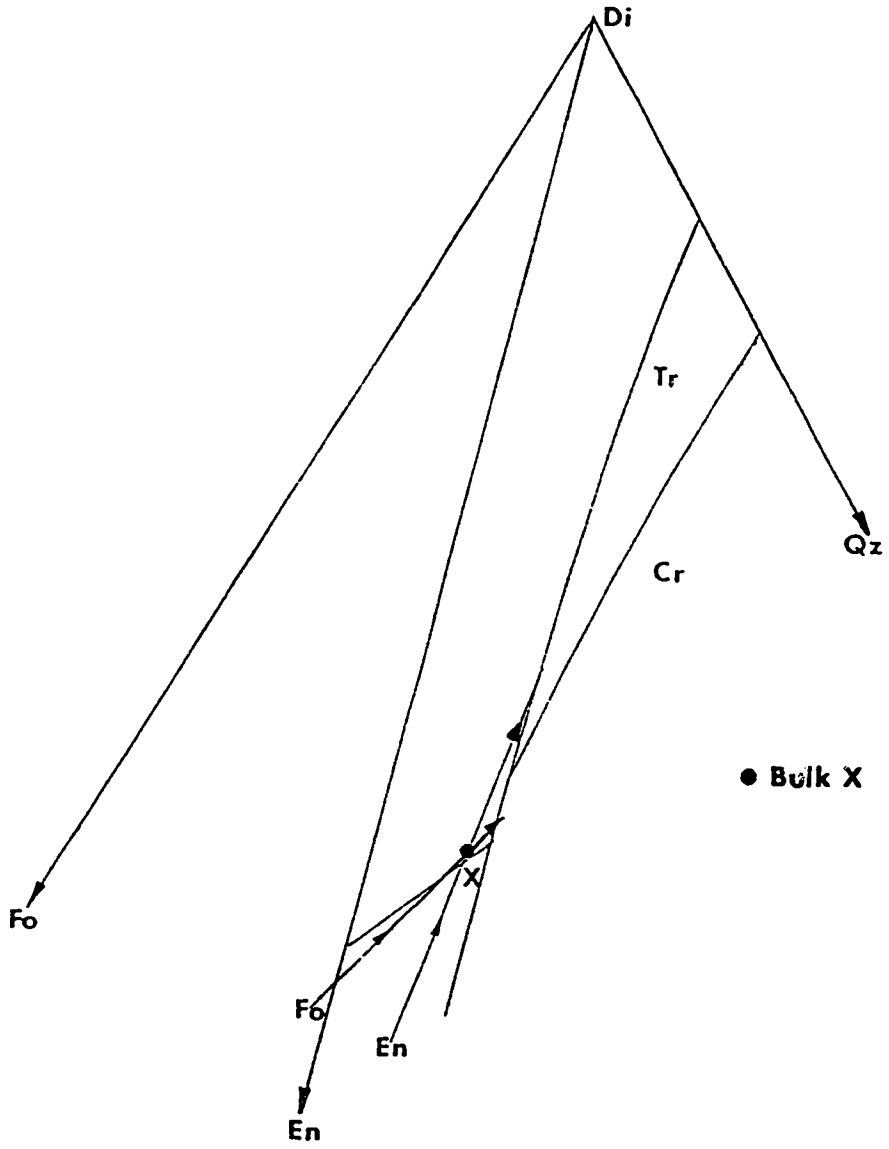

Figure 37. Crystallization of olivine or clinopyroxene will cause early crystallization and accumulation of cristobalite or tridymite respectively if the phase boundaries are not shifted when the SiO_2 component is considered to be granitic glass.

The existence of Pr_{ss} (hy) in the brown glass is undeniable: 75 - 82% of the BGL normative composition is represented as hypersthene. It must be concluded that something unexpected has occurred in the cooling and crystallization process of the CRBG with respect to the system Di-Fo-Qz. An immiscibility field must somehow intersect the tie line where Di_{ss} and Pr_{ss} coexist making it possible for the Pr_{ss} component to occur as a liquid rather than in the expected crystalline form.

ARGUMENTS AGAINST IMMISCIBILITY

Microprobe analysis reveals, however, chemical evidence that appears to contradict the possibility of immiscibility in the CRBG. Chemical analysis of the glass phases in several Wanapum flows indicate a marked departure from the theoretical partition coefficients of the elements Ti and P in the brown and colourless glasses. Data from Watson (1976) shows that P, and Ti should segregate preferentially into the mafic glass phase. The structure of the ferroandesitic melt is more able to accommodate the large incompatible elements than is the highly ordered, polymerized, silicic melt. In the case of phosphorus, partitioning should cause an enrichment by a factor of 20 in the mafic glass relative to the silicic glass. This process is less pronounced in alkalic melts than their tholeiitic counterparts (Philpotts 1982). Data form Philpotts (1982) shows enrichments of enrichments of 8.5 and 25.5 for TiO_2 and P_2O_5 respectively in mafic glasses relative to silicic glasses in rocks of tholeiitic affinity. These ratios dropped to 3.6 and 2.9 in rocks of alkalic compositions. Microprobe analysis of CRBG samples show an enrichment that is opposite to that predicted by Watson (1976) or the alkalic rocks of Philpotts (1982) for TiO_2 and possibly for P_2O_5 (up to 0.3 wt% TiO_2 in BGL versus 0.2 - 1.3 wt% TiO_2 in CGL) Similarly, REE's should be enriched in the mafic glass. However, as with Ti and P their enrichment in colourless glass is contradictory to the proposed partition coefficients, and are not concurrent with data from Kuo *et al.* (1988) where Ti and P observe predicted partitioning coefficients. The only trace elements that seem to follow Watson's (1976) partition coefficients in this study are Cs and Ba both of which are enriched in the colourless glass.

Partitioning of P_2O_5 between the brown and colourless glass is uncertain. Values of 0.16% and 0.29% are found in two of the 17 samples of colourless glass examined, the rest show no P_2O_5 content. The brown glasses similarly show no P_2O_5 content. There is, therefore, no clear evidence of any enrichment of P_20_5 in the granitic glass. As previously discussed apatite crystallization preferentially removed P_2O_5 from the melt before the glasses attained their present chemical nature.

The oddity that occurs is the preferential coexistence of apatite with the granitic glass phase, Plate 9. If apatite crystallized before the glass phase split there should be an equal, random coexistence of apatite with both glass phases. The same argument cannot be used for Ti, as it occurs in quantities of 0.2 - 1.3% in the granitic glass and is generally below detection limits in the mafic glass.

The addition of magmatic water as a concentrated phase to the residual liquid may affect the partitioning of Ti and P in the melts. (Simple systems models such as Watson (1976) are at best approximations to complex, multicomponent magma systems) The overall effects of the additional phases in the multicomponent natural systems on conclusions drawn from simple experimental systems are uncertain. However, in most situations where immiscibility has been discussed; experimental systems (Watson 1976, Roedder 1978), lunar basalts (Roedder and Weiblen 1973) and terrestrial basalts (Meyer and Sigurdsson 1978, Naslund 1983, Kuo *et al.* 1988) the preferential partitioning of P and Ti into the mafic melt seems to be the norm.

One possible explanation may be a four component equilibrium system between BGL, CGL, apatite and magnetite in the final stage before complete solidification. Another factor affecting element partitioning may be the extreme alkalinity of the system as it neared solidification.

A final argument against immiscibility arises as a result of the altered nature of the mafic glass phases. The presence of chlorophaeite is documented in basalts by many authors (Peacock and Fuller 1928, Meyer and Sigurdsson 1978). The nature of water causing this alteration is important. If the water is a concentrated magmatic phase, in equilibrium with the magma (Sheppard 1986), then the chemistry of the system may be relatively unchanged. Conversely, meteoric water will tend to remove material from the system as the flux of water is being constantly renewed.

A positive test for the type of water involved lies in oxygen isotope composition. $\delta^{18}O$

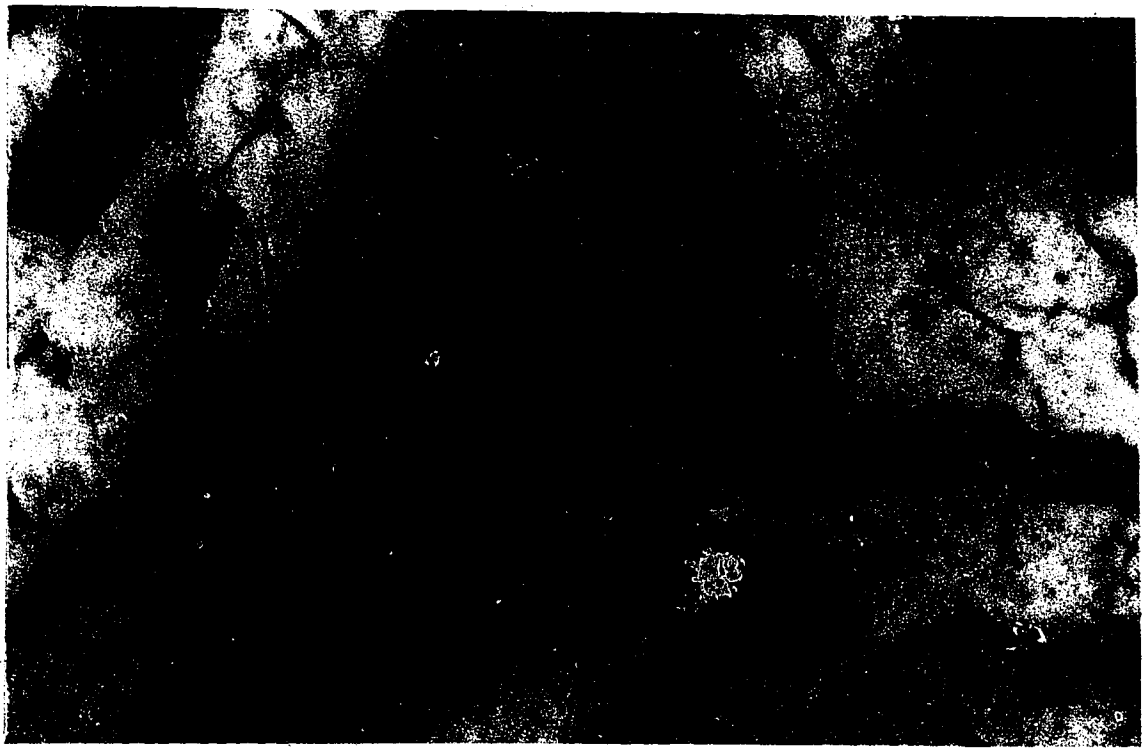

Plate 9. Typical occurrence of apatite within colourless glass from 6983. Field of view is 0.55 mm, plane polarized light conditions.

values from glass phases in the CRBG range from +10.5 - +12.8‰, Table 12. This is generally consistent with the $\delta^{18}O$ range from magmatic waters. Sheppard (1986) determined the average values of magmatic waters to be between +5 - +13‰. Primary magmatic waters, those originating at depth and travelling to the location of emplacement with the lava generally fall in the interaction between a mafic material and the concentrated magmatic water in the residuum rather than the interaction of ground water with the mafic material.

Alternately, based on simple calculations for the exchange of isotopes between ground water and rocks produce the same results.

$1000 \ln\alpha_{(min\text{-}water)} = 25‰ @25°C$

$= {}^{18}O_{(min)} - {}^{18}O_{(water)} = 25‰$

$= {}^{18}O_{(min)} - -13 = 25‰$

$= {}^{18}O_{(min)} = +12‰$

Where -13 is the average meteoric water in Idaho, extrapolated from Dansgaard (1964), and 25‰ is the partitioning coefficient of oxygen between water and rock at 25°C.

The value determined for the secondary minerals in the equation are very similar to that seen in the glasses in the CRBG glasses. This alteration of the rocks in many cases seems to be confined to an isotopic exchange: most minerals appear fresh and unaltered.

This puts a controlling factor on arguments about immiscibility based on chemical evidence if the rocks have exchanged with an external chemical system. However, most chemical arguments are based on major element data which in most phases do not seem to have been significantly altered. It seems likely that alteration for the most part may be confined to isotopic exchange between the rocks and fluids in the system. The only exception to this would seem to be the mafic glass phase which appears highly altered in most samples suggesting that the chemistry may have changed as a result of the weathering process. This does not in any way preclude the possibility that the chlorophaeite is an altered, brown, mafic glass in the residuum of the system. It does however

Table 12.

Sample #	$\delta^{18}O$
6909 BGL	+ 12.81
6910 BGL	+ 10.59
6983 CGL	+ 11.24

Table 12. $\delta^{18}O$ values of glass separates from the Columbia River Basalt Group. Experimental procedure is as described by Clayton and Mayeda (1963), and is accurate to ± 0.02‰.

raise questions concerning the mafic material such as: what was its original composition?, and what materials and in what quantities have been lost or gained from the fluids?

Arguably, some of the evidence presented thus far seems to contradict the theory of liquid immiscibility. However, textural relationships, and major and trace element variations corresponding with experimental systems indicating immiscibility cannot be ignored, the challenge is to account for the partitioning of Ti and P in this system.

SUPERCOOLING

Observed textures and grain sizes, small average crystal size (<0.5mm), and rare phenocryst occurrence are suggestive of a rapid cooling rate in the CRBG. The long acicular habit of apatite crystals is especially indicative of rapid cooling. Laths of apatite exhibit a bimodal length:width ratio. Common to most member units is a 20 - 25:1 length:width ratio which occurs in apatite crystals included within the colourless glass phase, plate 10. In addition, each unit has a further, more individual, apatite occurrence with length:width ratios ranging form 30 - 90:1, plate 10, this is consistent with 50:1 l:w ratios of apatite from upper Yakima flows (Schmincke 1967). These high l:w ratios are the cross cutting apatites that grow across grain boundaries. These crystals are usually solitary and do not account for a high percentage of the apatite present.

Due to the length of time required to ensure plagioclase nucleation in cooling basic magmas (10^5 hrs) Gibb (1974) concluded that units of the Picture Gorge may have been supercooled. Lofgren (1980) describes a progression of feldspar crystal morphology from thin tabular, to elongate skeletal, to dendritic and finally to spherulitic with increasing amount of supercooling. A comparison of these textures and the tabular nature of observed in the CRBG correspond to the texture Lofgren (1980) describes with supercooling 40°C below the liquidus.

Gibb (1974) concluded that the nucleation and subsequent growth of plagioclase and pyroxene was suppressed approximately 50°C . This would account for the nearly equal occurrence of olivine and clinopyroxene in the sample FG10104 (from Waters 1961). The rocks from this study show a general increase in modal abundance from olivine to plagioclase in all members. Data from Waters (1961) shows no more than occasional equality in the three phases. In most cases plagioclase and clinopyroxene are enriched by a factor of 20 of more with respect to olivine.

It is therefore unlikely that the amount of supercooling was on the order of 40°C in the

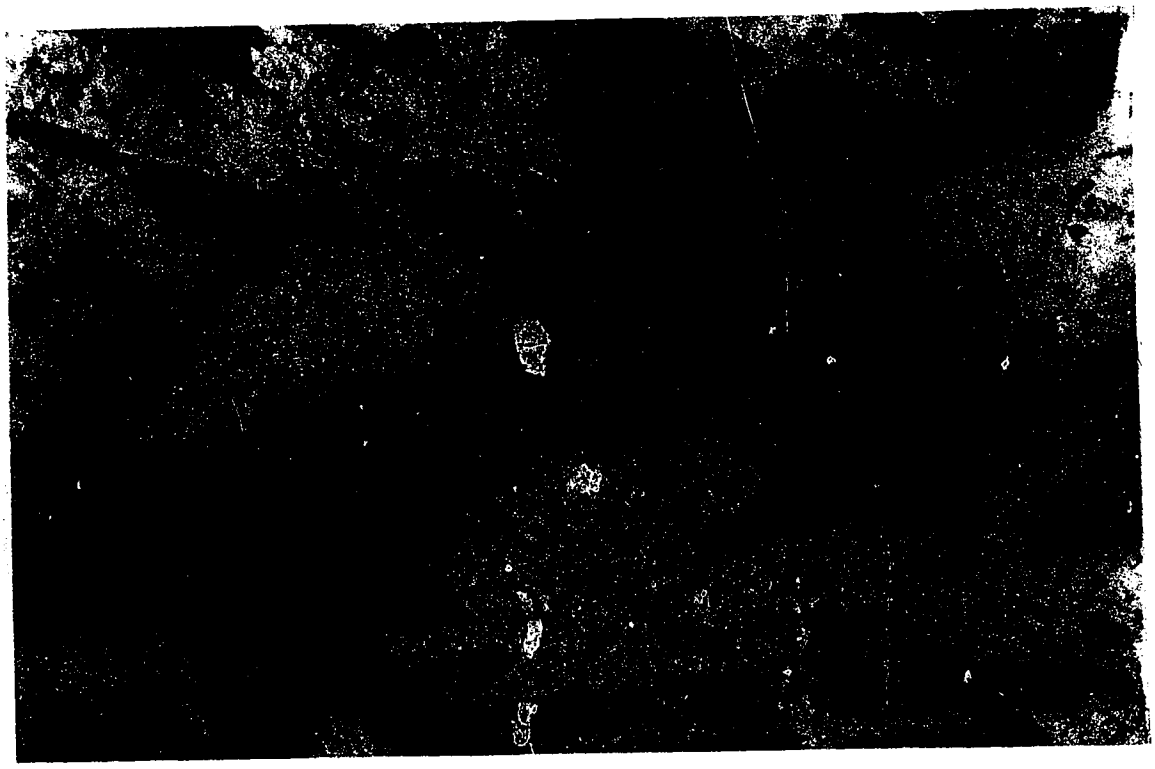

Plate 10. High length:width ratio of apatite crystals and cross cutting of mineral boundaries are evident in the large central crystal from 3AS7. Field of view is 1.4 mm, plane polarized light conditions.

CRBG lava units. Suppressions of 20°C (1198°C to 1180°C) may delay the onset of plagioclase nucleation, (Gibb 1974 data). Lofgren (1980) determined that plagioclase should be reverse zoned if super cooling has occurred. Gibb (1974) lists a petrographic complication: there is no reverse zoning in Waters' (1961) sample FG10104. Similarly, there is no evidence of reverse zoning in the samples from this study. Crystal spectrometers tuned to Na and Ca were traversed across the various zones in a plagioclase phenocryst similar to that in plate 11. Ca counts rose from 75 cps to 7500 cps going from rim to core while Na counts dropped from 200 cps to 10 cps. The increased Ca content in the core supports normal zoning in this sample.

This evidence suggests that supercooling of the CRBG was not pervasive. It may however have affected units on an individual basis such as that represented by Waters' (1961) sample FG10104. Even such isolated occurrences must be examined to ensure that all the theoretical constraints are met. However, a sound argument based on fine grain size can be made for rapid cooling of the extruded magmas.

PETROGENESIS

Views concerning petrogenesis, emplacement methods,and the ultimate origin of the CRBG vary greatly. However, each in turn must address certain fundamental parameters. Firstly, the sequential order of the individual flows is not accompanied by simple compositional evolution patterns of the flows. Commonly less evolved units overlie more evolved units. Secondly, the individual flows are highly varied with respect to chemical and isotopic signatures. Units that have undergone little chemical differentiation do not have typical primitive melt $^{87/86}Sr$ ratios or ^{18}O compositions. Thirdly, in many units evidence of fractionation, primarily of olivine and to a lesser extent of plagioclase and pyroxene are evident, but geophysical evidence (Hill 1977) does not support the presence of dense cumulate layers that should be associated with this process. Catchings and Mooney (1988) model deep crustal sills beneath the CRBG based on high velocity seismic data. However, simple volumetric calculations show this layer to be insufficient to produce the volume of the CRBG from simple fractionation of a typical melt of the upper mantle. Finally, evidence from glass phases requires that very little fractionation of plagioclase or clinopyroxene be involved in the petrogenetic model. Lack of phenocrysts and chemical differentiation from the base to tops of flows indicate that the magmas were emplaced and cooled without significantly altering whole rock composition. In such a model glass phases are a result of nonfractional crystallization of the bulk magmas. The following discussion will deal systematically with the major theories of CRBG genesis.

SILL MODEL

The first major petrogenetic theory concerning the emplacement of the CRBG to be considered is that of Cox (1980). In this model the primary magma source is a Mg-rich mantle picrite which undergoes subsequent fractionation to produce the highly evolved nature of the surface basalts. The picritic magma is emplaced at or near the crust mantle boundary in sill-like bodies where pre-eruption fractionation occurs.

To counter arguments that dense sill like bodies have not been located by geophysical methods (Hill 1977), Cox (1980) suggests that as fractionation progresses the sill will differentiate into a lower ultramafic layer which will appear as mantle material consistent with findings by Catchings and Mooney (1988). This will be overlain by gabbroic material that will appear to be lower crust. The Moho in this area will now appear to be at the boundary separating the upper and lower units of the differentiated sill. In a consideration of Lesotho lavas Cox and Hornung (1966) determined that a 1.5 km lava pile on the surface represented 15% fractionation and was associated with a 0.26 km thick layer of gabbroic cumulates overlying 0.53 km of dunite material. Comparison of CRBG data with that of Lesotho (Cox and Hornung 1966) suggests, on the basis of Fe/Mg ratios, that the African basalts are somewhat more fractionated.

If the CRBG represents only 10% fractionation the volume of the dense cumulate layer should be on the order of 20,000 km^3. A body of such dimensions should be easily located by geophysical methods such as those carried out by Hill (1972). In fact, such a body has now been found (Catchings and Mooney 1988). Data found in figures 6, 7, and 11 from MacDonald *et al.* (1987) suggests that some ferrobasalts in Askja represent 65% fractional crystallization, ferroandesites represent roughly 84%, and finally rhyolites 91% crystallization of the bulk parental magma. The chemical composition of icelandites (ferroandesites) are very similar to that of the Wanapum formation of the CRBG. This indicates that CRBG flows may represent in the order of

65% fractional crystallization of a parental magma similar to the Askja magma. This requires a volume of cumulate layers of roughly 330,000 - 382,000 km^3. If confined to the immediate area of the dyke swarms the layer of cumulates would be on the order of 1/2 to 1 times the thickness of the local crust (Lambert, 1987 pers. comm.). This volume is of the order of 2x that which may reside in the sill proposed by Catchings and Mooney (1988). This argument further supports the lack of validity of crystal fractionation as the sole process of formation of the CRBG due to the lack of geophysical evidence to support sufficiently large volumes of associated cumulates. However, to this end Cox (1980) postulates that repeated injection/fractionation in the sill will produce a broad diffuse seismic Moho. This will account for the lack of dense cumulate bodies which are masked by the diffuse Moho.

The highly varied nature of the basalts is attributed to highly varied polybaric fractionation processes (Cox 1980, Cox and Jamieson 1974). The fractionation of olivine, pyroxene, and plagioclase occurs over a large pressure range, 35 Kbar to 1 atmosphere. Plagioclase is removed in high quantities as a late stage in a low pressure regime (Cox 1980). Hooper *et al.* (1984) modelled the fractionation of the CRBG using a model described by Wright and Doherty (1970). Conclusions from this modelling were that in no cases could crystallization alone account for the variation between Imnaha and the later Grande Ronde units. Similar modelling when accounting for the assimilation of country rock (Carlson 1984) or recharge of the magma system as proposed by O'Hara and Matthews (1981) still fail to model the fractionation process that will derive the Grande Ronde from the Imnaha.

Incompatible trace element variation diagrams presented in this study contradict the supposition of high amounts of either pyroxene or plagioclase fractionation. Variation diagrams such as Fe/Zn (Figure 19) should show marked decreases in Fe and Zn, if these elements are concentrated in the pyroxene structure (Rankama and Sahama 1950, and Vlasov 1966) and pyroxene removal has occurred. Rather, the observed trend is a relatively constant Fe value associated with

rising Zn contents. This trend provides compelling evidence that major pyroxene fractionation has not occurred.

Trace element data concerning plagioclase fractionation is less conclusive. Elements used to trace the selective removal of plagioclase are Ca and Sr, both enriched in the plagioclase structure (Rankama and Sahama 1950, and Vlasov 1966), and K, Rb, and Ba all enriched in the K-feldspar (which is part of the CGL component in the CRBG). The variation diagrams K-Ba, and K-Rb both show the expected trends associated with plagioclase removal, systematic increases in K, Rb, and Ba as a result of all these elements being incompatible with the plagioclase structure. (figures 20 and 21 respectively). However, data concerning Ca and Sr are not as definitive. The Ca-Sr variation diagram (figure 19) should show a clear decrease in the contents of each element if plagioclase fractionation has occurred. Similarly, Sr-Rb (figure 18) should show decreasing Sr contents associated with increasing K and Rb in the residual material. Again, as with Ca-Sr this trend is not observed. In addition, the lack of Eu anomalies (B.V.S.P. 1981, Nelson 1983, Hooper *et al.* 1984 Hooper 1985) do not indicate plagioclase fractionation. The glass phases, formed as a post eruptive event, do indeed exhibit the predicted negative Eu anomalies which result from the crystallization of the plagioclase in these flows.

The final and perhaps most compelling evidence against fractionation of partially melted upper mantle material producing these flood basalts is isotopic. Heavy oxygen isotopes are concentrated in quartz relative to other minerals (Faure 1977, Taylor 1968) and ^{18}O values generally increase as a function of fractionation from ultramafic to acidic rocks (Faure 1977, Taylor and Sheppard 1986). Typical ocean ridge basalts, considered to be primary partial melts of the depleted upper mantle, consistently exhibit $\delta^{18}O$ values of $+5.6\pm0.3‰$ (Taylor and Sheppard 1988). Andesites have similar values ranging from +5.5 - +7.4‰. Finally, granites and associated igneous rocks range from +7 - +13‰ (Faure 1977, Taylor 1968, Taylor and Sheppard 1986).

Data collected from the CRBG show a variation in $\delta^{18}O$ values from unit to unit in the flood basalt province, table 13. The basal Imnaha has a $\delta^{18}O$ value of +5.6‰ Picture Gorge values range from +6.26 - +6.64‰ the Grande Ronde unit ranges from +6.79 - +7.32‰ and finally the Wanapum ranges from +6.75 - +7.08‰ Due to the very highly varied chemical nature of the Saddle Mountain Basalts no samples from this unit were analyzed. Taylor and Sheppard (1986) state that oxygen isotope variations greater than 1 per mil should be suspected as being representative of a process other than simple fractionation. The $\delta^{18}O$ variation with the CRBG samples is mostly less than 1 per mil. Also, isotope values do not concur with evolved chemical signatures. Picture Gorge unit which is less chemically derived than the underlying Imnaha unit, has a higher ^{18}O ratio indicative of greater amounts of fractionation.

Some evidence would suggest that the model of partial melt of upper mantle material in a series of basal crustal sills followed by fractionation and later emplacement proposed by Cox (1980) is an oversimplification of the CRBG's origin. While the model satisfies chemical/sequential parameters, where primitive units such as Picture Gorge overlie more derived units such as the Imnaha by emplacing magmas from separate sills at different times, it fails to satisfy isotopic/chemical parameters. Units such as the Imnaha and Wanapum have more chemically evolved signatures than their isotopic signatures would suggest.

CRUSTAL CONTAMINATION

The second major petrogenetic theory put forward for the origin of the CRBG is proposed by Carlson (1984), who explains incompatible element enrichment, as well as radiogenic and stable isotope values, by a mixing procedure involving a typical upper mantle source as a crustal component. In the next section a brief description of the five components proposed by Carlson (1984) will be discussed and compared to data collected through the course of this thesis.

Component one, C1, has $^{87/86}Sr$ ratios < 0.7035 and $\delta^{18}O$ = +5.5‰. Carlson (1984) interprets this component as depleted upper mantle. C1 best corresponds to Picture Gorge and isolated occurrences within the Imnaha. $\delta^{18}O$ values determined in this thesis for Imnaha units are +5.6‰ Picture Gorge units are higher ranging from +6.3 - +6.5‰. $^{87/86}Sr$ ratios determined by Lambert (1987 unpublished, the body of samples used by Lambert was the same as those used in this thesis), for Picture Gorge units are, 0.703, Imnaha data is not available. The combination of data from this study and that of Lambert (1987 unpublished) would seem to confirm the validity of C1 as proposed in this model.

Component two, C2, has higher $^{87/86}Sr$ ratios = 0.704, and $\delta^{18}O$ values are > +6.0‰. The most likely interpretation of C2 is contamination of a mantle region very similar to C1 by subducted sediments. Based on data presented by Church (1976), Carlson (1984) estimated that only 2% of subducted sediments would be required to produce the isotopic composition of C2. This component is considered to best be represented by units in the Imnaha. The Imnaha sample from this study has a lower $\delta^{18}O$ value of +5.6‰ ($^{87/86}Sr$ values from Lambert (1987 unpublished) are unavailable for comparison.

Component three, C3, is characterized by low $\delta^{18}O$ values (< +6.0‰), and higher $^{87/86}Sr$ ratios, (0.7075). C3 is represented by sample in Saddle Mountains units; Asotin, Elephant Mountain,

and Martindale. Due to the varied nature of the Saddle Mountains members $\delta^{18}O$ values were not determined. $^{87/86}Sr$ values taken from B.V.S.P. (1981) range from 0.708 - 0.713. Based on arguments presented by Semkin and DePaolo (1983) C3 probably represents a mixture of remobilized lower crust added to typical upper mantle material. Another possible explanation of C3 is that it represents an enriched subcontinental lithospheric unit (Carlson 1984 Morris and Hart 1983). The inherent problem with C3 representing any great amount of surface material is that the mixing process must be very consistent over a long period of time in order to produce the extreme volumes of chemically similar material. Also, these units are not stratigraphically continuous, therefore requiring duplication of the mixing process to a high degree at different times and locations throughout the history of the region.

Component four, C4, has very high $^{87/86}Sr$ ratios and $\delta^{18}O$ values (Carlson 1984) and is responsible for the variation seen in the Grande Ronde and various units in the Saddle Mountains. C4 is interpreted as crustal contaminant, most likely ancient granitic material from the lower crust. Prestvik and Goles (1985) concur with the occurrence of a deep crustal component as a source of contamination. This is in part based on the lack of calderas and collapse structures in the area. These structures should occur if a large volume of magma were stored in shallow crustal sills and then extruded.

Component five, C5, also has high $^{87/86}Sr$ ratios and ^{18}O values (Carlson 1984). The existence of C5 is necessary to account for anomalous Pb isotope ratios in various members of the Saddle Mountains unit. Pb data are not available to this thesis for comparison. Again, C5 is interpreted as another continental source of contamination, but has more highly enriched isotope signatures. These are probably a result of remobilization of the lower crust that has been affected by metamorphism up to granulite facies.

Carlson (1984) attributes the majority of CRBG volcanism, Imnaha, Picture Gorge, and

Grande Ronde, to a melting of mantle material similar to C2. The highly enriched incompatible element nature of the basalts is a result of extensive fractionation of a plagioclase and pyroxene assemblage in deep crustal or mantle reservoirs (Cox 1980). This model also incorporates extensive assimilation of a granitic crustal material, C4, (Carlson 1984, Heltz 1980). In a similar fashion Hooper (1985) models three small sequential units within the Saddle Mountains using mixing processes involving components C2 and C4 of Carlson (1984). This initial mixing is associated with an additional process such as crystal fractionation or differing amounts of initial partial melt to account for differences in these units.

The later stage eruptions of the Wanapum differ chemically from the preceding units. These variations are interpreted as representing partial melting and associated fractionation and contamination of distinct, separate reservoirs. The Saddle Mountains Basalts have a highly varied chemical nature ranging from very primitive to highly derived. Based on $\delta^{18}O$ values Carlson (1984) interprets these basalts as representing a deep, pristine mantle source. The varied chemical nature between flows is a function of the extent of crustal contamination which affects the individual units before extrusion. Variations within flows are due to varying amounts of melt produced, heterogeneous mixing of contaminants, and differences in bulk chemistry of the contaminant.

It is, at first, difficult to find fault with this hypothesis. DePaolo (1983) argues that crustal contamination is unlikely, on the basis of the lack of associated rhyolitic volcanism in this province. Evidence from this study indicates that this clearly is not justified given the large quantities of rhyolitic, colourless, glass present. A similar argument may be presented based on the extreme rarity of xenoliths of country rock associated with the feeder dykes of the CRBG (Tauenbeck 1969). A further argument was proposed by DePaolo (1983) based on Nd isotopic values. This argument was based on a semantic difference of interpretation of the same data by the two authors. New Nd isotope data are not available to this study for the purpose of comparison and as such will not be treated further. The final argument proposed by DePaolo (1983), suggesting that trace element

enrichment can be easily accounted for by simply tapping a less depleted, more pristine mantle source is valid and forms the first real contradiction to this model.

Another argument that seems to indirectly contradict this model is the required consistency of process to produce such large volumes of homogeneous material. If the partial melt of mantle material occurs at a pseudoinvariant point as described by Presnall (1969) then the initial melt products as determined by the process must be uniform. Therefore, the resultant differences between flows, and within flows must be a result of the mixing procedure. For a voluminous formation such as the Grande Ronde to be the result of continuous, constant mixing of crustal components C4, and C5 with the primary melt C2, and to exhibit such large scale homogeneity seems very unlikely (Hooper *et al.* 1984). Hooper *et al.* (1984) also point out that the mixing process must be very efficient to mix the two materials to a homogeneous state before extrusion. Again, this is a highly unlikely situation.

A further evidence against this model is the trace elemental abundances of elements controlled by plagioclase and pyroxene removal. The CRBG does not exhibit a negative Eu anomaly associated with plagioclase removal in whole rock data (B.V.S.P. 1981, Hooper *et al.* 1984). Similarly, increasing Fe and Zn contents in whole rock analysis do not support the removal of large amounts of pyroxene, which preferentially removes Fe and Zn, as a process of magma genesis.

The explanation of the colourless and brown glasses recorded in this study in the context of this model could be two fold. Firstly, they could be a result of an immiscible nature of the residual glass phases as the mixed bulk magma cooled. The second possibility is that the colourless glass represents the melt produced by the assimilation of granitic material which did not mix with the basaltic primary melt. There are two reasons why the latter is not likely. Firstly, there is little evidence of xenoliths of country rocks within the CRBG (Tauenbeck 1969). More compelling is the improbability that the assimilated country rock would exhibit the same anomalously high Fe/Mg

ratio as the mafic glass in the basalts, or possess the isotopic characteristics of the CRBG.

Additional arguments based on oxygen isotopes will further negate this line of reasoning. The incorporation of 20% granitic material with $\delta^{18}O$ ranging from +7 - +12‰ (Faure 1977, Taylor 1986, and Taylor and Sheppard 1986) with typical upper mantle derived products with $\delta^{18}O$ values of +5.6‰ should produce higher $\delta^{18}O$ values than are seen in these basalts (Nelson 1983) Table 13. If the model incorporates some fractionation, as it does, this too should serve to increase the concentration of heavy oxygen in the residual glass. Data presented by Taylor and Sheppard (1986) suggests that an assimilation of 20% granitic material may increase the concentration of heavy oxygen to roughly +10‰. By the time that $^{87/86}Sr$ ratios have risen to 0.705 (the average for the CRBG). This points to problems with the model of large scale crustal contamination.

A final argument may be presented in the mechanism of assimilation. The heat required to melt country rock is generally thought to come from the excess heat given off as a result of crystallization (latent heat of crystallization). In this model large amounts of crystallization must occur in the sills or dykes in order to facilitate the assimilation of the contaminant. Resultant bodies of sufficient amounts of crystalline material have not been found by standard geophysical methods (Hill 1972, Catchings and Mooney 1988).

The crustal contamination model proposed by Carlson (1984) has many distinguishing features. All the observed chemical and spatial trends can be produced without great amounts of fractionation. However, the arguments against this model point to a number of weaknesses involving problematic consistency, isotopic values and the lack of dense, crystalline bodies. These difficulties must be addressed in order to satisfy all parameters seen in the CRBG. To this end a new model to explain the origin of this flood basalt province based on the partial melting of eclogite as the primary source of these basalts will be proposed.

Table 13.

Sample	Unit	$\delta^{18}O$
6909	Wan.	+ 6.91‰
6913	G.R.	+ 6.84‰
6916	P.G.	+ 6.60‰
6919	P.G.	+ 6.58‰
6922	P.G.	+ 6.33‰
6931	G.R.	+ 7.32‰
6946	Imn.	+ 5.71‰
6983	Wan.	+ 7.10‰
6893 *	Wan	+ 6.89‰

Table 13. $\delta^{18}O$ values from representative whole rock samples of type Columbia River Basalts (Lambert et. al. 1989). Experimental procedure is after Clayton and Mayeda (1963). Accuracy is ± 0.02%.

* 6983* is a plagioclase separate rather than a whole rock sample.

ECLOGITE MODEL

General Considerations

The model proposed here for the generation of the CRBG is the "eclogite model". It suggests that the initial partial melt is not a typical upper mantle source such as that which produces MORB. Heltz (1980) similarly concluded that the parental material responsible for the Ice Harbor unit must be an Fe-rich pyroxenite rather than lherzolite of harzburgite. Prestvik and Goles (1985) discuss the possibility of producing trace element enriched magmas from partial melt product of a subducted lithospheric slab in a discussion of the Saddle Mountains unit. Clearly, the trace element enrichment, and sequential problems encountered in the CRBG requires a more complex magma genesis mode than simple melting of a typical upper mantle source. The eclogite model was initially proposed to account for the extreme variability in observed incompatible trace element chemistry of the Saddle Mountains units. However, it can be expanded to include the other units and the isotopic and spatial problems encountered in the CRBG.

In this model the precursor event is the formation of MORB. This process occurs at a mid-ocean ridge millions of years prior to the subduction of the slab. The partial melt of lherzolite followed by olivine removal is the accepted model of genesis of MORB's. However, when the slab is partially melted the processes that formed the slab are still imprinted on the partial melt products. It is from this ridge environments that these basalts obtain a signature indicative of large amounts of olivine fractionation, seen in the variation diagrams.

Partial melting of eclogite and small amounts of associated sediments will serve a number of purposes when considering the genesis of the CRBG. The imprint of olivine removal is already present in the partial melt product thereby negating the need for large scale olivine removal from the primary CRBG melts. Similarly, the large enrichments of incompatible can be accounted for

without large scale fractionation. Two-stage partial melting of mantle peridotite and recycled eclogite may enrich incompatible elements by up to 80 X with respect to the mantle (B.V.S.P. 1981). Incompatible elements are enriched in the late stage low temperature phases which are among the first phases to melt with addition of heat to the slab. Nelson (1983) and subsequently Prestvik and Goles (1985) have similarly concluded that the Grande Ronde unit may have undergone tow or three stages of fractionation/enrichment in order to account for the trace element and ^{18}O data.

Thompson (1977) and Barrash *et al.* (1983) provide evidence for the subduction of the Farallon plate beneath the North American continent at the time when the CRBG feeder dykes were active. This is based on the variations in the trend of dyke swarms throughout the region which is probably a result of relative motion of the slab as it moved beneath the continental margin (Barrash *et al.* 1983).

The necessary conditions for partial melt to occur are addition of heat, reduction of pressure, or an increase in volatile content to flux the process. Any of these three methods are conceivably possible in the CRBG. The addition of heat in the form of a diapir of mantle plume is quite likely based on the primitive nature of some units. Thompson (1977) presents evidence for the presence of a diapir beneath the Columbia River region from 10 - 13 million years ago.

The reduction of pressure is also a possibility , less likely, but none-the-less possible. Many authors (Swanson *et al.* 1975, McDougall 1976, Barrash *et al.* 1983, Catchings and Mooney 1988) have proposed widespread extensional rifting associated with the continental margin in the Mid-Miocene. Rifting is presumed to extend to a depth consistent with the magma chambers, the base of the crust, to facilitate magma emplacement. It does not seem likely that the rifts will extend further down, to the slab, to initiate melting. However, the release of pressure associated with deep rifting in the crust surface may relieve enough pressure at the slab surface to initiate, or sustain a partial melting process.

Water, as a flux, can be easily derived by one of two methods in this model. Increased pressure acting on the layer of sediments as they are drawn down into the mantle may liberate interstitial water. Similarly, the dewatering of hydrous minerals within the slab and the sediments as a result of increased pressure may add water to the system. Either method could liberate the required water to flux the partial melting reaction.

Radiogenic isotope values such as extreme $^{87/86}Sr$ values in units such as Saddle Mountains are accounted for by contamination of the magma by the sedimentary veneer that was drawn down into the mantle by the slab. Based on major element variation diagrams the plagioclase removal has not occurred during the formation of the CRBG. If however, plagioclase removal has occurred the subsequent introduction of a crustal component may explain why chemical evidence does not support the removal of plagioclase from this system.

The opposite arguments can be applied to this situation and the argument against crustal contamination. In this model the contamination is much less, that is the ratio of cumulates to magma is much less than on the diagram from Taylor and Sheppard (1986). Therefore the amount of contamination which is necessary to cause the desired isotopic ratios is quite small. In this way enrichment of K, Ba, Rb, Sr, and Ca need not be attributed to the masking of plagioclase fractionation by later contamination. They are a result of either small amounts of plagioclase fractionation or small amounts of contamination. The very high $^{87/86}Sr$ ratios in the Saddle Mountains units are accounted for by larger amounts of contamination here than in other units.

The Glass Problem

In this model the colourless glass cannot be attributed to simple melting of the sedimentary source. Again the argument of similarity of Fe/Mg ratios arise. As such the high ^{18}O, +10 ,

values of the glasses must be accounted for if they are not a contamination signature. Three possible explanations for the 10 per mil glasses are possible. First, this is a result of surface weathering and interaction with ground water as discussed earlier. Secondly, there may be a result of extreme Rayleigh fractionation of heavy oxygen into the residual silicic phase in the cooling system. Thirdly, the ^{18}O may be partitioned into the remaining melt as a function of the crystallization process. Crystallizing olivine, clinopyroxene, and to a much greater extent magnetite will enrich the residuum in heavy oxygen. The effect of crystallizing plagioclase will neither increase or decrease the melt in heavy oxygen content. This is a result of the plagioclase and whole rock having very similar ^{18}O values in the analyzed CRBG samples.

If crystallization of these basalts were to occur in the following order: olivine, clinopyroxene, plagioclase, and finally magnetite as suggested by various phase diagrams and modal mineralogy the sequence of ^{18}O enrichment in the residuum should be similar to that shown in figure 38. Initial olivine and clinopyroxene crystallization will tend to increase the residual melt in heavy oxygen. When magnetite begins to crystallize at roughly 60% solidification, the very low $\delta^{18}O$ values of magnetite, roughly +3.3 - +3.5‰ (Taylor 1968) the result will be a marked increase in ^{18}O in the residuum during the final 20% crystallization while magnetite is forming.

The large negative europium anomaly in the glass phases is formed in a similar fashion. Europium is concentrated in the residuum until plagioclase begins to crystallize. At this point most of the Eu is drawn into the plagioclase structure and the result is a negative Eu anomaly in the residuum.

^{18}O behaved in the same manner, but no phase such as quartz began to crystallize that could have preferentially removed the heavy oxygen isotope from the melt. Hence the positive ^{18}O anomaly seen in the glass phases today. The result of this process is the relative enrichment of the glasses in ^{18}O and the depletion in Eu with respect to the crystalline phases of the CRBG.

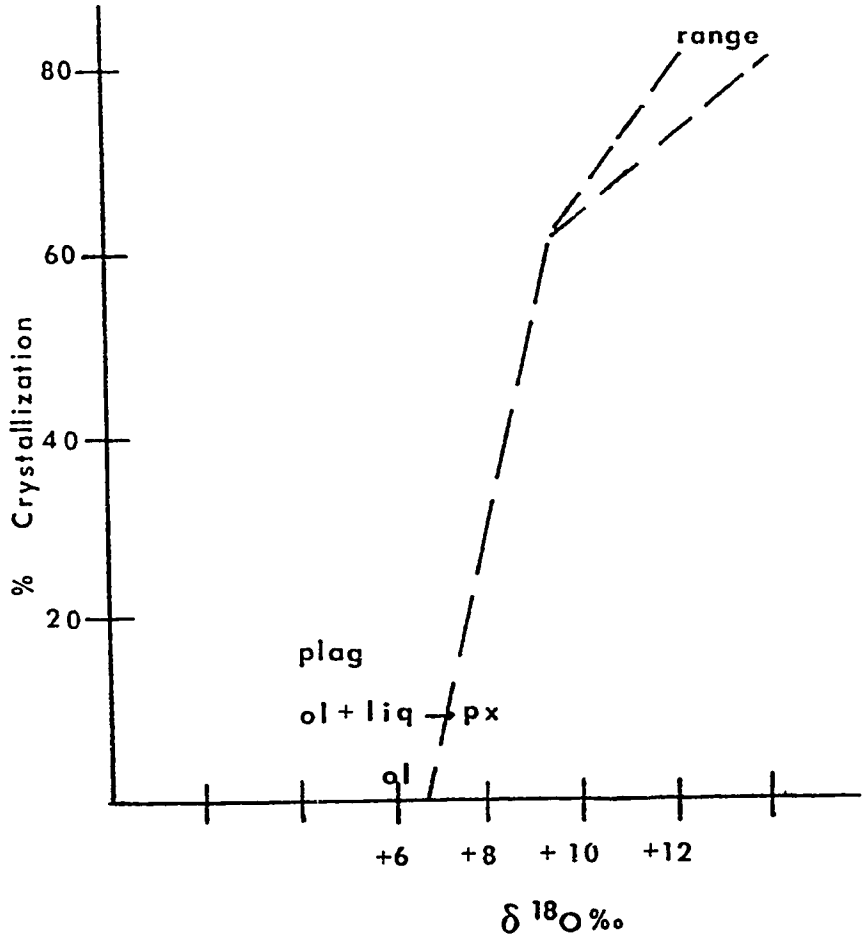

igure 38. Generalized representation of the process for ^{18}O enrichment of the glass phases in ıe CRBG in the context of the eclogite model of emplacement.

Glass phases in this model are a result of crystallization of the magmas under equilibrium conditions. As discussed elsewhere in this section, once the residuum had been preferentially enriched in SiO_2 it split into two immiscible phases. The chlorophaeite represents an alteration of the brown glass as a result of reaction with the magmatic water, which was wholly concentrated in the residuum. At a value of 0.84% H_2O in MWGM (Table 11) and 20% glass in the rock, the original melt would have had 0.17% H_2O by weight, a perfectly respectable mantle value.

This model serves to explain all the chemical, spatial, and isotopic constraints in the CRBG. There is no need for unrelated large scale consistency in mixing processes in different locations. All characteristics are a result of sampling a mantle that is homogeneous on a relatively large scale, yet heterogeneous on an even larger scale. Trace element data consistent with olivine removal is accounted for in a removed environment, yet the signature remains. Similarly, very little fractionation is required which fits well with geophysical data (Hill 1972) which does not provide compelling evidence for large scale dense cumulate bodies.

CONCLUSIONS

Petrographic and chemical evidence demonstrate the existence of two glass phases within the CRBG. Electron microprobe analysis of these glasses reveals that the colourless glass is very rich in: Si (75%), Al (13 - 15%), Na (3 - 4%), and K (6 - 7%), and closely resemble the composition of the granites from the Isle of Skye (Thompson 1969). Moreover, this granitic glass is similar to K-rich granites as described by Pearce *et al.* (1984). The granitic glass commonly contains numerous crystals of apatite, but, P is only detected in the colourless glass in two analyses.

The brown mafic glass which commonly occurs in large drops in the colourless glass is quite commonly altered to a red-brown material. Peacock and Fuller (1928), Waters (1961), Schmincke (1967), and Hearn *et al.* (1984) describe this alteration product as chlorophaeite. The analysis of the brown glass phases are consistent with that of chlorophaeite: Fe (25 - 28%), Mg (8 - 10%), Si (45 - 47%), and H_2O (1 - 24%). In many instances the chlorophaeite of brown glass appears isotropic. Meyer and Sigurdsson (1978) describe a similar occurrence of chlorophaeite in Icelandic basalts. However, as has been discussed, it is the conclusion of this study that the smectite/chlorophaeite is the alteration product of a mafic glass and as such the term brown glass has been used to describe this phase in order to maintain consistency in comparisons between it and the colourless glasses.

The existence of glass phases in the CRBG raises some interesting questions. Primarily, the relationship between the two glasses must be addressed. Textural evidence (the existence of bubbles of brown glass within colourless glass) would immediately suggest an immiscible nature between the two. Boundaries between the two are sharp and chemically well defined, with large chemical differences due to the individual compositions occurring over distances of less than 2 μm.

Trace and major element variation patterns based on the residual glasses indicate that the

crystallization of olivine, clinopyroxene, plagioclase, and magnetite has concentrated Si in the residual melt. The MWGM composition confirms SiO_2 enrichment, containing 69.9% SiO_2 with respect to 49 - 50% SiO_2 in the average Wanapum whole rock analyses. Secondly, in order to polymerize the residual melt and stabilize the two immiscible liquids a system of Al_2O_3 modification or removal is required (Wood and Hess 1977). A very large negative Eu anomaly in the glass phases supports plagioclase removal and Al depletion.

Further chemical evidence based on REE patterns also support immiscibility in the CRBG glass phases. Both glasses exhibit sub-parallel REE patterns and a distinct, equal, negative Eu anomaly. his suggests that both glass phases coexisted at a time after plagioclase crystallization has occurred. The similarity of the negative Eu anomaly dispels the supposition that the smectite is, in this case, an alteration product of olivine as described by Meyer and Sigurdsson (1978) in Iceland. Olivine crystallization occurs prior to the onset of plagioclase crystallization. The olivine structure does not preferentially incorporate REE's and as such will not exhibit the large depletion in Eu, as a result of plagioclase removal, which is which is apparent in mineral and glass phases which formed subsequent to plagioclase removal.

Theoretically, immiscibility in this system can be modelled in two experimental systems. We take first the system K_2O-FeO-Al_2O_3-SiO_2 (Roedder 1952,1978). The addition of Na_2O to the K_2O apex and MgO to the FeO apex of the quaternary system more fully accounts for CRBG chemistry. With these additions the compositions of colourless glass and MWGM both plot within the fields of immiscibility as defined by Roedder (1978). The supposition that these additions will not drastically change the phase relationships in this system is supported in principle by the extreme similarity of the individual phase systems of the original and the added elements along the joins defined by the system. In all cases where one system exhibited immiscibility, the phase relations in the system of the added component did too. Examination of these systems confirmed that the requirement of SiO_2 enrichment in the residuum to facilitate immiscibility (Hess *et al.* 1975,

Rutherford *et al.* 1976). None of the individual phase systems exhibited immiscibility at SiO_2 contents less than 60 - 65%.

Similarly, the immiscibility in this system can be interpreted in terms of the system Fo-Di-Qz (Schairer and Yoder 1961) with FeO and alkalies added.In the natural system, the CRBG, it will be necessary to consider the silica component of the experimental system to be granite (colourless glass). The lowering of the melting temperature associated with granite rather than pure end member quartz will have the net effect of shifting the phase boundaries on this system towards the SiO_2 apex. Once this shift has occurred the whole rock basalts can be plotted in or very near to the field bounded by the En-Di join and the invariant line separating Di_{ss} and Ol, and the invariant line separating Di_{ss} and Pr_{ss}.

Crystallization of olivine or clinopyroxene will drive the composition across the diagram to the Di_{ss}-Ol invariant line, where a phase is lost when olivine reacts with the liquid to produce Di_{ss}. This reaction will continue until the local minimum is reached. The liquid will then move through the field of Di_{ss} with two degrees of freedom until it reaches the invariant line Tr-Di_{ss}, where Tr_{ss}, (or colourless glass) will begin to form. Subsolidus relationships in the system Di-En are such that for the majority of starting compositions, dissolution of Di_{ss} and Pr_{ss} will occur. As such, the end composition of this system will be Di_{ss} (clinopyroxene), tridymite (colourless glass), and Pr_{ss} (brown glass which is 80% normative hypersthene). This predicted end composition models the final phases in the CRBG quite accurately. The oddity that occurs is the occurrence of Pr_{ss} as a liquid rather than a crystalline phase. The co-occurrence of clinopyroxene with orthopyroxene has not been noted in this body of data. It must therefore be concluded that within the context of the system Fo-Di-Qz the crystallization of the CRBG encounters an unknown phase relationship within the field of Di-En such that the Pr_{ss} component is expressed as a liquid rather than as a solid phase. This could be the intersection of an immiscibility field with the solidus of the Di-Fo-Sio_2 -(Na alkalies) system.

The combination of the aforementioned arguments would seem to point to a strong likelihood of immiscibility having occurred at some point during the cooling process. The major drawback to this supposition is based on experimentally determined partitioning coefficients of the incompatible trace elements between acidic and basic melts (Watson 1976). Watson's (1976) experimental data supported by many studies of naturally occurring immiscible liquids (Roedder and Weiblen 1973, Meyer and Sigurdsson 1978, Roedder 1978, and Nelson 1983) suggest that Ti, and P and the REE's should all strongly partition into the unpolymerized basic melt with respect to the coexisting acidic melt. Microprobe and instrumental neutron activation analysis data indicate that in the CRBG this has not occurred. Ti and P, as are the REE's, are enriched in the acidic glass by a factor of 2 - 10. This would seem to be compelling evidence that the glasses were not immiscible.

Another argument against immiscibility is based on the stable isotope signature of the glasses. It can be shown that the +10 - +12% $\delta^{18}O$ values of these glasses can be produced by an interaction with local meteoric waters with $\delta^{18}O$ values of roughly -13 (Dansgaard 1964). If the glasses are alteration products the arguments for immiscibility based on chemistry are weakened. However, this can be countered by producing the isotopic signature of the glasses by simple partitioning of the heavy oxygen as the system crystallized. In such an argument the chlorophaeite will represent an alteration product of brown glass (Pr_{ss}), by a concentrated magmatic water rather than a meteoric water.

To conclude the discussion of immiscibility there are sufficient data in support of immiscibility to conclude that the glass phases are immiscible products. However, this must be qualified by stating that the apparent immiscibility in this system for some unknown reason does not seem to follow conventional elemental partitioning as described in experimental systems (Watson 1976) or natural systems (Roedder and Weiblen 1973). An experimental melting study of these glasses may shed more light on the immiscibility process in the CRBG residual melts.

Another post eruptive process that may affect the formation of glasses in these rocks is supercooling. Gibb (1974) experimentally describes a suppression of the nucleation temperature of plagioclase of nearly 50°C in the Picture Gorge unit. his and the equal occurrence of olivine, pyroxene, and plagioclase phenocrysts, an assemblage which is only possible if plagioclase nucleation was suppressed seem to support the occurrence of supercooling in the Picture Gorge unit. Data from this study do not confirm this observation. There is a general increase in phenocryst occurrence from olivine to pyroxene to plagioclase. Another indication of supercooling is reverse zoning of plagioclase (Lofgren 1980). Microprobe analysis of zoned plagioclase in Wanapum samples from this study does not reveal any reverse zonation. The data from this study would seem to indicate that supercooling is a localized, unit confined process in the CRBG. However, the extremely fine grain size high length:width ratios present in apatite crystals are evidence of a very rapid cooling process.

The general lack of phenocrysts and large scale homogeneity of the individual flows of the CRBG dictate that the petrogenetic model produces an enriched magma with little fractionation. As such, models such as that of fractionating of deep crustal sills (Cox 1980) are not a suitable method of flood basalt genesis beneath the Columbia Plateau. Similar arguments, in addition to isotopic discrepancies and problems with large scale mixing efficiency can be applied to models requiring crustal contamination (Carlson 1984). The preferred model of magma genesis in this study is that of the partial melt of eclogite producing an enriched mantle source.

The eclogite model easily accounts for isotopic, chemical/sequential problems, homogeneity, and the extreme trace element enrichment in the CRBG without requiring extreme amounts of fractionation. In this model the first stage of elemental enrichment occurs at the mid-ocean ridge. The production of MORB gives the basaltic slab the signature of olivine fractionation that is still apparent when the flood basalts are erupted. This is the first stage enrichment process. The basalt

composition is enriched in incompatible elements with respect to the mantle by the partial fusion process. The second stage of enrichment occurs when the subducted basalt/eclogite is partially fused beneath the continental margin. The combination of these two processes may enrich some elements by 80 X or more with respect to the mantle. The descent of the Farallon plate beneath Western North America (Thompson 1977, Barrash *et al.* 1983) provides the subducting body required by this model. The initiation of fusion of the eclogite slab is likely due to the influence of heat from a mantle diapir during the Mid-Miocene when the CRBG was erupted (Thompson 1977). This is supported by the very primitive chemical nature of some of the Picture Gorge units (Carlson 1984, this study). Another possible cause of the partial melt is the addition of water as a fluxing agent released by the dewatering of the sedimentary veneer on the slab or the dewatering of hydrous minerals in the slab. These possibilities are substantiated by the extreme $^{87/86}Sr$ ratios in the Saddle Mountains unit and minor enrichments in K, Ba, Rb, and Sr in the absence of plagioclase fractionation in some units. These observations are likely of a small degree of crustal contamination.

The subcontinental wedge is now enriched by the partial melt products derived from the slab and the incorporation of a small amount of subducted sediments. Homogeneity within large scale flows is due to melting at a pseudoinvariant point as described by Presnall (1969). The mantle source is homogeneous on a large scale (to produce homogeneity within flows), yet on a larger scale is heterogeneous, in order to account for differences between flows. This model is similar to the plum pudding model described by Morris and Hart (1983). Chemical/sequential parameters dictate that where primitive material overlies evolved materials the source regions are different, the former not as enriched by the partial fusion process as the latter.

This model does not require substantial subcontinental fractional crystallization as do the models proposed by Cox (1980) and Carlson (1984). Large scale fractionation (other than olivine) is inconsistent with trace and major element variation diagram findings. It is similarly inconsistent with geophysical data, the lack of evidence for the existence of large dense cumulate bodies (Hill

1970).

The colourless glass phase in this model need not be represented by a partial melt of crustal material, or an alteration product to satisfy the it's stable isotope signature. The $\delta^{18}O$ values of the glasses are a function of partitioning of heavy oxygen between mineral phases and the residuum as the melt cooled.

The eclogite model is able to resolve the major problems associated with other models of flood basalt genesis. It fulfils the chemical/sequential and isotopic signature problems of the CRBG whole rock compositions. It also provides a mechanism for large scale homogeneity within flows without having to propose long term consistency of magma mixing in separate chambers. And finally, the requirement from glass data that an enriched magma be emplaced such that major and trace element patterns can be attained by equilibrium crystallization is also met.

BIBLIOGRAPHY

Baksi, A.K., and Watkins, N.D., (1973) Volcanic production rates: comparison of ocean ridges, islands and the Columbia Plateau basalts. Science, V180, pp. 493-497.

Barrash, W., Bond, J., and Venkatakrishnan, R., (1983) Structural evolution of the Columbia Plateau in Washington and Oregon. American Journal of Science, V283, pp. 897-935.

Basaltic Volcanism Study Project (B.V.S.P.), (1981) Basaltic Volcanism on the Terrestrial Planets. Pergamon Press, New York, 1286 pp.

Beeson, M.H., Frecht, K.R., Reidel, S.P., and Tolan, T.L., (1985) Regional correlations within the Frenchman Springs Member of the Columbia River Basalt Group: new insights into the Middle Miocene tectonics of Northwestern Oregon. Oregon Geology, V47 #8, pp. 87-95.

Best, .G., (1982) Igneous and Metamorphic Petrology, W.H. Freeman and Co., 630 pp.

Bowen, N.L., and Anderson, O., (1914) In: Stone R.L., editor, (1947) Phase Diagrams for Ceramists, Part II. The American Ceramic Society. Columbus, Ohio. 152 pp.

Bowen, N.L., and Schairer, J.F., (1932) In: Stone, R.L., editor (1947) Phase Diagrams for Ceramists, Part II. The American Ceramic Society. Columbus, Ohio. 152 pp.

Boyd, F.R., and Schairer, J.F., (1962) The system $MgSiO_3$-$CaMgSi_2O_6$. Carnegie Institute of Washington Yearbook. V62, pp. 68-74.

Brown, G.M., Emeleus, C.H., Holland, J.G., and Phillips, R., (1970) Mineralogical, chemical and petrological features of Apollo 11 rocks and their relationships to igneous processes.In: Levenson, A.L., editor Proceedings Apollo 11 Lunar Science Conference. *Geochimica et Cosmochimica Acta.* Supplement 1. V1, pp. 195-219.

Carlson, R.W., (1983) Comment and reply on "Implications of oxygen-isotope data and trace-element modelling for a large scale mixing model for the Columbia River basalt. Geology. V11, pp. 735-736.

Carlson, R.W., (1984) Isotopic constraints on the Columbia River flood basalt genesis and the nature of the subcontinental mantle. *Geochimica et Cosmochimica Acta* V48 #1, pp. 2357-2373.

Carlson, R.W., Lugmair, .W., and McDougall, J.D., (1981) Crustal influence in the generation of continental flood basalts. Nature. V289, pp. 160-162.

Carlson, R.W., Lugmair, D.W., and McDougall, J.D., (1983) "Columbia River volcanism: the question of mantle heterogeneity or crustal contamination" (reply to a comment by D.J. DePaolo).*Geochimica et Cosmochimica Acta.* V47 #4, pp. 845-847.

Carlson, R.W., Lugmair, D.W., and McDougall, J.D., (1983a) Columbia River volcanism: the question of mantle heterogeneity or crustal contamination. *Geochimica et Cosmochimica Acta.* V45 #12, pp. 2483-2499.

Carmichael, I.S.E., (1964) The petrology of Thingmuli a tertiary volcano in Eastern Iceland. Journal of Petrology. V5 #3, pp. 435-460.

Carter, P.T., and Imbrahim, M., (1952) In: Resner, M.K., editor, (1964) Phase Diagrams for Ceramists 1964 Supplement, Volume II, Figures 1-2066. American Ceramic Society. Columbus, Ohio. 603 pp.

Catchings, R.D., and Mooney, W.D., (1988) Crustal structure of the Columbia Plateau evidence for continental rifting. Journal of Geophysical Research. V93 #B1, pp. 459-474.

Church, S.E., (1976) The Cascades Mountains revisited: A re-evaluation in light of new lead isotopic data. Earth and Planetary Science Letters. V76 #1, pp. 93-96.

Chamberlain, V.E., Lambert, R., St. J., Duke, M.J.M., and Holland, J.G., (1988) Geochemistry of the gneissic basement complex near Valemount, British Columbia: further evidence of a varied origin. Canadian Journal of Earth Sciences. V25 #11, pp. 1723-1739.

Clayton, R.N., and Mayeda, T.K., (1963) The use of bromine pentafluoride in the extraction of oxygen from silicates for isotope analysis. *Geochimica et Cosmochimica Acta.* V27, pp. 43-52.

Cox, K.G., (1980) A model for flood basalt volcanism. Journal of Petrology. V21 #4, pp.629-650.

Cox, K.G., (1983) The Karoo province of Southern Africa, In: Hawkesworth, C.J., and Norry, N.T., editors, Continental Flood Basalts and Mantle Xenoliths. Shiva Publishing Ltd., Nantwich, Cheshire. pp. 139-157.

Cox, K.G., and Hornung, G., (1966) The petrology of the Karoo basalts of Basutoland. American Mineralogist. V51 #2, pp. 1414-1432.

Cox, K.G., and Jamieson, B.G., (1974) The olivine-rich lavas of Nuanetsi: a study of polybaric magmatic evolution. Journal of Petrology. V15, pp. 269-301.

Criss, R.E., and Taylor, H.P. Jr., (1986) Meteoric-Hydrothermal systems, In: Valley, J.W., Taylor Jr., H.P., and O'Neil, J.R., editors, Reviews in Mineralogy, Volume 16, Stable Isotopes in "HIgh Temperature Geological Processes". Mineralogical Society of America, Washington, D.C., 570 pp.

Dansgaard, W., (1964) Stable isotopes in precipitation. *Tellus.* V16, pp. 436-438.

DePaolo, D.J., (1981) Trace elements and isotope effects of combined wallrock assimilation and fractional crystallization. Earth and Planetary Science Letters. V53, pp. 189-202.

DePaolo, D.J., (1983) Comment on "Columbia River volcanism: the question of mantle heterogeneity or crustal contamination" by R.W. Carlson, G.W. Lugmair, and J.D. McDougall. *Geochimica et Cosmochimica Acta.* V47 #14, pp. 814-845.

Dickin, A.P., (1981) Isotope geochemistry of Tertiary igneous rocks from the Isle of Skye, N.W. Scotland. Journal Petrology. 22 #2, pp. 155-189.

Dixon, S.J., and Rutherford, M.J., (1977) Trondjhemites as late stage immiscible liquids from fractionating oceanic basalts. (Abstract) EOS, Transactions of the American Geophysical Union. V58, pp. 520.

Dodds, R.K., (1970) The age of the "Columbia River Basalts" near Astoria Oregon. In: Gilmore, E.H., and Stradling, D., editors. Proceedings of the Second Columbia River Basalt Symposium, Cheyne, Eastern Washington State College Press. pp. 73-96.

Faure, G., (1977) Principles of Isotope Geology. John Wiley and Sons, New York, 464 pp.

Gibb, F.J.G., (1974) Supercooling and the crystallization of plagioclase from a basaltic magma. Mineralogical Magazine. V39, pp. 641-653.

Gilmore, E.H., and Stradling, D., editors (1970) Proceedings of the Second Columbia River Basalt Symposium. Cheyne, Eastern Washington State College Press, 333 pp.

Glasby, G.P., editor (1977) Marine Manganese Deposits. Elsevier Oceanographic Series. Elsevier Scientific Publishing Company, New York, 523 pp.

Glickson, A.Y., (1976) Trace element geochemistry and origin of early Precambrian acid igneous series, Barberton Mountain Land, Transvaal. *Geochimica et Cosmochimica Acta.* V40, pp. 1261-1280.

Goldschmidt, V.M., (1937) The principles of distribution of chemical elements in minerals and rocks. Journal of the Geochemical Society of London. V74, pp. 65-673.

Goles, G.G., (1980) Miocene basalts of the Blue Mountains province in Oregon part I: compositional types and their geophysical settings. Journal of Petrology. V27 #4, pp. 495-520.

Greig, J.W., (1927) Immiscibility in silicate melts. American Journal of Science. V13, pp. 133-154.

Hargraves, R.B., editor (1980) Physics of Magmatic Processes. Princeton University Press, Princeton, New Jersey, 586 pp.

Hawkesworth, C.J., and Norry, N.T., (1983) Continental Flood Basalts and Mantle Xenoliths. Shiva Publishing Ltd. Nantwich, Cheshire, 272 pp.

Hearn, P.P., Steinkampf, W.C., and Brown, Z.A., (1984) Characterization of secondary alteration in the Columbia River basalt by backscattered electron imaging and energy-dispersive X-ray spectroscopy. In: Roming, and Goldstein, editors, Microbeam Analysis, San Francisco Press, pp. 143-145.

Heltz, R.T., (1978) The petrogenesis of the Ice Harbor member, Columbia River Plateau, Washington: A chemical and experimental study. Unpublished PhD Thesis, Pennsylvania State University. 228 pp.

Heltz, R.T., (1980) Chemical and experimental study of the Ice Harbor member of the Yakima basalt subgroup: Evidence for intracrustal storage and contamination. Transactions of the American Geophysical Union. (abstract) V61, pp. 68.

Henderson, P., (1982) Inorganic Geochemistry, Pergamon Press, New York, 353 pp.

Hess, H.H., and Poldervaart, A., editors, (1967) Basalts: The Poldervaart Treatise on rocks of Basaltic Composition Interscience Publishers, New York, Volume I pp. 1-482, Volume II pp. 483-862.

Hess, P.C., (1980) Polymerization model for silicate melts. In: Hargraves, R.B., editor, Physics of Magmatic Processes. Princeton University Press, Princeton, New Jersey, 586 pp.

Hess, P.C., Rutherford, M.J., Guillemette, R.N., Rhyerson, F.J., and Tuchfeld, H.A., (1975) Residual products of fractional crystallization of lunar magmas: an experimental study. Proceedings

of the 6th Lunar Science Conference. V1, pp. 895-909.

Hoffer, J.M., (1980) Plagioclase mineralogy of the Rock Creek flow, Columbia River basalt. In: Gilmore, E.H., and Stradling, D., editors, Proceedings of the Second Columbia River Basalt Symposium. Cheyne, Eastern Washington State College Press, pp. 51-54.

Holden, G.S., and Hooper, P.R., (1976) Petrology and chemistry of a Columbia River basalt section, Rock Canyon, West-Central Idaho. Geological Society of America Bulletin. V87, pp. 215-225.

Holmgren, D.A., (1970) K/Ar dates and paleomagnetics, the type Yakima basalt, Central Washington. In: Gilmore, E.H., and Stradling, D., editors, Proceedings of the Second Columbia River Basalt Symposium. Cheyne, Eastern Washington State College Press, pp. 189-200.

Hooper, P.R., (1974) Petrology and chemistry of the Rock Creek flow, Columbia River basalt, Idaho. Geological Society of America Bulletin. V85, pp. 15-26.

Hooper, P.R., (1982) The Columbia River basalts. Science, V215 #4593, pp. 1463-1468.

Hooper, P.R., (1985) A case of magma mixing in the Columbia River Basalt Groups: the Wilkin Creek, Lapawi, and Asotin flows, Saddle Mountains Formation. Contributions to Mineralogy and Petrology. V91, pp. 66-73.

Hooper, P.R., Kleck, W.D., Knowles, C.R., and Theissen, R.L., (1984) Imnaha basalt, Columbia River Basalt Group. Journal of Petrology. V25 #2, pp. 473-500.

James, D.E., (1981) The combined use of oxygen and radioactive isotopes as indicators of crustal contamination. Earth and Planetary Science Letters. V9, pp. 311-344.

Kracek, F.C., (1930) In: Stone, R.L., editor (1947) Phase Diagrams For Ceramists Part II. American Ceramic Society, Columbus, Ohio, 152 pp.

Kracek, F.C., (1939) In: Stone, R.L., editor (1947) Phase Diagrams for Ceramists Part II. American Ceramic Society, Columbus, Ohio, 152 pp.

Kuo, L-C., Lee, J.H., Essene, E.J., and Pecor, D.R., (1988) Occurrence, chemistry, and origin of immiscible silicate glasses in a tholeiitic basalt. a TEM/AEM study. Contributions to Mineralogy and Petrology. V94, pp. 90-98.

Kushiro, I., (1969) Synthesis and stability of iron-free pigeonite in the system $MgSiO_3$-$CaMgSi_2O6$ at high pressure. Carnegie Institute of Washington Yearbook. V67, pp. 80-83.

Kyser, T.K., Cameron, W.E., and Nisbet, E.G., (1986) Boninite petrogenesis and alteration history: constraints from stable isotope compositions of boninites from Cape Vogel, New Caledonia, and Cyprus. Contributions to Mineralogy and Petrology. V93, pp. 222-226.

Lambert, R. St J., Marsh, I.K., and Chamberain, V.E., (1988) The occurrence of interstitial granite glass in the Columbia River Basalt Group and its petrogenetic implications. Geological Society of America Symposium, Hooper, P.R., and Reidel, S.P., editors, pp. unknown at thesis publication date.

Lindsley, D.H., (1967) The join hedenbergite-ferrosilite at high pressures and temperatures. Carnegie Institute of Washington Yearbook. V65, pp. 230-232.

Lofgren, G.E., (1973) Experimental crystallization of synthetic plagioclase at prescribed cooling rates. Transactions of the American Geophysical Union (abstract). V54, pp. 482.

Lofgren, G.E., (1980) Experimental studies on the dynamic crystallization of silicate melts. In: Hargraves, H.B., editor. Physics of Magmatic Processes, Princeton University Press, Princeton, New Jersey, 585 pp.

MacDonald, R., Sparks, R.S.J., Sigurdsson, H., Mattey, D.P., McGarvie, D.W., and Smith, R.L., (1987) the 1875 Askja volcano, Iceland: combined fractional crystallization and selective contamination in the generation of rhyolitic magma. Mineralogical Magazine. V51 #2, pp.100-121.

Mangan, M.T., Wright, T.L., Swanson, D.A., and Byerly, G.P., (1987) Regional correlation of Grande Ronde basalt flows Columbia River Basalt Group, Washington, Oregon, and Idaho. Geological Society of American Bulletin. V97 #11, pp. 1300-1318.

McDougall, I., (1976) Geochemistry and origin of basalt of the Columbia River group, Oregon and Washington. Geological Society of America Bulletin. V87, pp. 777-792.

McIntosh, H.B., Rait, J.R., and Hay, R., (1937) In: Stone, R.L., editor, (1947) Phase Diagrams for Ceramists Part II. American Ceramic Society. Columbus, Ohio, 152 pp.

Meyer, P.S., and Sigurdsson, H., (1983) Interstitial acid glass in Iceland Basalts. Lithos. V11, pp. 231-241.

Morris, J.D., and Hart S.R., (1983) Isotopic and incompatible element constraints on the genesis of island arc volcanoes form Cold Bay and Amak Island, Aleutians and implications for mantle source. *Geochimica et Cosmochimica Acta.* V47 11, pp. 2015-2030.

Muehlenbachs, K., (1973) The oxygen isotope geochemistry of siliceous volcanic rocks from Iceland. Carnegie Institute of Washington Yearbook. V72, pp. 593-597.

Muehlenbachs, K., (1986) Alteration of the oceanic crust and the ^{18}O history of sea water. In: Valley, J.W., Taylor, H.P., and O'Neil, J.R., editors. Reviews in Mineralogy, Volume 16, Stable Isotopes in High Temperature Geological Processes. Mineralogical Society of America, Washington, D.C., 570 pp.

Naslund, H.R., (1983) The effect of oxygen fugacity on liquid immiscibility in iron-bearing silicate melts. American Journal of Science. V283, pp. 1034-1055.

Nathan, S., and Fruchter, J.S., (1974) Geochemical and palaeomagnetic stratigraphy of the Picture Gorge and Yakima (Columbia River group) in central Oregon. Geological society of America Bulletin. V85, pp 63-65.

Nelson, D.O., (1983) Implications of oxygen isotope data and trace-element modelling for a large scale mixing model for the Columbia River basalt. Geology. V11, pp. 248-251.

Novohatski, I.A., Belov, .F., Gorokh, A.V., and Savinskaya, A.A., (1965) In: Resner, M.K., editor. (1969) Phase Diagrams for Ceramists 1975 Supplement, Volume 4, Figures 4150-4999. American Ceramic Society. Columbus, Ohio, 513 pp.

O'Hara, M.J., and Matthews, R.E., (1981) Geochemical evolution in a periodically replenished, periodically tapped continuously fractionated magma chamber. Journal of the Geological Society of London. V138 #3, pp. 237-277.

Ol'shanski, Y.I., (1951) Equilibrium of two immiscible liquids in silicate systems of the alkaline earth metals. In: Resner, M.K., editor. (1969) Phase Diagrams for Ceramists, 1969 Supplement, Volume 2, Figures 2046-4149. American Ceramic Society. Columbus, Ohio, 625 pp.

Peacock, M.A., and Fuller, R.E., (1928) Chlorophaeite, sideromelane and plagonite from the Columbia River Plateau. American Mineralogist. V13 #7, pp 360-382.

Pearce, J.A., Harris, N.B.W., and Tindle, A.G., (1984) Trace element discrimination diagrams for the tectonic interpretation of granitic rocks. Journal of Petrology. V24 #4, pp. 956-983.

Philpotts, A.R., (1979) Silicate liquid immiscibility in tholeiitic basalts. Journal of Petrology. V20 #1, pp. 99-118.

Philpotts, A.R., (1982) Compositions of immiscible liquids in volcanic rocks. Contributions to Mineralogy and Petrology. V80, pp. 210-218.

Presnall, D.C., (1969) The geometric analysis of partial fusion. American Journal of Science. V267, pp. 1178-1194.

Prestvik, T., and Goles, G.G., (1985) Comments on petrogenesis and the tectonic setting of the Columbia River basalts. Earth and Planetary Science Letters. V72, pp. 65-73.

Rankama, K., and Sahama, T.H.G., (1966) Geochemistry. The University of Chicago Press, Chicago, Illinois, 912 pp.

Rankin, G.A., and Merwin, .E., (1916) In: Stone, R.L., editor, (1947) Phase Diagrams for Ceramists. American Ceramic Society, Columbus, Ohio, 152 pp.

Reidel, S.P. (1983) Stratigraphy and petrogenesis of the Grande Ronde basalt from Deep Canyon County,Washington, Oregon, and Idaho. Geological Society of America Bulletin. V94, pp. 519-542.

Resner, M.K., editor, (1964) Phase Diagrams for Ceramists 1964 Supplement, Volume 2 Figures 1-2066. American Ceramic Society, Columbus, Ohio, 625 pp.

Resner, M.K., editor, (1975) Phase Diagrams for Ceramists 1974 Supplement, Volume 4 Figures 4150-4999. American Ceramic Society. Columbus, Ohio, 513 pp.

Roedder, E., (1951) Low temperature liquid immiscibility in the system K_2O-FeO-Al_2O_3-SiO_2. American Mineralogist. V36, pp. 282-286.

Roedder, E., (1952) In: Resner, M.K., editor, (1964) Phase Diagrams For Ceramists 1964 Supplement, Volume 2 Figures 1-2066. American Ceramic Society, Columbus, Ohio, 603 pp.

Roedder, E., (1978) Silicate liquid immiscibility in the system K_2O-FeO-Al_2O_3-SiO_2: an example of serendipity. *Geochimica et Cosmochimica Acta*. V42 #11, pp. 1597-1617.

Roedder, E., and Weiblen, P.W., (1973) Petrology of some lithic fragments from Luna 20. *Geochimica et Cosmochimica Acta*. V37 #4, pp. 1031-1052.

Ross, M.E., (1983) Chemical and mineralogical variations within four dykes of the Columbia River Basalt Group, Southeastern Columbia Plateau in Washington and Oregon. American

Journal of Science. V283, pp 897-935.

Rutherford, M.J., Hess, P.C., Rhyerson, F.J., Campbell, H.W., and Dick, P.A., (1976) The chemistry, origin, and petrogenetic implications of lunar granite and monzonite. Proceedings of the 7th Lunar Science Conference. V2, pp. 1723-1740.

Schmincke, H.U., (1967) Stratigraphy and petrology of four upper Yakima basalt flows in South-Central Washington. Geological Society of America Bulletin. V78, pp. 1385-1422.

Semkin, S.C., and DePaolo, D.P., (1983) Sm-Nd and Rb-Sr constraints of cenozoic basalt petrogenesis and mantle heterogeneity in the SW great basin. (abstract) Transactions of the American Geophysical Union. V64, pp. 338.

Smith, D.G.W., and Gold, C.M., (1979) EDATA2 a fortran IV computer program for processing wavelength and/or energy-dispersive electron microprobe analyses. In: Newberry, D.E., editor, Proceedings of the 14th Annual Conference of the Microbeam Analysis Society. San Antonio, Texas, pp. 273-278.

Smith, G., editor, (1981) Phase Diagrams for Ceramists 1979 Supplement, Volume 5 Figures 5000 -5590. American Ceramic Society. Columbus, Ohio, 330 pp.

Swanson, D.L., Wright, T.L., and Heltz, R.T., (1975) Linear vent systems and estimated rates of magma and eruption for the Yakima basalt on Columbia Plateau. American Journal of Science. V275, pp. 877-905

Swanson, D.L., Wright, T.L., Hooper, P.R., and Bentley, R.D., (1979) Revisions to the stratigraphic nomenclature of the Columbia River Basalt Group. United States Geological Survey Bulletin 1456-G. United States Government Printing Office, Washington, D.C., 59 pp.

Tauenbeck, W.H. (1970) Dykes of the Columbia River basalt in Northeastern Oregon, Western Idaho, and Southeastern Washington. In: Gilmore, E.H., and Stradling, D., Editors, Proceedings of the Second Columbia River Basalt Symposium, Cheyne, Eastern Washington State College Press, pp. 73-96.

Taylor, H.P., (1968) The oxygen isotope geochemistry of igneous rocks. Contributions to Mineralogy and Petrology. V19, pp. 1-71.

Taylor, H.P., (1980) The effects of assimilation of country rocks by magmas on $^{18}O/^{16}O$ and $^{87}Sr/^{86}Sr$ systematics in igneous rocks. Earth and Planetary Science Letters. V47, pp. 243-254.

Taylor Jr., H.P., (1986) Igneous Rocks II: isotopic case studies in circumpacific magmatism. In: Valley, J.W., Taylor, H.P., and O'Neil, J.R., editors (1986) Reviews in Mineralogy Volume 16, Stable Isotopes in High Temperature Geological Processes. Mineralogical Society of America, Washington, D.C., 570 pp.

Taylor Jr., H.P., and Sheppard, S.M.F., (1986) Igneous rocks I: processes of isotopic fractionation and isotopic systematics. In: Valley, J.W., Taylor, H.P., and O'Neil, J.R., editors (1986) Reviews in Mineralogy, Volume 16 Stable Isotopes in high Temperature Geological Processes. Mineralogical Society of America, Washington, D.C., 570 pp.

Thompson, R.N., (1969) Tertiary granites and associated rocks of the Marsco area, Isle of Skye. The Quarterly Journal of the Geological Society of London. V124 #496, pp. 349-385.

Thompson, R.N., (1977) Columbia/Snake River, Yellowstone magmatism in the context of Western U.S.A. cenozoic geodynamics. Tectonophysics. V39, pp. 621-636.

Valley, J.W., Taylor, H.P., and O'Neil, J.R., editors, (1980) Reviews in Mineralogy Volume 16, Stable Isotopes in High Temperature Geologic Processes. Mineralogical Society of America, Washington, D.C., 570 pp.

Vlasov, K.A., editor, (1966) Geochemistry and Mineralogy of Rare Elements and Genetic Types of their Deposits. Volume I. Israel Program for Scientific Translations Ltd. Jerusalem, 688 pp.

Wager, R.L., (1956) A chemical definition of fractionating stages as a basis for comparison of Hawaiian, Hebredian, and other basic lavas. *Geochimica et Cosmochimica Acta.* V9, pp. 217-248.

Wager, R.L., and Brown, G.M., (1967) Layered Igneous Rocks. W.H. Freeman and Company. San Francisco, 588 pp.

Walters, S.G., and Ineson, P.R., (1983) Clay minerals in basalts of the South Pennines. Mineralogical Magazine. V47, pp. 21-26.

Waters, A.C., (1961) Stratigraphic and lithographic variations in the Columbia River Plateau. American Journal of Science. V259, pp. 583-611.

Watkins, N.D., and Baksi, A.K., (1974) Magneto-stratigraphy and oroclinal folding of the Columbia River, Steens, and Owynee, basalts in Oregon, Washington, and Idaho. American Journal of Science. V274, pp. 148-189.

Watson, E.B., (1976) Two-liquid partition coefficients: experimental data and geochemical implications. Contributions to Mineralogy and Petrology. V56, pp. 119-134.

Wollast, R., (1961) In: Resner, M.K., editor, (1969) Phase Diagrams for Ceramists, 1969 Supplement Volume 3 Figures 2046-4149. American Ceramic Society, Columbus, Ohio, 625 pp.172

Wood, M.I., and Hess, P.C., (1977) (abstract) The role Al_2O_3 in the immiscible silicate melts. EOS Transactions of the American Geophysical Union. V58, pp. 520.

Wright, T.L., Grolier, M.J., and Swanson, D.A., (1973) Chemical variation related to the stratigraphy of the Columbia River basalt. Geological Society of America Bulletin. V84, pp. 371-385.

Wright, T.L., Swanson, D.A., Heltz, R.T., and Byerly,G.R., (1977) Major oxide, trace element, and glass chemistry of Columbia River basalt samples collected between 1971 and 1977. United States Geological Survey Open File Report 79-711, 151 pp.

Appendix 1
Methods of Data Acquisition

The data presented in the following appendices was obtained by the listed methods. A full account of analytical procedures associated with each follows in Appendix 5.

Whole Rock Major Element Data -- XRF analytical technique.
Whole Rock Trace Element Data -- AAS analytical technique.
BGL/CGL Major Element Data -- Microbeam analysis.
CIPW Norms -- Hand Calculation.
Glass Separates Trace Element Data -- INAA.
MWGM composition -- Hand Calculation.
Bubble Boundaries -- Microbeam Analysis.

Appendix 1-A
Saddle Mountain Whole Rock Geochemistry

	6915 a.	6932 b.	6932	6933 a.	6934 b.	6934	6935	6936
SiO_2	50.17	56.78	56.15	56.28	51.17	50.88	50.22	49.54
Al_2O_3	15.70	13.25	13.57	13.40	15.91	15.21	14.19	13.82
Fe_2O_3	2.89	2.95	2.97	3.00	2.82	2.82	3.70	3.88
FeO	8.54	8.86	8.93	8.84	8.36	8.51	11.21	11.37
MgO	6.12	3.26	3.08	3.07	6.06	6.30	4.05	4.26
CaO	11.18	5.81	6.00	6.14	11.00	10.89	8.72	8.90
Na_2O	2.58	2.85	3.02	2.98	2.53	2.60	2.50	2.59
K_2O	0.60	2.81	2.72	2.77	0.68	0.63	1.15	1.44
TiO_2	1.76	2.34	2.37	2.42	1.75	1.73	3.34	3.54
MnO	0.20	0.16	0.19	0.19	0.19	0.19	0.21	0.21
S	0.03	0.04	0.05	0.06	0.04	0.00	0.18	0.12
Total	99.77	99.11	99.05	99.15	99.81	99.99	99.51	99.67
qz	2.56	10.44	10.54	0.76	1.66	5.87	3.34	2.11
ap	0.45	1.96	2.09	1.92	0.45	0.45	1.24	0.85
il	3.34	4.45	4.50	4.60	3.32	3.29	6.43	6.73
or	3.60	16.58	15.05	16.34	4.01	3.71	6.78	8.49
alb	21.81	24.10	25.58	25.19	21.34	21.98	21.13	21.89
an	29.43	15.05	15.43	14.09	28.06	27.95	24.10	21.82
cor	.	.	.	.	.	.	.	.
ol	.	.	.	.	.	.	.	.
hy	16.10	15.07	14.66	13.68	15.45	16.57	15.98	14.62
diop	20.77	6.57	6.74	8.11	20.53	20.19	12.87	16.45
mt	4.19	.	4.31	4.35	4.10	4.09	5.37	5.63
Total	99.85	95.48	99.80	99.82	99.82	99.79	99.97	99.93
U	2.	2.	3.	1.	2.	5.	5.	1.
Th	3.	2.	5.	6.	2.	5.	2.	2.
Pb	13.	10.	19.	11.	9.	13.	13.	7.
Nd	26.	52.	49.	51.	17.	15.	41.	41.
Ce	38.	67.	66.	74.	50.	48.	94.	95.
La	21.	47.	47.	45.	19.	21.	39.	38.
Ba	275.	3753.	3578.	3360.	295.	280.	488.	509.
Nb	14.	21.	23.	21.	14.	15.	24.	27.
Zr	142.	504.	515.	527.	145.	142.	253.	267.
Y	32.	52.	51.	51.	33.	31.	49.	50.
Sr	225.	261.	269.	261.	218.	221.	223.	227.
Rb	22.	53.	48.	52.	19.	21.	34.	44.
Ga	17.	19.	17.	15.	21.	21.	24.	18.
Zn	87.	97.	98.	07.	91.	86.	113.	120.
Cu	64.	1.	7.	1.	66.	61.	15.	16.
Ni	42.	1.	5.	1.	39.	43.	8.	8.
Co	32.	10.	16.	14.	33.	33.	25.	29.
Cr	88.	1.	1.	1.	87.	92.	20.	30.

	3AS4	3AS6	3AS12 a.	3AS12 b.	3AS13	3AS15 a.	3AS15 b.
SiO_2	53.95	52.40	56.18	56.57	56.71	56.39	56.68
Al_2O_3	13.88	13.58	13.74	13.37	13.29	12.64	12.66
Fe_2O_3	3.20	3.28	3.04	3.00	3.07	3.18	3.08
FeO	9.03	9.55	9.14	8.95	8.60	9.15	9.13
MgO	4.29	5.61	3.26	3.74	3.44	3.72	3.90
CaO	8.21	8.99	6.77	6.88	6.79	6.81	6.68
Na_2O	3.24	2.96	3.40	3.34	3.22	3.17	3.16
K_2O	1.64	0.97	1.70	1.61	1.95	2.03	1.93
TiO_2	2.06	2.05	2.14	1.97	1.95	2.23	2.08
MnO	.	.	0.19	0.18	0.21	0.20	0.20
S	0.04	0.08	0.07	0.01	0.08	0.09	0.20
P_2O_5	0.26	0.26	0.42	0.38	0.47	0.43	0.43
Total	99.80	99.69	100.55	100.00	99.95	99.89	99.94
qz	5.03	3.93	9.61	9.92	10.61	8.78	10.31
ap	0.56	0.56	0.91	0.82	1.02	0.93	0.96
il	3.91	3.89	4.07	3.74	4.03	4.24	3.95
or	9.67	5.72	10.03	9.50	11.50	11.98	11.39
alb	27.39	25.02	28.74	28.23	27.22	26.79	26.71
an	18.47	20.89	17.20	16.72	16.04	14.25	14.65
cor	.	.	.	.	.	.	.
ol	.	.	.	.	.	.	.
hy	13.57	16.87	13.46	14.14	12.81	15.56	14.39
diop	17.02	13.41	11.40	12.41	12.13	14.00	12.98
mt	4.64	4.76	4.41	4.35	4.45	4.26	4.21
Total	99.84	99.55	99.73	99.82	99.81	96.79	99.55
U	2.	1.	2.	3.	3.	3.	1.
Th	1.	1.	6.	6.	4.	6.	3.
Pb	16.	13.	14.	19.	17.	18.	20.
Nd	17.	27.	34.	31.	29.	35.	33.
Ce	50.	53.	53.	70.	65.	60.	50.
La	21.	23.	31.	22.	27.	30.	36.
Ba	644.	503.	655.	669.	713.	747.	730.
Nd	14.	13.	14.	14.	13.	14.	14.
Zr	180.	172.	192.	202.	201.	212.	202.
Y	36.	38.	40.	41.	42.	43.	43.
Sr	309.	311.	304.	316.	308.	291.	292.
Rb	49.	35.	50.	48.	55.	62.	56.
Ga	21.	20.	18.	16.	17.	20.	19.
Zn	106.	104.	106.	99.	98.	106.	111.
Cu	33.	29.	5.	7.	10.	9.	11.
Ni	10.	7.	1.	2.	2.	1.	2.
Co	33.	31.	26.	24.	23.	21.	26.
Cr	28.	48.	13.	26.	24.	24.	23.

Appendix 1-B
Grande Ronde Whole Rock Geochemistry

	6905	6911	6912	6913	6916	6931	6937
SiO_2	54.37	56.57	56.49	55.83	53.14	53.95	54.42
Al_2O_3	15.02	14.47	13.98	13.55	14.88	13.32	14.18
Fe_2O_3	2.67	2.76	2.84	3.05	2.94	2.95	2.99
FeO	8.05	8.41	8.71	9.20	9.20	8.98	9.31
MgO	4.33	2.95	3.31	3.70	4.47	4.29	4.30
CaO	8.96	6.95	6.86	7.05	8.68	8.11	7.90
Na_2O	2.88	3.63	3.28	3.21	3.29	3.36	3.14
K_2O	1.10	1.90	2.06	1.79	1.00	1.38	1.37
TiO_2	1.79	1.86	1.98	2.10	1.83	1.96	1.89
MnO	0.18	0.04	0.04	0.21	0.21	0.21	0.20
S	0.02	.	.	.	0.06	0.05	.
P_2O_5	0.28	0.03	0.28	0.28	0.31	0.27	0.40
Total	100.01	99.84	99.83	98.99	100.01	98.83	100.00
qz	8.21	8.18	9.45	8.77	4.[illegible]	5.06	6.86
ap	0.61	0.65	0.61	0.61	0.67	0.58	0.87
il	3.40	3.58	3.76	3.99	3.48	3.72	3.54
or	6.49	11.21	12.15	10.56	5.90	8.14	8.08
alb	24.34	30.68	27.72	27.30	27.81	28.32	26.54
an	24.79	17.55	17.33	17.26	22.86	19.95	20.55
cor	.	.	.	.	.	.	.
ol	.	.	.	.	.	.	.
hy	13.45	11.55	12.75	13.85	15.46	14.25	13.68
diop	14.71	12.51	12.41	13.22	15.06	15.34	13.32
mt	3.87	3.37	4.12	4.42	4.27	4.28	4.43
Total	99.87	99.28	99.89	99.89	99.82	99.64	99.87
U	2.	3.	2.	2.	3.	3.	3.
Th	2.	5.	4.	5.	1.	3.	2.
Pb	10.	16.	11.	19.	17.	14.	14.
Nd	28.	33.	27.	25.	25.	29.	21.
Ce	43.	53.	60.	55.	30.	48.	53.
La	30.	22.	19.	25.	25.	18.	38.
Ba	527.	702.	737.	750.	493.	547.	625.
Nb	13.	13.	13.	14.	12.	18.	13.
Zr	164.	192.	196.	200.	253.	147.	187.
Y	36.	37.	36.	36.	13.	13.	31.
Sr	328.	300.	290.	313.	160.	173.	311.
Rb	32.	54.	55.	56.	36.	38.	41.
Ga	18.	13.	20.	25.	30.	31.	23.
Zn	99.	101.	105.	112.	31.	42.	100.
Cu	38.	19.	11.	8.	33.	27.	50.
Ni	20.	4.	5.	4.	10.	2.	26.
Co	62.	25.	24.	27.	27.	26.	26.
Cr	64.	14.	15.	75.	39.	24.	24.

	6938	6939 a.	6939 b.	6940	6941	6942	6947
SiO_2	57.37	54.31	54.51	55.41	53.40	57.36	54.34
Al_2O_3	13.15	13.48	13.52	13.24	14.03	13.14	13.74
Fe_2O_3	2.90	3.17	3.13	3.11	2.93	2.92	3.10
FeO	8.92	9.46	9.35	9.49	8.49	8.94	9.28
MgO	3.30	4.08	4.17	4.14	5.72	3.37	4.20
CaO	6.19	7.69	7.77	6.96	9.20	6.52	7.99
Na_2O	3.25	3.03	2.86	3.38	3.01	3.30	2.93
K_2O	1.97	1.87	1.79	1.54	0.97	1.55	1.55
TiO_2	2.24	2.33	2.27	2.15	1.67	2.01	2.43
MnO	0.18	0.21	0.23	0.18	0.20	0.19	0.20
S	.	.	0.03	0.02	.	.	0.03
P_2O_5	0.52	0.36	0.37	0.40	0.38	0.40	0.41
Total	98.99	99.99	100.00	100.01	100.00	98.90	100.20
qz	11.92	6.75	7.82	7.93	4.68	11.24	8.18
ap	1.13	0.78	0.80	0.87	0.82	0.87	0.89
il	4.26	4.43	4.31	4.07	3.17	3.82	4.62
or	11.62	11.03	10.56	9.03	5.72	10.91	9.14
alb	27.47	25.61	24.17	28.55	25.44	27.89	24.77
an	15.46	17.64	18.75	16.39	21.89	15.56	19.75
cor	.	.	.	.	.	.	.
ol	.	.	.	.	.	.	.
hy	13.88	13.94	14.46	15.53	16.44	13.50	13.73
diop	9.88	15.07	14.41	12.89	17.44	11.82	14.27
mt	4.21	4.60	4.54	4.51	4.25	4.24	4.50
Total	99.83	99.85	99.82	99.79	99.85	99.87	99.85
U	3.	3.	3.	4.	2.	2.	1.
Th	3.	8.	9.	4.	1.	9.	4.
Pb	12.	14.	17.	20.	13.	17.	15.
Nd	31.	29.	33.	34.	23.	33.	35.
Ce	60.	60.	58.	43.	48.	65.	84.
La	30.	22.	32.	26.	17.	27.	23.
Ba	821.	654.	621.	644.	460.	732.	590.
Nb	13.	17.	14.	14.	10.	16.	17.
Zr	234.	182.	187.	192.	135.	199.	212.
Y	46.	36.	42.	40.	34.	39.	43.
Sr	312.	304.	317.	314.	370.	354.	322.
Rb	63.	43.	46.	50.	28.	61.	42.
Ga	20.	18.	23.	11.	18.	25.	28.
Zn	107.	110.	109.	99.	85.	100.	101.
Cu	7.	43.	46.	17.	49.	11.	58.
Ni	1.	12.	14.	4.	19.	4.	12.
Co	20.	24.	26.	25.	30.	25.	23.
Cr	7.	30.	39.	18.	74.	17.	27.

	6948	6949	6950	6951	6952	6953	6954
SiO_2	52.65	54.06	55.28	55.46	55.29	55.56	55.86
Al_2O_3	13.90	13.41	13.81	14.67	14.31	14.01	13.56
Fe_2O_3	3.14	3.20	2.85	2.71	2.76	2.92	2.98
MgO	5.55	3.77	4.24	3.96	4.33	4.01	3.41
CaO	9.23	7.91	7.51	8.32	8.42	7.91	7.13
Na_2O	2.72	3.45	3.47	3.08	3.02	3.13	3.13
K_2O	0.95	1.67	1.40	1.44	1.19	1.26	2.16
TiO_2	2.24	2.48	2.00	1.83	1.69	1.87	2.16
MnO	0.21	0.24	0.19	0.18	0.20	0.19	.
S	0.06	0.01	0.01	0.01	0.01	.	0.01
P_2O_5	0.34	0.42	0.39	0.29	0.31	0.37	0.48
Total	100.00	99.99	99.92	100.03	100.00	100.02	100.00
qz	5.74	5.68	7.07	8.35	8.44	9.20	9.00
ap	0.74	0.91	0.85	0.63	0.66	0.80	10.40
il	4.26	4.71	3.80	3.40	3.21	3.55	4.10
or	5.60	9.85	8.26	8.49	7.02	7.37	12.45
alb	22.99	29.46	29.33	26.10	25.53	26.46	26.46
an	22.89	16.16	18.18	21.91	21.92	20.47	16.71
cor	.	.	.	.	.	.	.
ol	.	.	.	.	.	.	.
hy	16.93	11.85	14.55	12.60	14.52	14.21	12.80
diop	16.12	16.90	13.68	14.46	14.71	13.57	12.98
mt	4.56	4.64	4.14	3.93	4.00	4.24	4.32
Total	99.83	100.13	99.86	99.87	100.00	99.87	99.86
U	4.	4.	1.	3.	3.	2.	4.
Th	4.	3.	2.	1.	3.	1.	4.
Pb	13.	15.	18.	11.	14.	14.	15.
Nd	25.	28.	21.	25.	23.	20.	33.
Ce	58.	50.	55.	53.	60.	58.	67.
La	18.	21.	17.	23.	13.	19.	23.
Ba	481.	619.	556.	530.	582.	607.	711.
Nb	15.	16.	13.	11.	12.	12.	14.
Zr	181.	227.	187.	172.	155.	171.	207.
Y	39.	42.	38.	36.	33.	37.	43.
Sr	321.	305.	342.	313.	306.	322.	319.
Rb	26.	45.	46.	36.	34.	33.	55.
Ga	27.	21.	20.	22.	18.	25.	15.
Zn	95.	105.	96.	89.	98.	94.	103.
Cu	84.	71.	71.	37.	11.	23.	24.
Ni	23.	11.	11.	6.	4.	5.	9.
Co	32.	27.	29.	27.	30.	29.	28.
Cr	53.	29.	26.	19.	21.	22.	18.

	6955	6956
SiO_2	57.17	55.91
Al_2O_3	13.51	13.17
Fe_2O_3	2.74	3.04
FeO	8.09	9.34
MgO	3.06	3.74
CaO	7.12	7.15
Na_2O	2.78	3.15
K_2O	2.30	1.73
TiO_2	2.56	2.11
MnO	0.01	.
S	.	.
P_2O_5	0.41	0.44
Total	99.34	98.78
qz	12.76	9.48
ap	0.89	0.96
il	4.87	4.01
or	13.57	10.21
alb	23.50	26.63
an	17.58	16.67
cor	.	.
ol	.	.
hy	10.20	14.23
diop	12.52	13.26
my	3.98	4.41
Total	98.67	99.86
U	2.	2.
Th	6.	7.
Pb	13.	17.
Nd	32.	33.
Ce	55.	58.
La	29.	31.
Ba	1392.	759.
Nb	15.	14.
Zr	227.	191.
Y	48.	40.
Sr	335.	316.
Rb	57.	48.
Ga	17.	12.
Zn	121.	103.
Cu	12.	41.
Ni	5.	11.
Co	31.	24.
Cr	17.	16.

Appendix 1-C
Picture Gorge Whole Rock Geochemistry

	P.G	Hi.Mg	Lo.Mg	6917	6918	6919	6920
SiO_2	50.20	50.21	51.30	49.28	49.17	49.75	49.99
Al_2O_3	15.36	15.49	15.34	16.31	17.31	14.97	15.45
Fe_2O_3	2.84	2.88	3.19	2.78	2.63	2.96	2.94
FeO	8.58	8.65	9.58	8.44	7.79	8.92	8.79
MgO	6.21	6.67	4.84	6.32	6.10	6.71	5.91
CaO	10.84	10.46	9.42	10.95	11.33	11.09	11.05
Na_2O	3.16	2.94	3.28	3.11	3.13	2.96	3.12
K_2O	0.53	0.57	0.74	0.46	0.47	0.42	0.54
TiO_2	1.55	1.56	1.79	1.77	1.53	1.73	1.72
MnO	0.21	0.20	0.23	0.20	0.19	0.22	0.20
S	0.01	.	.	0.01	0.01	0.01	.
P_2O_5	0.28	0.22	0.33	0.36	0.33	0.26	0.27
Total	100.15	99.85	100.04	100.00	100.00	99.99	99.89
qz	1.34	1.49	1.50	.	.	.	.
ap	4.36	0.72	0.76	0.83	0.56	0.56	0.58
il	2.96	3.40	3.40	3.36	3.29	2.79	3.27
or	3.13	3.37	4.37	2.72	2.42	2.48	3.10
alb	26.74	24.88	27.75	26.32	25.02	25.05	26.37
an	26.16	27.39	24.95	29.21	26.30	26.32	26.54
cor	.	.	.	.	.	.	.
ol	.	.	.	6.41	3.55	4.44	3.21
hy	22.90	16.39	16.26	8.51	11.78	13.22	10.20
diop	10.09	16.29	16.42	18.59	22.08	19.50	21.75
mt	4.18	4.63	4.63	4.03	4.30	4.05	4.27
Total	100.76	101.56	100.04	99.98	99.56	98.41	99.30
U	.	.	2.	4.	2.	5.	2.
Th	.	.	2.	1.	1.	1.	2.
Pb	.	.	11.	9.	10.	11.	10.
Nd	.	.	25.	9.	.	15.	13.
Ce	.	.	31.	34.	12.	26.	24.
La	.	.	12.	5.	4.	16.	8.
Ba	.	.	297.	277.	287.	278.	279.
Nb	.	.	8.	6.	8.	8.	9.
Z	.	.	84.	73.	96.	89.	102.
Y	.	.	29.	25.	33.	31.	33.
Sr	.	.	281.	287.	267.	252.	279.
Rb	.	.	15.	12.	19.	16.	21.
Ga	.	.	14.	16.	19.	17.	18.
Zn	.	.	68.	63.	80.	75.	83.
Cu	.	.	200.	170.	247.	208.	248.
Ni	.	.	41.	49.	45.	43.	44.
Co	.	.	41.	39.	31.	37.	35.
Cr	.	.	205.	155.	144.	137.	146.

P.G. represents the type Picture Gorge sample. High Mg and Lo Mg represent the averages of high and low Mg content Picture Gorge samples respectively.

	6921	6922	6923	6924	6925	6926	6927
SiO_2	50.16	51.27	51.08	51.91	50.52	53.25	51.25
Al_2O_3	15.45	15.14	15.57	15.27	14.21	15.05	15.01
Fe_2O_3	2.88	2.62	2.72	2.81	3.25	2.82	2.91
FeO	8.55	7.96	8.38	8.56	10.15	8.53	8.99
MgO	6.33	6.64	5.89	4.98	5.38	4.53	6.17
CaO	11.12	11.18	10.40	10.16	9.96	9.49	10.17
Na_2O	3.01	3.14	3.54	3.41	3.50	3.42	3.10
K_2O	0.31	0.34	0.46	0.74	0.55	0.70	0.47
TiO_2	1.59	1.29	1.46	1.63	1.95	1.63	1.49
S	0.02	.	.	.	0.01	0.01	.
P_2O_5	0.28	0.27	0.30	0.29	0.31	0.36	0.31
Total	100.00	100.01	100.00	99.97	100.02	100.01	99.08
qz	.	.	.	1.06	.	4.11	0.80
ap	0.60	0.58	0.60	0.63	0.67	0.78	0.67
il	3.02	2.45	2.77	3.10	3.69	3.10	2.88
or	1.72	2.00	2.71	4.36	3.24	4.13	2.77
alb	26.20	26.54	29.22	28.82	29.57	28.91	26.20
an	27.31	26.19	25.22	24.16	21.41	23.66	25.63
cor	.	.	.	.	.	.	.
ol	2.29	0.68	3.00	.	1.95	.	.
hy	12.81	15.10	11.16	13.57	12.78	13.69	18.03
diop	21.29	22.44	20.02	20.07	21.47	17.42	18.70
mt	4.18	3.90	3.95	4.08	4.72	4.09	4.22
Total	99.43	99.88	99.40	99.85	99.51	99.79	99.90
U	1.	4.	6.	5.	2.	2.	1.
Pb	1.	2.	2.	1.	2.	4.	1.
Th	12.	8.	12.	13.	10.	8.	12.
Nd	16.	15.	13.	11.	19.	21.	23.
Ce	25.	30.	30.	31.	10.	34.	31.
La	11.	9.	13.	10.	18.	17.	12.
Ba	304.	282.	341.	319.	397.	468.	331.
Nb	8.	8.	10.	10.	9.	8.	7.
Zr	94.	91.	110.	132.	121.	22.	88.
Y	32.	32.	34.	39.	44.	41.	36.
Sr	254.	230.	242.	222.	197.	236.	210.
Rb	14.	9.	10.	19.	18.	22.	88.
Ga	18.	19.	22.	30.	19.	22.	17.
Zn	71.	70.	78.	84.	88.	85.	80.
Cu	218.	185.	190.	238.	304.	234.	265.
Ni	41.	48.	38.	30.	19.	18.	42.
Co	32.	35.	32.	30.	27.	26.	33.
Cr	136.	153.	128.	91.	46.	51.	91.

	6928	6929 a.	6930 b.	6930
SiO_2	50.07	50.69	49.81	51.41
Al_2O_3	15.27	14.86	14.32	14.55
Fe_2O_3	2.79	2.76	2.93	2.80
FeO	8.44	8.35	8.76	8.60
MgO	7.43	7.57	8.79	6.62
CaO	10.62	10.83	10.59	10.42
Na_2O	2.94	2.74	2.45	3.11
K_2O	0.48	0.28	0.31	0.46
TiO_2	1.47	1.46	1.58	1.55
MnO	0.22	0.20	0.22	0.21
S	.	.	.	.
P_2O_5	0.26	0.25	0.25	0.27
Total	100.19	98.99	99.02	100.02
qz	.	0.18	.	0.49
ap	0.60	0.54	0.54	0.58
il	2.79	0.77	3.00	2.94
or	2.84	1.65	1.83	2.71
alb	24.88	23.19	20.73	26.29
an	27.05	27.42	27.16	24.36
cor	.	.	.	.
ol	4.44	.	1.85	.
hy	13.22	20.89	21.12	17.54
diop	19.50	20.09	19.18	20.89
mt	4.05	4.00	4.25	4.06
Total	101.27	97.73	99.66	99.86
U	5.	3.	2.	2.
Th	1.	1.	2.	5.
Pb	11.	12.	9.	12.
Nd	15.	14.	17.	16.
Ce	26.	29.	24.	43.
La	16.	10.	5.	16.
Ba	278.	246.	381.	315.
Nb	8.	7.	7.	9.
Zr	89.	90.	87.	103.
Y	31.	31.	31.	33.
Sr	252.	271.	245.	251.
Rb	16.	14.	11.	13.
Ga	17.	15.	14.	11.
Zn	75.	74.	77.	75.
Cu	208.	215.	185.	214.
Ni	37.	35.	34.	34.
Co	36.	33.	34.	33.
Cr	131.	138.	142.	131.

Appendix 1-D
Wanapum Whole Rock Geochemistry

	6900	6901	6902	6903	6904	6906	6907	6908
SiO_2	49.95	50.37	49.11	50.11	51.08	50.15	51.94	51.60
Al_2O_3	14.04	13.22	13.39	13.52	13.51	14.44	13.41	13.69
Fe_2O_3	3.66	3.74	3.97	3.79	4.62	4.14	4.63	4.51
FeO	11.31	11.63	11.74	11.49	11.13	10.78	10.40	10.47
MgO	4.13	4.43	4.43	3.97	4.62	4.14	4.63	4.52
CaO	8.56	8.27	9.02	9.00	8.33	8.81	8.50	8.52
Na_2O	2.69	2.76	2.67	2.37	2.75	2.86	2.67	2.63
K_2O	1.43	1.17	1.25	1.31	1.12	1.03	1.34	1.31
TiO_2	3.37	3.44	3.64	3.72	3.06	3.09	2.81	2.87
MnO	0.23	0.23	0.24	0.21	0.22	0.22	0.22	0.22
S	.	.	.	.	.	.	.	.
P_2O_5	0.62	0.74	0.51	0.59	0.56	0.53	0.53	0.52
Total	99.99	100.00	99.97	99.98	100.00	100.97	100.00	99.93
qz	4.32	5.21	3.67	6.56	5.52	3.09	6.07	5.84
ap	1.35	1.61	1.11	1.26	1.22	1.15	1.15	1.13
il	6.41	6.54	6.92	7.05	5.82	5.93	5.34	5.45
or	7.61	6.72	7.14	6.93	6.31	7.96	7.96	8.02
alb	22.74	23.33	22.57	20.01	23.24	24.17	22.57	22.23
an	22.41	20.30	20.96	22.73	21.34	22.56	20.60	21.52
cor	.	.	.	.	.	.	.	.
ol	.	.	.	.	.	.	.	.
hy	16.22	17.43	15.26	14.56	17.54	15.07	16.04	16.05
diop	13.33	13.22	17.00	15.01	13.55	14.70	14.99	14.20
mt	5.32	5.43	5.76	5.88	5.25	5.17	5.08	5.12
Total	99.71	99.79	100.39	99.99	99.79	99.80	99.80	99.56
U	2.	3.	5.	3.	3.	2.	4.	2.
Th	1.	2.	1.	4.	3.	1.	1.	2.
Pb	11.	12.	10.	6.	10.	14.	10.	12.
Nd	38.	33.	40.	36.	27.	32.	31.	27.
Ce	70.	70.	65.	70.	77.	67.	60.	72.
La	26.	31.	30.	32.	35.	30.	30.	23.
Ba	598.	644.	615.	590.	612.	589.	607.	611.
Nb	21.	20.	21.	19.	17.	19.	16.	16.
Zr	233.	214.	226.	226.	197.	199.	192.	189.
Y	52.	50.	52.	50.	43.	44.	41.	41.
Sr	291.	266.	274.	290.	287.	288.	309.3	05.
Rb	44.	40.	39.	41.	28.	40.	41.	41.
Ga	21.	13.	24.	14.	20.	18.	21.	21.
Zn	117.	110.	119.	121.	105.	101.	106.	102.
Cu	14.	16.	16.	13.	24.	28.	26.	28.
Ni	9.	8.	9.	8.	7.	14.	14.	10.
Co	40.	32.	34.	43.	48.	47.	30.	23.
Cr	21.	22.	22.	22.	33.	34.	41.	40.

	6909	6910	6914	3AS7	3AS7	3AS9	3AS9	3AS10
SiO_2	51.88	51.27	53.31	5.136	51.21	51.15	51.10	51.15
Al_2O_3	13.82	13.71	13.20	14.47	13.48	12.95	12.63	12.67
Fe_2O_3	3.45	3.55	3.41	3.39	3.72	3.74	3.43	3.91
FeO	10.22	10.74	10.14	10.34	10.91	11.36	11.12	11.14
MgO	4.27	4.41	4.38	4.22	4.43	4.66	4.65	4.96
CaO	8.57	8.41	8.04	8.27	8.43	8.30	8.67	8.45
Na_2O	2.92	2.67	2.61	2.75	3.07	3.07	3.04	2.83
K_2O	1.37	1.26	1.25	1.55	0.90	1.02	0.98	1.07
TiO_2	2.70	3.03	2.85	2.77	2.98	3.02	3.15	3.09
MnO	0.22	0.23	0.21	0.21	0.23	0.23	0.24	0.23
S	0.05	0.09	0.08	0.19	0.09	0.06	0.04	0.07
P_2O_5	0.54	0.63	0.55	0.57	0.55	0.49	0.46	0.46
Total	100.01	100.00	99.51	100.09	100.05	100.05	99.51	100.03
qz	5.02	6.01	9.41	4.75	4.93	4.20	4.56	11.00
ap	1.17	1.37	1.20	1.24	1.20	1.04	1.00	1.00
il	5.13	5.76	5.42	5.26	5.66	5.74	5.78	5.87
or	8.06	7.37	7.15	9.14	5.31	6.02	5.78	6.31
alb	24.68	22.57	22.06	23.24	25.95	25.95	25.90	23.92
an	20.54	21.72	20.20	22.54	20.33	28.53	18.33	17.56
cor	.	.	.	.	.	.	.	.
ol	.	.	.	.	.	.	.	.
hy	14.68	16.59	15.96	16.36	16.16	16.72	14.87	5.81
diop	15.31	13.19	12.91	12.26	14.87	16.21	18.33	17.56
mt	5.01	5.20	4.95	4.92	5.40	5.43	5.70	5.61
Total	99.60	99.78	100.04	99.71	99.81	99.84	100.04	95.74
U	4.	4.	.	4.	3.	3.	2.	4.
Th	1.	2.	.	1.	2.	3.	3.	3.
Pb	10.	11.	.	15.	15.	17.	16.	13.
Nd	32.	34.	.	34.	32.	33.	33.	36.
Ce	55.	43.	.	53.	60.	70.	76.	58.
La	23.	35.	.	26.	25.	32.	41.	27.
Ba	596.	573.	.	588.	607.	592.	585.	582.
Nb	16.	16.	.	16.	18.	16.	15.	16.
Zr	187.	191.	.	193.	195.	190.	183.	191.
Y	43.	42.	.	44.	45.	47.	47.	41.
Sr	315.	302.	.	322.	306.	309.	311.	306.
Rb	39.	43.	.	44.	45.	47.	46.	41.
Ga	15.	17.	.	19.	15.	20.	16.	18.
Zn	108.	104.	.	112.	118.	119.	120.	112.
Cu	20.	29.	.	18.	23.	18.	24.	14.
Ni	8.	10.	.	8.	12.	8.	11.	11.
Co	27.	32.	.	24.	21.	26.	16.	40.
Cr	21.	42.	.	35.	33.	36.	35.	38.

Appendix 1-E
Imnaha Whole Rock Geochemistry

	6943	6944	6945	6946
SiO_2	52.31	52.40	51.05	51.25
Al_2O_3	13.47	14.03	15.15	13.71
Fe_2O_3	3.39	3.25	3.11	3.47
FeO	10.26	9.63	9.19	10.28
MgO	4.38	4.37	4.64	4.75
CaO	8.19	8.60	9.03	8.80
Na_2O	3.32	3.18	3.37	3.47
K_2O	1.21	1.12	1.18	1.08
TiO_2	2.81	2.75	2.65	2.71
MnO	0.21	0.20	0.18	0.21
S	0.04	0.03	.	0.03
P_2O_5	0.45	0.46	0.46	0.48
Total	100.04	100.02	100.01	100.24
qz	4.38	5.13	1.41	2.65
ap	0.98	1.00	1.00	1.04
il	5.34	5.26	5.04	5.15
or	7.14	6.61	6.96	6.37
alb	28.06	26.88	28.48	27.56
an	18.26	20.68	22.71	19.57
cor	.	.	.	.
ol	.	.	.	.
hy	14.67	13.51	14.02	15.14
diop	16.11	15.69	15.72	17.34
mt	4.92	4.61	4.51	5.04
Total	99.86	99.37	99.86	99.83
U	6.	6.	3.	2.
Th	3.	5.	3.	1.
Pb	12.	15.	15.	11.
Nd	33.	32.	33.	36.
Ce	60.	53.	55.	60.
La	30.	31.	26.	26.
Ba	454.	491.	436.	449.
Nb	20.	19.	18.	17.
Zr	251.	244.	220.	226.
Y	50.	50.	42.	47.
Sr	258.	310.	363.	290.
Rb	41.	30.	38.	34.
Ga	18.	21.	20.	23.
Zn	104.	100.	98.	100.
Cu	101.	130.	141.	176.
Ni	15.	20.	63.	22.
Co	25.	24.	32.	23.
Cr	29.	33.	85.	51.

Appendix 2-A
Brown Glass Major Element Composition

	6908 (a)e	6908 (b)e	6944 (a)e	6944 (b)e	6946 (a)e	6946 (b)e	6946 (c)e	6946 (d)e
SiO_2	46.4	47.0	49.3	46.3	46.0	46.5	46.7	46.0
Al_2O_3	5.2	4.8	3.4	2.5	4.2	2.2	3.6	4.0
* FeO	26.6	25.7	25.4	30.5	27.4	30.5	27.1	26.9
MgO	8.3	7.9	10.9	5.1	9.6	5.7	8.8	10.3
CaO	2.1	2.1	1.4	1.7	1.6	1.4	1.5	1.7
Na_2O	.	.	0.4	.	0.6	0.2	0.4	0.7
K_2O	0.5	0.4	0.3	0.2	0.4	0.2	0.2	0.4
TiO_2	.	.	0.3	.	.	.	.	.
MnO	0.2	0.3	.	0.3	0.2	0.7	0.3	0.2
P_2O_5	.	.	.	.	.	.	.	.
+ H_2O	10.7	11.8	8.6	13.4	10.0	12.6	12.5	9.8
Total	100.0	100.0	100.0	100.0	100.0	100.0	100.0	100.0
qz	5.5	8.0	5.8	10.4	0.9	8.8	5.2	.
ap	.	.	.	.	.	.	.	.
il	.	.	.	.	.	.	.	.
or	2.6	2.2	1.4	1.3	2.4	1.2	2.4	1.9
alb	.	.	4.4	0.2	5.1	1.7	3.4	6.8
an	10.9	10.4	7.3	7.1	8.7	5.3	8.4	7.7
cor	5.2	4.1	.	.	.	.	.	.
ol	.	.	.	.	.	.	.	1.3
hy	76.8	76.1	80.4	77.5	82.6	80.7	80.8	79.7
diop	.	.	0.6	3.0	1.0	4.3	.	2.3
mt	.	.	.	.	.	.	.	.
Total	101.0	100.89	99.9	99.5	100.6	100.0	100.2	99.7

. In electron microprobe data represents a value below detection limits.

e Energy dispersive analysis technique.

w Wavelength dispersive analysis technique.

* All Fe is expressed as FeO. All CIPW Norms are calculated with all iron expressed as FeO. Fe_2O_3 was entered into the equation as 0.

+ Water is calculated as the difference between the total of the oxides and 100.

	6954 e
SiO_2	46.3
Al_2O_3	2.5
* FeO	26.1
MgO	11.6
CaO	1.8
Na_2O	0.7
K_2O	0.6
TiO_2	.
MnO	0.2
P_2O_5	.
+ H_2O	9.1
Total	100.0
qz	.
ap	.
il	.
or	3.54
alb	5.90
an	8.99
cor	.
ol	4.58
hy	75.17
diop	0.35
mt	.
Total	98.63

Appendix 2-B
Colourless Glass Major Element Composition

	3AS7 (a)e	3AS7 (b)e	3AS7 (c)e	6906 (a)e	6906 (b)e	6907 (c)e	6908 (a)e	6908 (b)e
SiO_2	75.7	77.0	75.2	72.1	73.4	73.9	69.6	74.4
Al_2O_3	14.8	12.8	12.1	12.5	12.5	13.0	13.4	19.8
* FeO	1.2	0.9	1.3	1.3	1.3	1.6	4.2	1.8
MgO	0.4	0.3	0.3	0.4	0.3	0.4	1.0	0.4
CaO	0.4	0.4	0.2	0.3	0.3	1.5	0.4	0.4
Na_2O	1.9	2.0	2.6	4.0	2.6	3.7	3.7	1.8
K_2O	7.2	6.9	7.1	6.2	7.4	5.7	4.8	6.1
TiO_2	1.0	0.9	0.8	0.5	0.6	0.7	1.1	0.8
MnO	.	.	.	.	.	.	.	.
P_2O_5	.	.	.	.	.	.	.	0.2
+ H_2O	0.1	0.0	0.0	0.2	0.1	0.0	0.1	0.0
Total	100.0	100.0	100.0	100.0	100.0	100.0	100.0	100.0
qz	36.03	37.92	31.94	22.45	26.27	27.15	23.01	38.30
ap	.	.	.	.	.	.	.	0.34
il	2.05	1.65	1.48	1.00	0.95	.	2.16	1.57
or	42.49	40.96	41.90	33.90	43.73	33.69	28.03	36.18
alb	15.72	16.73	22.14	33.90	22.00	31.31	31.36	15.50
an	0.99	0.89	3.01	2.20	2.48	2.85	6.58	1.13
cor	1.04	0.50	.	1.55	0.60	.	.	4.39
ol	.	.	.	.	.	.	.	.
hy	1.39	0.98	1.86	2.00	2.56	3.44	7.62	2.76
mt	.	.	.	.	.	.	.	.
Total	99.59	99.73	102.33	98.90	98.60	99.40	99.82	100.17

. In electron microprobe analyses represents a value below detection limits.

e Energy dispersive analysis technique.

w Wavelength dispersive analysis technique.

* All CIPW Norm are calculated with all Fe represented as FeO. Fe_2O_3 was entered into the equation with a value of zero.

+ Water was calculated as the difference between the sum of the oxides and 100.

	6908 (b)e	6910 (a)e	6910 (b)e	6910 (c)e	6944 (a)e	6944 (b)e	6946 e	6983 w
SiO_2	74.2	75.5	76.8	74.5	75.4	65.0	69.8	77.0
Al_2O_3	12.8	12.1	1.25	13.0	13.4	19.8	14.6	11.0
* FeO	2.3	1.3	0.6	1.3	1.1	0.9	1.1	0.2
MgO	0.5	0.5	0.3	0.4	0.4	0.5	1.5	1.7
CaO	0.3	0.4	0.2	0.3	0.3	1.5	0.3	2.9
Na_2O	2.1	1.7	3.0	2.0	3.5	7.3	3.5	2.9
K_2O	6.5	7.2	6.2	7.4	5.8	4.5	7.4	5.1
TiO_2	1.3	1.3	0.3	1.0	0.2	0.5	0.4	0.7
MnO	.	.	.	.	.	.	.	.
P_2O_5	.	0.3	.	.	.	.	.	.
+ H_2O	0.0	1.8	0.0	0.0	0.0	0.0	1.4	0.9
Total	100.0	100.0	100.0	100.0	100.1	100.0	100.0	100.0
qz	34.30	37.30	34.26	32.79	31.14	1.27	31.14	38.49
ap	.	0.63	.	.	.	.	.	.
il	1.14	2.45	0.51	1.82	0.38	1.00	0.38	1.33
or	38.07	42.31	36.59	43.73	34.10	26.56	34.10	30.14
alb	17.92	14.37	25.44	17.07	29.40	58.74	29.40	24.54
an	1.63	0.19	1.09	1.53	1.28	7.50	1.28	1.94
cor	2.36	1.35	0.87	1.68	1.40	2.97	1.40	.
ol	.	.	.	.	.	.	.	.
hy	4.41	1.37	1.54	1.81	2.65	1.98	2.65	2.63
diop	.	.	.	.	.	.	.	0.04
mt	.	.	.	.	.	.	.	.
Total	99.83	99.97	100.30	100.43	100.35	100.02	100.43	99.10

Appendix 2-C
Glass Phases Trace Element Analysis

6909 CGL		6983 CGL	
La	17.9 ± 0.3	67.5	± 0.7
Ce	113.0 ± 0.2	138.0	± 2
Nd	58.0 ± 3	72.0	± 5
Sm	12.6 ± 0.25	16.7	± 0.7
Eu	1.59 ± 0.11	3.67	± 0.04
Tb	2.02 ± 0.02	2.85	± 0.05
Dy	102.0 ± 1.6	na	
Yb	5.96 ± 0.52	8.43	± 0.3
Lu	0.81 ± 0.04	1.2	± 0.02
Sc	5.19 ± 0.44	4.58	± 0.17
Rb	137.0 ± 71	75.0	± 7
Cs	3.3 ± 0.3	4.4	± 0.5
Ba	1330.0 ± 50	596.0	± 42
Hf	16.1 ± 0.3	17.8	± 0.2
Ta	1.4 ± 0.16	2.05	± 0.06
Th	1605.0 ± 0.2	1806.0	± 0.3
Mn	381.0 ± 9	na	
Co	9.00 ± 9	3.06	± 0.06

6909 BGL		6983 BGL	
La	17.9 ± 0.3	33.3	± 1.6
Ce	41.1 ± 0.4	76.1	± 0.9
Nb	na	na	
Sm	5.99 ± 0.25	7.86	± 0.86
Eu	0.94 ± 0.024	0.89	± 0.09
Tb	1.03 ± 0.05	na	
Dy	6.05 ± 0.06	na	
Yb	3.31 ± 0.17	4.05	± 0.51
Lu	0.52 ± 0.02	0.62	± 0.04
Sc	6.38 ± 0.23	7.36	± 0.05
Rb	25.0 ± 4	15.0	± 1
Cs	2.7 ± 0.2	0.9	± 0.3
Ba	153.0 ± 21	93.0	± 50
Hf	2.62 ± 0.09	1.08	± 0.31
Ta	0.39 ± 0.03	0.62	± 0.14
Th	3.49 ± 0.07	7.92	± 0.13
Mn	2420.0 ± 20	na	
Co	12.0 ± 0.1	19.6	± 0.3

Trace element data from instrumental neutron activation analysis.

na Element not analyzed.

Appendix 3
Mean Wanapum Glass Mixture

	Avg. BGL x 0.25	+	Avg. CGL x 0.75	=	MWGM
SiO_2	52.4	+	74.4	=	69.0
Al_2O_3	5.6	+	13.0	=	11.2
* FeO	29.4	+	1.6	=	8.4
MgO	9.1	+	0.4	=	0.9
CaO	2.3	+	0.5	=	0.9
Na_2O	0.3	+	2.6	=	2.1
K_2O	0.5	+	6.6	=	5.1
TiO_2	**0.0	+	0.9	=	0.6
S	.	+	.	=	0.0
P_2O_5	.	+	.	=	0.0
Total	100.0		100.0		98.4

Mean Wanapum Glass Mixture is calculated by adding the average compositions of BGL and CGL as determined in this study together. The ratio of 3:1 CGL:BGL is in accordance with the average modal occurrence of the glass phases in the the samples as determined by point counting methods.

* All Fe is expressed as FeO.

** Although this element is present in some analysis it is not present in all sample, when expressed to 1 significant figure after the decimal as in this table 0 is the appropriate entry.

Appendix 4
Crystal Spectrometer Count Rates Across Bubble Boundaries
Bubble Boundaries

6983a

	Fe	Si	Mg	K
	56.	1477.	126.	950.
	54.	1512.	143.	868.
	52.	1617.	156.	846.
	71.	1362.	136.	833.
***	182.	1229.	888.	824.
	721.	945.	427.	111.
	758.	877.	456.	85.
	808.	923.	478.	91.
	837.	879.	492.	81.
	788.	929.	464.	108.

6983b

	Fe	Si	Mg	K
	835.	946.	478.	100.
	813.	903.	524.	119.
	747.	955.	502.	126.
	706.	854.	525.	190.
+++	704.	868.	504.	203.
+++	129.	1252.	270.	965.
	54.	1387.	176.	1284.
	83.	1426.	187.	1259.
	105.	1357.	184.	1213.
	80.	1381.	210.	1232.

6983c

	Fe	Si	Mg	K
	43.	1404.	33.	1025.
	58.	1405.	33.	1151.
	54.	1454.	41.	1133.
	114.	1350.	53.	1158.
	+++	89350.	61.	1114.
+++	300.	986.	164.	684.
	737.	945.	331.	315.
	765.	928.	310.	195.
	801.	915.	296.	199.
	824.	971.	294.	171.

6983d

	Fe	Si	Mg	K
	785.	921.	354.	168.
	788.	985.	354.	194.
	740.	950.	310.	209.
	715.	990.	272.	267.
***	535.	1117.	188.	423.
	142.	1387.	100.	1042.
	58.	1448.	37.	1192.
	157.	1488.	47.	1083.
	48.	1483.	37.	1138.
	35.	1467.	27.	1059.

6983e

	Fe	Si	Mg	K
	62.	1388.	28.	1167.
	51.	1410.	20.	1148.
	77.	1397.	33.	988.
	95.	1356.	41.	1002.
+++	80.	1224.	60.	1011.
+++	349.	975.	164.	555.
	663.	929.	256.	302.
	777.	924.	285.	202.
	813.	919.	320.	165.
	837.	946.	319.	159.

Counts per second encountered by crystal spectrometers as the automated stage was driven across various bubble boundaries. Microprobe conditions were 15 kV accelerating voltage, and 0.6 nA probe current, count times were 10 seconds at each location, and locations are 1 μm apart.

*** Area believed to be directly on the boundary between the two glass phases.

+++ Spectrometer believed to have crossed the actual glass/glass boundary between the points marked +++.

Appendix 5
Analytical Procedure

SAMPLE PREPARATION

Sample preparation for all analytical procedures began with the individual blocks of basalt. Visible signs of alteration were removed from the sample. The samples were then scrubbed with a wire brush in a hot soapy solution, rinsed and allowed to air dry.

The samples were then cut for thin section preparation for later petrographic and microprobe procedures. Thin sections were prepared in the thin section laboratory at the University of Alberta by Mr. Peter Black. Next, the remaining sample material was broken into inch cubes and passed through a jaw crusher. The chips from the jaw crusher were further crushed in a swing mill utilizing an agate mortar and pestle.

The powder from the swing mill was divided into three portions, one was sent to Dr. J.G. Holland for XRF analysis, another was passed into solution via standard techniques, and the third was sieved to obtain mineral separates.

The sieve section that passed 120 mesh but not 200 mesh was also collected and washed to remove dust. This portion (the first) were grains were almost uniformly of single mineral composition. This was the portion from which all mineral separates were taken.

The method for obtaining mineral separates was as follows. Brown glass was collected by placing all the material in Tetrabromoethane (TBr_4). Brown glass was the only phase that floated in TBr_4. The portion that sunk in this separation was collected for later separation of the CGL phase. The floating section was collected, washed with acetone, and placed in an equal volume of TBr_4 with 10 ml of acetone added. The section that sunk in this second separation was discarded, the floating section, BGL, was collected for analysis.

The fraction that sunk in the original TBr_4 solution contained; pyroxenes, olivine, plagioclase, colourless glass, opaques, and any compound grains that still remained. This fraction was passed through a succession of progressively diluted TBr_4 until a floating fraction remained that contained only CGL, and occasional plagioclase and compound CGL/plagioclase grains. The remainder, ferro-magnesian minerals, sunk. This fraction was collected and not used further in the course of this study.

The floating fraction, containing CGL and plagioclase, was passed through successively diluted TBr_4 until the CGL floated and the plagioclase and compound grains sunk. The floating section, CGL, was collected, washed in acetone and placed in the previous solution of TBr_4 with a further 1 ml of acetone added. The final floating portion was collected, hand picked to remove any obvious impurities and labelled CGL.

The plagioclase section that sunk in the first plagioclase/CGl separation was then added to a more concentrated TBr_4 solution (2 ml of undiluted TBr_4 was added to the dilute solution to increase specific gravity). The fraction that sunk was discarded. The floating fraction was collected, washed, and hand picked and finally labelled plagioclase separate.

ANALYTICAL PROCEDURES

Atomic Absorbtion Spectroscopy

Once passed into solution the solutions were analyzed by atomic absorbtion spectrometry techniques to determine whole rock trace element composition. AAS analysis was performed by comparing solutions with unknown elemental concentrations to standard solutions of known concentration of a given element. The sample concentration was determined by fitting the full peak height of the sample to a curve generated by known concentrations. In all cases every effort was made to compare similar concentrations of standard and unknown. In cases where suitable standards did not exist known standards were diluted with distilled water to prepare standards of lower concentration. All standards were reanalyzed at the end of each procedure to determine if any drift of the machine had occurred during the procedure.

The estimated accuracy of this procedure is ± 2% for most data. Extreme compositions such as U, Th, and Ba may be ± 5%. Errors are largely due to the inaccuracies in the curve drawn from the known standards, the fitting of unknown data to this curve, and manual peak height measurement. Additional inaccuracies due to the dilution process of known standards are a factor in those concentrations below 10 pp. Finally, errors in standard concentration are passed through to the final results.

X-Ray Fluorescence

Powders of all whole rock samples were sent to Dr. J.G. Holland at the University of Durham, England for XRF analysis. Dr. J.G. Holland's analytical procedure is fully discussed in Brown *et al.* (1970).

Instrumental Neutron Activation Analysis

INAA was performed on powdered mineral separates of two glass pairs, BGL and CGL from samples 6908 and 6944. Analyses were performed at the University of Alberta's SLOW-POKE reactor facility by M.J.M. Duke. The analytical procedure utilized is fully described in the Appendix to Chamberlain *et al.* (1988).

Oxygen Isotope Analysis

Powdered mineral and glass separates were analyzed to determine ^{18}O concentrations. All determinations were carried out by Mrs. E. Toth using the methods described by Clayton and Mayeda (1963), accuracy using this procedure is ± 0.02%.

Microbeam Analysis

Electron microprobe analysis was performed at the University of Alberta by the author with the assistance of Mr. S. Launspach.

The first step in all analysis was the selection of the area on the sample to be analyzed. This was accomplished by examination first by optical means by a standard optical microscope. Potential areas for analysis were marked for later identification. Once loaded into the microprobe the optical system was used to locate the approximate areas as marked for examination. The precise area to be examined was determined using backscattered electron images to locate areas that appeared to be the most homogeneous.

Due to the nature of glasses and the possibility of introducing error in the analysis due to volatilization of the sample at the beam/sample interface the beam was rastered over as large

an area as homogeneity of the sample permitted. In most cases this was on the order of 10μm x 10μm.

Microprobe conditions during energy dispersive work were 15 kV accelerating voltage, 32 nA aperture current, beam current was approximately 3.5 nA. Count time at all locations were 8 x 30 seconds . During wavelength dispersive runs the probe operating conditions were 15 kV accelerating voltage, 60 nA aperture current and approximately 7.5 nA beam current, count times were 100 seconds on the peak and 40 seconds on the background either side of the peak. Microprobe raw data was processed by the EDATA2-M software program (Smith and Gold 1979). Analytical uncertainties with these procedures are ± 1 - 1.5% for major elements(Si - Ti), and ± 5 - 10% for trace elements (Mn and P).

The bubble boundary traces were obtained by first finding a suitable bubble boundary by backscattered electron image. Then the four crystal spectrometers were positioned to detect Si, K, Fe, and Mg radiation. The automated stage was then computer driven by a series of 1 μm steps from an area of colourless glass into an area of brown glass. At each location computerized scalers recorded the number of counts encountered in the ten second counting interval. These numbers were recorded and used purely in a qualitative manner to determine whether the bubble boundaries were sharp and well defined or gradational. Microprobe conditions were 15 kV accelerating voltage, 60 nA aperture current, approximately 7.5 nA beam current and count times at each location were 10 seconds.

NON-ANALYTICAL PROCEDURES

CIPW Norm Calculations

CIPW norms were calculated using the procedure as described in Best (1982) using data obtained from various analytical procedures.

Point Counting

All point counts were done manually counting 1500 points on each slide. Point counting on very fine grained material has inherent shortcomings such as 3-D effects, optical limitations, and human error. The modal proportions attained are believed to be accurate within ± 8 -10% at the 99% confidence level. Point count data was most significant in determining the ratio of BGL:CGL in Wanapum samples in order to calculate MWGM. The accuracy of the point counting even if in error by10% will not alter the composition of MWGM enough to alter any of the arguments presented in this thesis.

Mean Wanapum Glass Mixture

Mean Wanapum Glass Mixture is calculated by mixing BGL and CGL compositions (determined by microprobe) in a ratio of 3:1 in keeping with modal proportions of the glass phases in the Wanapum as determined by point counting.